A CLIMATOLOGY OF BLACK BAY

LAKE SUPERIOR

A CLIMATOLOGY OF BLACK BAY

LAKE SUPERIOR

by

Francis E. Roy

A Project Report

Submitted in partial fulfillment of the
requirements for the Degree of
MASTER of ENGINEERING

School of Graduate Studies

Department of Civil Engineering and Applied Mechanics

McMaster University
Hamilton, Ontario, Canada
September 1982

MASTER OF ENGINEERING (1982) McMaster University

Hamilton, Ontario

TITLE: A Climatology of Black Bay

AUTHOR: F.E. Roy, B.Sc (M.E.), University of Manitoba

SUPERVISOR: Dr. C.R. Murthy

NUMBER OF PAGES: viii, 131 including Appendices

ABSTRACT

Black Bay is a major hatchery for lake herring (Coregonus artedii, Leseur) on the North shore of Lake Superior. Selgeby (1978) observed and documented the rapid spring dispersal of herring larvae. This preliminary study has been directed towards the identification of some of the mechanisms of this dispersal. It is based on data obtained from two specifically set current meter stations and a bathythermograph survey conducted in the spring of 1978, as well as data from existing meteorologic and stream flow records. A spectral analysis of the current meter record was done to determine the main energy components of the flow. Evidence indicates that transports in the Bay are driven by several mechanisms which are common to coastal estuaries, including a psuedo-tide, river inflow, and circulation due to longitudinal density (thermal) gradients, as well as surface winds. It is proposed that the passage of the thermal bar through the Bay may also be a significant influence on the dispersal of the herring larvae. The distinct seasonal character of the climatology is evident, though more data is needed to properly document it. Reasons for the attractiveness of the Bay to the herring as a hatchery are suggested, as is one vulnerability of the system to contamination by surface run-off.

ACKNOWLEDGEMENTS

I wish to thank Dr. C.R. Murthy for his encouragement and guidance in his role as Student Advisor.

Special acknowledgement is made to Mr. F.M. Boyce of the National Water Research Institute, Canada Centre for Inland Waters, for initially suggesting Black Bay as a research topic, and providing data from his field work during the February - June period of 1978. His interest, guidance and encouragement has been a great help in completing this project.

Thanks also is extended to Mr. F. Chiocchio of NWRI for his contribution in processing the field data into a useable form and providing the results of the spectral analysis of the current data.

To others of the NWRI Staff who supported my investigation through their willing assistance and discussion, thank you.

To those unsung, who maintain the meteorological and stream flow data collection and processing network in Canada, thank you also; it would be impossible without your efforts.

Although support and advice was wide-spread and freely given, in the final analysis, the interpretations, with all their possibilities for error and omission, are acknowledged to be mine.

F.E. Roy

Burlington, Ontario

1982

TABLE OF CONTENTS

TABLE OF CONTENTS (con't)

--" It is a common mistake to think that all that matters in science is logic and the understanding and application of fixed laws. In fact, imagination plays a decisive role in science and especially in natural science. For even though we can hope to get the facts only after many sober and careful experiments, we can fit the facts themselves together only if we can feel rather than think our way into the phenomena."--

Werner Heisenberg

"Physics and Beyond -
Encounters and Conversations"

Harper Torchbooks
Harper and Row, 1971

1. INTRODUCTION

Black Bay is the central one of the three major bays on the north shore of Lake Superior; the other two being Nipigon Bay to the East and Thunder Bay to the West.

According to Selgeby (1978), the Black Bay herring fishery is the largest remaining in Lake Superior and contributes more than 50 per cent of the total catch from Ontario's waters. The decline of herring populations in Lake Superior since the 1950's has prompted several studies, mostly of biological factors. Concern for the health of the Black Bay Fishery has generated a need to learn something of the physical behaviour of the Bay, particularly during the critical period of herring larvae dispersal in May (MacCallum, 1976).

In response to this need, a joint field program was undertaken from February through mid-June, 1978, by the National Water Research Institute and the Ontario Ministry of Natural Resources. The objective was to monitor the behaviour of the Bay during the spring period. Unfortunately, this program of measurements was not entirely successful. Two current meters, one on each station, obtained no data at all, and a third meter got no data after 12 April. The temperature data program was not as well documented as it might be, so that the data collected is useful only in qualitative terms, its accuracy being open to question. In spite of this, the amount of information

obtained was judged satisfactory to provide a basis for a climatological study of the Bay.

Black Bay has not been the subject of previous significant examination. It is generally established that mixing in large fresh water bodies is due to the influx of energy from the wind, the sun, and in-flowing or out-flowing streams. The summer currents in the shallow estuarine water of Saginaw Bay in Lake Huron have been shown to be driven principally by wind stress (Danek and Saylor, 1977). The formation and structure of the thermal bar in the Keweena Bay of Lake Superior has been examined and documented in some detail by Spain et al., 1976. There have been many observations of the influence of river inflows on the currents in lakes and bays (Hamblin and Carmack, 1978).

The bathymetry and geography of Black Bay makes it particularly interesting. Its shallower upper portion represents a large receiver for energy from the wind and sun. Its narrowing, deepening, relatively long channel connection to Lake Superior permits the development of gradients which tend to focus this energy into fairly steady longitudinal circulations. The data set available for study here is valuable in that it spans both ice-covered and ice-free regimes, and through the period of peak river discharge. The bathythermograph data runs late enough into the summer to provide initial evidence of stratification. This situation presents the opportunity

to examine the effects of the main forcing functions of circulation in a fresh water estuary in some isolation. The ice-covered period displays the effects of river flow without wind. The middle period displays the combined effects of peak river flow, heat input and wind. The later period provides some evidence of longitudinal circulation due to density (thermal) gradient in the absence of significant river flow.

It has been suggested (Fischer, 1979) that estuaries have individual personalities made up of the physical character of their geography, the character of their tributary rivers, and the seasonal variation of the weather. This report is an attempt to establish those factors of "personality" which govern the seasonal movements of the waters of Black Bay and thereby identify features which may influence the rapid dispersal of lake herring larvae during the spring period.

2. DESCRIPTION OF BLACK BAY

Black Bay is located on the North shore of Lake Superior (48°35' N, 88° 30' W) between Thunder Bay to the West and Nipigon Bay to the East (Canadian Hydrographic Service, 1977; EMR Canada, 1977) (Figure 1).

The Bay has a long axis bearing approximately 30° - 210° and is approximately 60 km long by 10 km wide. It lies between Sibley Peninsula on the north-west and Black Bay Peninsula on the south-east.

A group of Islands, the largest of which is Edward Island, obstructs the Bay entrance from the lake. Consequently, there are three channels out of the Bay. Between the east side of Edward Island and Black Bay peninsula is Magnet Channel. This is both narrow (1200 m minimum) and shallow (10 m minimum). The main channel into the lake is Montreal Channel which lies between the west side of Edward Island and shoal water around Cranberry Island. It is V-shaped in section, has soundings of 53 m, and a top width of approximately 3 km. Finally, between Cranberry Island and the Sibley Peninsula, lies Middlebrun Channel. This is shallow (12 m minimum) although wider than Magnet Channel (2 km).

For the purpose of this study, an arbitrary Bay exit has been set on the line from Kidd Point on the Sibley Peninsula, to

George Point on the Black Bay Peninsula. This line is up-bay from the split into the three channels out of the Bay, and is approximately a perpendicular to the main channel.

The Bay shape is characterized by a shallow (less than 10 m) almost circular inland end, about 17 km in diameter. The average bottom slope in this section is estimated as 0.044%. This is connected to the Bay exit by a progressively narrowing and deepening channel. At the inland end, it has a top width of approximately 10 km, is flat V-shape in section, and is 12 to 14 m deep in the center. The channel runs 26.5 km to the Bay exit, in a deepening, narrowing V-section. At the exit, between Kidd Point and George Point, the top width is 4.5 km and the channel depth is 37 to 40 m. The average bottom slope over this section is estimated as 0.097%.

Inside the exit, the Bay has a volume of approximately 3.4 km^3 over an area of 490 km^2. The hypsometric data, derived from mean chart soundings over 2 km square elements, are plotted in Figure 2. This illustrates the relatively large portion of the volume contained in depths of less than 10 m (Program BAY2, Appendix 5).

Black Bay Peninsula on the south-east, lies between the Bay and Lake Superior. This land area is steep-sided adjacent to the Bay, and drains mainly south-east, into the lake. To the north-east, a low swamp area, 10 km wide, separates the head of Black Bay from Nipigon

Bay. To the north and north-west are the drainage basins of the Black Sturgeon, Spruce, Wolf and Pearl Rivers, the major streams running into the Bay.

The Spruce - Black Sturgeon system has a drainage basin of approximately 2700 square km discharging into the north end of the Bay. The Water Survey of Canada maintains a stream flow monitor station (02AC002) at the Ontario Highway 17 crossing on the Black Sturgeon, approximately 10 km upstream from the river entrance to the Bay. This river is controlled by dams upstream.

The Wolf River discharges into the north-west side of the Bay, draining a basin of approximately 700 square km. The Water Survey of Canada has Station 02AC001 metering stream flow at the Highway 17 crossing, about 3 km upstream from the river entrance to the Bay. This river is also controlled by dams upstream.

The Pearl River, draining much of the north-west side of the Bay, enters on the west side, about half-way down the main channel. This river is not controlled.

There are several smaller streams draining into the north-west side of the Bay between the Wolf and Pearl Rivers. The drainage area covered by these has been integrated into the Pearl River Basin for this study, as they are not sufficiently large to

merit separate consideration. This gives a drainage basin of approximately 430 square km, assigned to the Pearl River.

On the lower north-west side lies the Sibley Peninsula. Drainage from this area enters the Bay by several small streams below the exit at Kidd Point - George Point.

The average annual discharge of the Black Sturgeon and Wolf Rivers combined, is about 33 $m^3 s^{-1}$. The peak daily average discharge of these Rivers in 1978 occurred on 3 June, and reached 102 $m^3 s^{-1}$.

The east side of the main channel of the Bay, the Black Bay Peninsula, is a steep bank from 45 to 60 m high, for a distance of 15 km up channel from Copper Point. It is considered that this topographical feature might have the local effect of inducing surface winds to flow predominantly up or down the main channel of the Bay.

3. DATA

3.1 Sources

The data for this study were obtained from two sources. The primary data set is that of currents and temperatures obtained from a field program conducted by the National Water Research Institute (NWRI) and the Ontario Ministry of Natural Resources (OMNR) (Boyce, 1978).

The supporting data set was obtained from continuous water survey and meteorological survey stations operated and reported on by various Branches of Environment Canada, as listed in Table 1.

The geographic location of the data collection stations are shown in Figure 1.

3.2 Current Meter Data

Two current meter stations, 78-3C-1A and 78-3C-2A were set by NWRI specifically for this study on a bay section at right angles to the main channel and 6 km up-Bay from the Kidd Point - George Point exit. Each station consisted of a string of three Geodyne Model 920-3 Current Meters, suspended in a taut mooring at depths of 4, 10 and 18 (bottom - 2 m) m. Station 1A was on the West side and 2A on the East side of the Channel, with approximately 2 km between them (Figure 3). Periods of data return are listed in Table 2.

The Geodyne Model 920-3 Current Meter measures current using a vertically mounted double S-shaped Savonius rotor which electromagnetically transmits 16 pulses/revolution to an electronic cumulative counter. Rotor starting speed is below 2.5 cm/s and maximum speed is over 360 cm/s. The instrument is accurate to within ±2.5 cm/s at 40 cm/s or less and within ±5 cm/s at speeds over 50 cm/s. Current direction is measured by an external vane coupled to the vane follower assembly which has a resolution of 2.8°. The vane follower is fluid damped. The recorded direction is the direction in which the current is flowing. The vane is accurate to within ±10° at 2.5 cm/s and to within ±2° at 13 cm/s. A magnetic compass establishes orientation of the instrument. By adding the direction vane and compass readings, current direction can be resolved within ±6° magnetic.

The instrument recorded the average current and direction for a 40 second period at 30 minute intervals in this application.

The current meter data were routinely processed to provide edited files of time/date and temperature, speed and direction for each 30 minute interval (Chiocchio and Kerman, 1978).

A co-ordinate system was aligned with the channel center-line down-Bay from the meter station with x being defined as the cross-Bay (east) and y as the along-Bay (north) axes. This co-ordinate system was inclined 15° East from Magnetic North.

Letting U and ϕ be the reading of speed and direction and B the inclination of the co-ordinate axes, then the components of velocity across and along the Bay are

$$u = U \cos (\phi - B)$$

$$v = U \sin (\phi - B)$$

The average components of velocity over some time interval T are then

$$\bar{u} = \frac{1}{N} \sum_{n=1}^{n=N} u_n \qquad N = \text{number of samples in the time interval}$$

$$\bar{v} = \frac{1}{N} \sum_{n=1}^{n=N} v_n$$

The average speed and direction over that time interval are then

$$\bar{U} = (\bar{u}^2 + \bar{v}^2)^{\frac{1}{2}}$$

$$\bar{\phi} = \tan^{-1}\left(\frac{\bar{u}}{\bar{v}}\right)$$

The current meter data have been processed to first, determine evidence of persistent flows over long time intervals and second, to determine the major energy components evident in the flows.

The list of daily average speed and direction were plotted as progressive vector diagrams (PVD) (Program PVD, Appendix 5). In studying the PVD, one must recognize that the presentation is that of current and direction at a fixed point in the time domain, i.e. Eulerian data, and be cautioned not to imply movement in space over time as with a Lagrangian drift. The value of the PVD in this case is to show the persistence in both direction and speed of the daily average currents during the period of interest. The diagrams are attached as Appendix 1.

The NWRI spectral analysis program, COHOV, designed to compute auto and cross spectra of complex valued (or vector) time series was used to compute and plot the Kinetic Energy Density and Cross Correlation Statistics. The record from each meter was separated into two seasons, the ice-covered from 78/02/11 to 78/03/28, and the ice-free from 78/05/01 to 78/06/09. The results of this treatment allow the association of periods of major energy densities contained in the original record to time scales of probable casual events. The spectral plots are attached as Appendix 2.

3.3 Temperature Data

The Geodyne 920-3 current meter includes a thermistor probe in the bottom end cap, adjacent to the current sensing rotor. This thermistor controls the frequency of a stable oscillator circuit. The frequency is counted for 1.825 seconds and recorded as temperature. The accuracy is 0.1°C over the range -2°C to +35°C.

As with the current speed and direction, the temperature record is routinely processed to provide temperature averaged over a given time interval. In this study, the daily averaged temperatures were used from the records listed in Table 2. These are plotted in Figure 4.

A second source of water temperature data was that obtained from a mechanical bathythermograph (MBT) survey of water temperature conducted by OMNR as summarized in Table 3. The MBT is a mechanical instrument carrying a gold plated glass slide in a holder and a thermally sensitive stylus. The slide holder translates longitudinally, driven by a bellows, in response to static water pressure. The stylus is driven by a Bourdon tube filled with xylene having a high thermal coefficient of expansion and moves laterally in reponse to water temperature. The unit is first field calibrated by recording surface temperature with a precision thermometer (surface bucket temperature), and then lowered on a line in a continuous fall to the bottom and

retrieved. The stylus scratches the coated slide as the slide moves, thus providing a graph of temperature against depth. The slide is then photographed against a calibrated grid for permanent record. The data requires digitizing for any extensive manipulation.

Selected casts have been used in conjunction with the temperature data from Stations 1A and 2A to derive depth averaged temperatures versus time in the region of the current meter section. These data were also plotted on the channel profile to obtain isothermal maps of the section against time (Appendix 3).

In addition to the MBT survey, the OMNR also made observations of surface water temperature at various points in the Bay over the period May 20 to August 2. Of particular interest here, were data gathered on a transect from Kidd Point to George Point, and also in the Montreal Channel off the south end of Edward Island.

Temperature data was also obtained from unpublished NWRI records of Lake Superior surveillance cruises over the period 1964 to 1973, (Robertson, 1973). This data was used to provide some indication of Lake Superior water temperature at 0, 20, 40 and 60 m depths from mid-April through late November, in Region 4 of the Lake outside the entrance to Black Bay. These data along with OMNR data are collected in Figure 5.

The temperature of the inflowing river water was not measured. Mean values of river thermograph readings at the stream flow monitoring stations for 1971 to 1975 were obtained from published records (Water Survey of Canada, 1976).

4. RESULTS

4.1 Currents

The results of the current meter measurements are detailed in the PVD of daily averaged currents (Appendix 1) and the Kinetic Energy Density and Cross Correlation Spectra (Appendix 2).

It is obvious from the PVD presentation that two distinct regimes are depicted reflecting the change in the condition of the Bay from one characterized by uniform flows under the protective ice cover up to the end of April to one characterized by some dynamic complexity in May and June.

4.1.1. Ice covered period

From 11 February through 17 April, the PVD shows a persistent flow regime at the 18 m level, down Bay on the West side and up Bay on the East. Flows at the 4 m level are not so organized, but indicate a trend up channel, the current on the East side being generally parallel to the shore, while that on the West side shows a more easterly component.

The spectral analysis results confirm this impression, indicating greater energy at the 18 m level than at the 4 m level, and

greater on the West side than on the East side. It also confirms the opposing direction of flows at the 18 m level. As well the spectral analysis results show a strong oscillation at a period of 7.8 hours.

Both this persistent flow pattern and strong oscillation would be expected to significantly influence Bay flushing time during this period.

Notable anomalies in the PVD pattern at the 18 m level between 8 and 20 March and after 17 April are evidence of ice cover decay in the region of the current meter section with some external forcing from other than river flows.

4.1.3 Ice free period

Observations at the 18 m level are confined to the East side only after April 12. From 1 May to 9 June (end of record) the flow regime is significantly altered. The nature of this change is grossly indicated by the monthly averaged values of along channel currents (Figure 6). It is evident that where during the ice covered period the concentration of flow energy was at the 18 m level, during the ice free period the currents increase significantly and concentrate at the 4 m level down channel on the west side and at the 18 m level up channel on the east side.

This is reflected in the magnitudes and directions displayed in the PVD as well as in the spectral analysis results.

The energy in the Bay oscillation at the 7.8 hour period is unchanged in the ice free period, although it is less significant relative to the larger period components in the spectra. This suggests that the contribution of this oscillation to Bay flushing is consistent throughout the whole year, and independent of local meteorological or river flow conditions.

4.2 Temperature

4.2.1 Current meter temperatures

The primary data are the daily averages of water temperature recorded by the current meters. These are graphed against time in Figure 4.

From the beginning of record to 16 April, the Bay temperature at the current meter station is generally less than 0.5° at the 4 m level and about 1.1° at the 18 m level. This indicates a small but stable gradient with the heavier water at the bottom, and a small heat flux from the water to the atmosphere.

Corresponding in time to the anomaly observed in the currents on the east side of the channel, the daily average temperature at the 4 m level rose from 0.5° to 0.8° between the 8 and 17 March, and then declined to 0.4° by 21 March. Minor increases in temperatures at the 18 m level on both east and west sides, suggest some vertical transfer of heat, which is consistent with the idea that meteorologically forced changes in surface currents may have temporarily affected flows at the 18 m level.

Over the period 25 March to 16 April, the temperature record returns to a steady condition.

The rise in surface water temperature at a relatively steady rate beginning around the 18 April signals the end of the stable regime characteristic of the ice covered period and the beginning of the spring heating cycle. This coincides with significant changes in the surface currents beginning on 17 April and is considered to reflect the decay and breakup of the ice-cover over the current meter station.

With the removal of the ice cover, one would expect to see the surface temperature rise above the bottom temperature, reflecting the new direction of heat flow from the atmosphere to the water, with the associated instability in density gradient leading to thermal turnover of the Bay.

This condition starts to be evident from 17 April to 4 May, but is interrupted by an abrupt rise in temperature at the 18 m level in advance of the surface temperature, creating a vertical temperature gradient opposite from that expected for a heat flux from the surface. This anomaly is associated with a significant arresting of the 18 m level current at the same time. This suggests the influx of heat to the bottom water from some other source than just convection from the surface.

Following this anomaly, both bottom and surface temperatures rise from 1.5 to 4° from 14 to 24 May, with very small temperature gradients indicated either vertically on the east side, or horizontally between the two surface meters. This is taken as evidence of the passage of a thermal bar.

After 29 May, temperature gradients are established consistent with the vertical transfer of heat from the surface to the bottom. Changes in heating rate appear to correlate to changes in daily average current directions indicating the wind to be significant in promoting mixing in the water column.

4.2.2 MBT data

The Mechanical Bathythermograph surveys conducted by OMNR extend the period of temperature observation beyond the 9 June when

the current meters were recovered. The first survey on 30 May shows the remnants of 4° water at the bottom of the channel below the 18 m level. The next survey of 2 June shows this now mixed to 6°. By 6 June just before the current meters were recovered, the Bay at the current meter section is uniformly mixed with a surface temperature of about 9° and a bottom temperature of about 7°. Thereafter, the MBT data for 15 and 21 June and 18 July give strong evidence of a cold (5°) water intrusion up Bay past the current meter section, indicating a fairly large scale, thermally generated lake-bay exchange in early summer.

4.2.3 River Temperature Data

The mean of river thermograph records 1971 to 1975, shows that the river temperature reaches 4° around 15 May and thereafter is generally warmer than Bay water temperatures observed. As already observed the Bay at the current meter section reaches 4° on 24 May. Consequently, after this date, the river discharge will generally be less dense than the Bay and its energy will remain in the upper levels of the Bay. This agrees with the earlier observation that during the ice free period, down channel flows appear stronger at the 4 m level on the west side.

4.2.4 Lake temperature data

The area weighted mean water temperature of Lake Superior in the coastal region adjacent to Black Bay is shown in Figure 5. This is historical data derived from 19 cruises from 1964 through 1973. The means of surface water temperature from the 1978 OMNR Survey in the Montreal Channel at the southend of Edward Island are shown for comparison. Similarly, mean surface water temperatures on the Kidd Point - George Point transect measured by the OMNR Survey are also shown.

The vertically averaged temperature of the Bay at the current meter station and the average temperature to the 40 m depth in the lake have been used to calculate the density anomaly between the lake and the Bay. The result is shown in Figure 7. This result shows that until about May 30, the Bay may be considered open ended since there is no significant density gradient between the Bay and the Lake. Thereafter, the rapid heating of the Bay makes it lighter than the Lake and by 9 June, a significant longnitudinal density gradient develops which would be expected to force an intrusion of cold lake water into the Bay. Such an intrusion is evident, as noted, from the MBT data.

4.2.5 Summary of temperature data

The main features of the temperature data are depicted in Figure 8.

Initially, the river flow, Bay and Lake are essentially equal in temperature. The river plume seeks a level characteristic of its density in the Bay Lake temperature gradient.

With the removal of the ice-cover, the upper Bay heats more rapidly than either the river or the deeper Lake. This leads to the formation of a thermal bar. For a short period, the river inflow is denser than the inshore Bay. The river plume flows through the upper Bay with little mixing.

By the end of May, the river and the upper Bay surface are equal in temperature. The river plume now mixes more readily with the upper Bay water, in the absence of large density gradients between the two water masses behind or inshore of the thermal bar.

In mid June, the river discharge is maximum and appears to hold the heavier lake water in balance much in the manner of an arrested wedge intrusion.

By mid July, the river discharge has declined, and the lake has intruded into the Bay establishing a stratification at the 10 m level.

5. DISCUSSION

5.1 A General Caveat

An estimated mass balance of the water in Black Bay, based on the monthly totals of river inflow, precipitation and changes in Lake Superior water level is listed in Table 4 for the period January to August, 1978. The important characteristic shown here is that even in the most active month of June, the bulk residence time of Bay Volume/Monthly Outflow is long, 17.8 months, and the average over the period is 47.1 months. The similar parameter for Kamloops Lake (Hamblin and Carmack, 1978) varies from 340 days in February to 15 days in June, with an annual average of about 60 days. By comparison to this, Black Bay is almost quiescent. In consequence, the sectionally averaged currents to be expected at the meter section are miniscule so that any conclusions drawn from limited observations, must be treated cautiously.

In light of these considerations, it is recognized that the failure of 3 of the 6 current meters placed (Table 2) severely limits the usefulness of the data set for detailed analysis on its own. For much of the period 10 February through 12 April, when at least 4 of the meters were operating, currents observed were often less than the 2.5 cm s^{-1} threshold of the instrument, and no accuracy can be claimed for current speed, while the accuracy for direction is ±10°. For the

period 12 April through 9 June, when currents were large enough for accurate observation, the total Bay section was monitored by only 3 meters. The loss of the meter at the 18 m level on the west side, was critical to establishing the credibility of any objective conclusion from this data set.

Having identified this general caveat, the value of this data set in providing some insight into the general flow regime in Black Bay cannot be argued seriously. When these insights are reinforced by others based on other data, or on observations drawn by others from similar situations, then the case for accepting the indications of the current meter data set is strengthened. The least that is achieved is the establishment of a preliminary climatology which can form the basis for more detail future study.

5.2 Breakup of the Ice Cover

In general, the data displays two distinct regimes which may be conveniently called ice-covered and ice-free.

The date of break up of the ice cover in the vicinity of the current meter station was not recorded by observation, but may be deduced from the data records. It is important to fix this date within a few days since it marks the opening of the Bay surface to

direct heating by the sun and atmosphere and, therefore, affects estimates of heat flow into the Bay, with consequent changes in the thermal regime.

The condition of the ice cover is reflected in the data. An episode suggesting open ice over the eastern meter string is evident from 5 through 21 March. Over this period, the current at the 4 m level is reversed. An anomaly in the flow at the 18 m level on the east side from 8 through 20 March infers a transfer of energy from the surface. Daily average temperature at 4 m rose from 0.5° to 0.8° between the 8 and 17 March, then declined to 0.4° by 21 March (Figure 4). The daily maximum air temperature on 9 March was 0.3°C. Winds on 9 March were of variable direction or swivelling, with a mean speed of 15.7 km/hr and a maximum of 26 km/hr. Winds remained moderate (daily maximum over 15 km/hr) and were generally down Bay or swivelling until 19 March, then were calm on 20, 21 March. This episode appears to have affected the currents at the 4 m level on the west side of the channel from 16 to 19 March as well. The return of both current and temperature to stable conditions from the 21 March to 16 April shows that the whole ice cover over the Bay remained intact, however.

Phillips (1978) provides charts of ice probability showing the percentage frequency for various concentrations of ice for 10 day intervals, based on an average of 140 surveys. The Thunder Bay chart

indicates that by 25 April, there is a 10 percent frequency of occurrence of 10/10 ice cover and a 55 percent frequency of occurrence of 1/10 ice cover.

The PVD of daily average current at the 4 m level on the east side of the Bay, shows a distinct reversal of flow direction on 17 April, while on the west side there is a similarly significant change in flow direction on 22 April.

The plot of daily average temperatures at the 4 m level shows water temperatures beginning to rise at a steady rate of 0.1°/day on the east side and 0.2°C/day on the west side, commencing on 20 April. This indicates a significant increase in heat flux from the surface. Heating of the surface water from 0 to 4°C will increase its density, creating an instability which will diffuse heat downward. The diffusion rate would be further increased by the action of wind on the unstable surface layers.

The wind record for this period shows three episodes of interest. For 18 through 20 April, a predominantly north wind (down channel) averaging 16.2 $km.h^{-1}$ with mid-day peaks of 30.2 $km.h^{-1}$ blew. On 21 April, the wind was south and south-west (up channel). Beginning around noon on 22 April and continuing through 24 April, the wind was again trending down channel, this time from the east and east-north-east, again with mid-day peaks of 32.0 $km.h^{-1}$. Winds

reduced in strength on 25 through 27 April, but held east-north-east. The third episode of strong winds ran from 28 through 30 April, with the direction from north-north-east.

These data of current, wind and temperature are considered to reflect a weakening and initial down channel movement of ice on 18 April, with the ice moving out from the east side of the channel first. Further ice from up the Bay was moved out down the west side of the channel over the period 22 to 24 April. By 28 April the Bay was fully open, so that the third wind episode could introduce sufficient energy to influence temperatures and current at the 18 m level. This is somewhat earlier than usual as reflected by Selgeby (1978), who implies the Bay is ice-free by 15 to 20 May, and by the historical record given by Phillips (1978).

With this significant boundary point established, the ice covered and ice free periods may now be discussed independently.

5.3 Ice Covered Period

5.3.1 The general pattern

The ice cover excludes major influxes of energy from wind, sun and atmospheric radiation. The lake water temperature outside the Bay is essentially the same as the Bay water. The sigificant influence of the lake on the Bay is its free oscillation in the fundamental

mode of 7.84 hours, which produces a kinetic energy density component in the Bay which is an order of magnitude greater than that of flow components at other frequencies. The bulk residence time averaged for February and March is 84.6 months.

The temperatures over the period at the current meter station remain notably steady, especially from 21 March to 20 April. If it is assumed that the vertical temperature gradient indicated is linear and typical of the whole Bay under the ice-cover, then the water at the 29 m depth (mid-channel below the current meters) would be approximately 1.8°C, at the 6 m depth typical of the mid-point of the upper Bay about 0.3°C, and under the ice about 0.02°C.

The current and temperature data obtained at the mid-channel station are not sufficient to fully depict the situation in Black Bay. What emerges from the PVD's and the spectral analysis for energy components with periods greater than 24 hours, is a clear pattern of flow at the 18 m level, down Bay on the west and up Bay on the east. At the 4 m level, there is a generally up Bay flow of much lower magnitude, with that at the west side meter having a more easterly component than that at the east side meter.

In the absence of other forcing mechanisms, these flows must be driven primarily by river discharge, temperature or density gradients between the river and Bay waters, and modified by geostrophic forces.

5.3.2 Inertial scale

One time scale of importance to this discussion is the Rossby Number (R_o) which is a convenient measure of the magnitude of the inertial properties of the flow relative to the Coriolis acceleration.

$$R_o \equiv \frac{U}{Lf_o}$$

The scales for flow speed (U), dimension (L), and local inertial frequency (f_o) are defined by the scale of the processes being examined. In this case, a characteristic dimension (L) to define the time of advective transport, is the cross channel dimension at the 18 m depth of the order 2.5×10^3 m. The local inertial frequency, f_o, at latitude 48° 35' is of the order 1.1×10^{-4} rad. s^{-1}. The flow speed used is dependent on the time scale of the process of interest. For example, 18 m currents averaged over a month, are of the order 1.2×10^{-2} ms^{-1}, daily average currents display a range from 2×10^{-2} to 2×10^{-4} ms^{-1}, while hourly average currents of the order 10^{-1} ms^{-1} are recorded. Hence

R_o (monthly) $\approx 4.4 \times 10^{-2}$

R_o (daily) $\approx 7.3 \times 10^{-2}$

R_o (hourly) $\approx 3.6 \times 10^{-1}$

Since the flow speeds are generally so small, it is expected that for flows of a period greater than 24 hours at least, the Coriolis acceleration due to the earth's rotation will influence the current path.

Another scale of the importance of rotation is the ratio of the characteristic basin scale, L, to the Rossby radii of deformation, $r = C/f_o$, where C is the propagation speed of wave motions.

For surface waves, the external Rossby radius is given by

$$r_e = \left(\frac{gH}{f_o^2}\right)^{\frac{1}{2}}$$

At the current meter section, H is of order 18 m, giving a value of r_e in the order of 120 km. Since the surface width of the channel is only 6 km, rotation may be neglected in the analysis of surface waves in this case.

For internal waves, the internal Rossby radius is given by

$$r_i = \frac{NH}{f_o}$$

As shown in the next section, N, the buoyancy frequency, is in the order of 5×10^{-3} radians per second during the ice covered

period. With the increased vertical density gradient at the end of May, it increases to 8×10^{-3}. These values give internal Rossby radii of 0.8 km and 1.3 km respectively. Since the channel width at the 18 m depth is about 2.5 km, L/r_i is greater than 1, and again, it is concluded that the earth's rotation will influence the motion of the longer period internal waves in the Bay.

5.3.3 Stability

Another time scale of importance is that relating to the stability of the water column. A measure of the scale of the density gradient is given by Fischer et al (1979) in the parameter

$$E' = \frac{1}{\rho o} \frac{\partial \rho e}{\partial z}$$

where

ρo is the water density of the mean temperature

$\frac{\partial \rho e}{\partial z}$ is the density gradient

During this period, the average temperature at 18 m level is about 1.1°C and at 4 m level about 0.4°C (Ref. Figure 4). For these conditions, E', is approximately 2.8×10^{-6} m^{-1} for fresh water.

Fischer shows that a water particle displaced vertically in a density gradient, will oscillate at a buoyancy frequency N.

$$N = (E'g)^{\frac{1}{2}}\ s^{-1}$$

The ratio of the advection time scale to this buoyancy time scale is the internal Froude Number

$$Fi = \frac{U}{H} \times \frac{1}{N}$$

For the same time scales as before, and a distance scale of channel depth ($H \approx 18$ m)

$$Fi\ (\text{monthly}) \approx 1.3 \times 10^{-1}$$

$$Fi\ (\text{daily}) \approx 2.5 \times 10^{-1}$$

$$Fi\ (\text{hourly}) \approx 1.3$$

This demonstrates that for the longer time scales, the density anomaly dominates the advection scale. Even though the density gradient is small, because the flow speeds are generally so small, it is expected that the density gradient will force in flowing water to seek a level characteristic of its temperature.

5.3.4 River inflow

Fischer et al (1979) cite several examples of river in-flows of both greater and lesser density than the resident reservoir or lake

water. The river plume may intrude a long way out on the surface if it is very light relative to the Bay; it may plunge directly and flow as a submerged plume down a convenient descending channel if it is very heavy; or it may plunge directly and then at some depth of equal density to the river, it may separate from the bottom and proceed as a sub-surface intrusion, if it is of intermediate density.

Hamblin and Carmack (1978) cite many instances where incoming river flows may influence or even dominate the circulations of the receiving bodies of water. They also point out that the influence of the earth's rotation on river in-flows to larger water bodies has been widely observed.

The temperature of the in-flowing river water into the Bay from the major rivers is not known. Mean values of thermograph records (Figure 10) indicate it would not exceed 0.5°. If it is of low velocity, under an ice cover, it may be super-cooled, i.e. less than 0°C. Dissolved solids and suspended bed load may contribute to some density anomaly. In any event, the in-flow situation in this case is unstable. The Bay is not stratified and has a low vertical temperature gradient. There is only a small temperature difference between the river and the Bay. The in-flowing water must entrain Bay water. If the Bay is warmer than the river, the river plume will flow on top of it and this will entrain water from below. It will then pick up heat and hence density and therefore tend eventually to sink

to some sub-surface equilibrium depth. If the Bay is colder than the river, the river plume will sink immediately, losing heat on the way, until an equilibrium is reached, at which point a sub-surface intrusion will occur. Since the equilibrium temperature of the river and entrained Bay water must have some value greater than 0°C, and since the vertical temperature gradient of the Bay water is so low, and since the river in-flows are of low energy, this equilibrium depth will be intermediate between the surface and the bottom of the Bay. The nature of this plume and entrainment exceed the scope of this report, but are worth further study in future.

As the kinetic energy of the in-flowing river water is transformed by entrainment processes from low volume high speed to high volume low speed, the internal Froude Number of the plume is reduced, and the plume stabilizes at a characteristic density level. As the plume moves further into the Bay, increasing the length characteristic of advection time, the Rossby Number decreases, and the Coriolis acceleration will direct the plume to the west side in the down Bay direction.

As the river in-flow entrains Bay water, continuity requirements will force a counter flow up the Bay. This counter flow will be made up of water which requires the least work to set it in motion. Because of the density gradient of the Bay water, entrained water would be replaced by a counter flow at the same depth. For example,

water entrained by the river plume at the surface before plunging, would be replaced by a surface counter flow, since extra work would be required to lift the deeper, heavier water up to the surface. Similarly, water entrained at lower levels after the plunge, would be replaced by counter flows at these levels, since extra work would be required to pull the lighter surface water down to that depth. Again, because of the low Rossby Number, these counter flows would tend to the east side of the Channel as they move north up the Bay. The velocities of such counter flows would tend to be lower than the river plume at some stable point down the Bay, since their mass flow balances the entrained water only.

5.3.5 Interpretation of Current Record

The situation at the current meter section may then be interpreted on the preceding ideas. The flows at the 18 m level depict the main river plume with entrained Bay water going down the west side, and the counter plume of replacement water from the lake or Bay going up the east side. The flows at the 4 m level depict a counter flow balancing surface water entrained by the river flow in the upper Bay.

It seems likely that the flows indicated by the current meters at the 18 m level are closely similar to the shore-bound flow stage discussed by Hamblin and Carmack in their analysis of currents

in Kamloops Lake. The river plume moving down the Bay stabilizes at its density level and is driven to the right hand shore by the Coriolis force. Being bounded by the shore, a cross-stream pressure gradient develops balancing the Coriolis force. To adequately document the extent of these shore-bound current plumes, more detailed temperature profiles are required to establish the cross-stream temperature gradient.

5.3.6 Estimate of flow distribution

An approximation of the relative distribution of the long term exchange flows in the Bay due to the river discharge during the ice-covered period may be made from the available data, with some loose assumptions.

The monthly mass balance gives an estimate of the net out-flow past the current meter section, which may be interpreted as an average rate of net discharge.

The meter section will be approximated by a triangular section 5 km wide by 29 m deep. It will be assumed that the monthly averaged N/S currents from each meter is the sectionally averaged current for the stream tube represented by that meter.

By continuity, the sum of flows in each stream tube through the meter section, must equal the net discharge through the meter section, Q_T. In nondimensional form, scaled to Q_T,

$$\sum_{n=1}^{n} \frac{U_n A_n}{QT} = 1 \qquad (1)$$

The definition of symbols is shown in Figure 3.

Assume that the flows in the upper layer are replacing water entrained by the river flow on the surface of the upper Bay before the plunge line. The depth of this upper layer (y_1) must then be equal or less than the mean depth of the upper Bay (Yu), otherwise extra energy is required to pull warmer (hence heavier) water up from a lower depth. Then $y_1 = Y_u$.

Assume the flow in the upper layer is homogenous with a cross-section average velocity represented by the average of meters 1 and 2.

Expanding 1

$$\langle \bar{U}_{1,2} \rangle \cdot (A_1 + A_2) + U_3 \bar{\bar{A}}_3 + U_4 \bar{\bar{A}}_4 = Q_T \qquad (2)$$

From the section dimensions, and setting $y_1 \approx 6$ m,

$$(A_1 + A_2) = (6 \times 5000) - 6\,(6 \times \frac{2500}{29})$$

$$= 26{,}900 \text{ m}^2$$

$$A_3 = \tfrac{1}{2}hw; \text{ but, } \frac{h}{w} = \frac{29-y_1}{2500-X_1} \approx \frac{23}{2300}$$

$$\text{Then } A_3 = \tfrac{1}{2} \cdot \frac{23}{2300} \cdot w^2 \qquad \text{for } 0 < w < 2000$$

$$A_4 = \tfrac{1}{2}\, H \cdot W - A_3 \qquad \text{where } W = 5000 - 2 \cdot (6 \times \frac{2500}{9}) \approx 4000 \text{ m}$$

$$H = 26 - 9 = 23 \text{ m}$$

Substituting in (2),

$$\langle \overline{U}_{1,2} \rangle \cdot 26{,}900 + \overline{U}_3 \cdot \tfrac{1}{2} \cdot \frac{23}{2000} \cdot w^2 + \overline{U}_4 \,(\tfrac{1}{2}HW - \tfrac{1}{2} \cdot \frac{23}{2000} \cdot w^2) = Q_T$$

$$2 \cdot \langle \overline{U}_{1,2} \rangle \cdot 26{,}900 + \frac{23}{2000} \cdot w^2 \cdot (\overline{U}_3 - \overline{U}_4) + U_4 \cdot H \cdot W = 2Q_T$$

The data for March 15 (- down or out, + up or in)

$$Q_T = -13.07 \text{ m}^3/\text{s}$$

$$\langle \bar{U}_{1,2} \rangle = 0.013 \text{ m/s}$$

$$\bar{U}_3 = -0.0097 \text{ m/s}$$

$$\bar{U}_4 = 0.0051 \text{ m/s}$$

$$H = 23 \text{ m}$$

$$W = 3966 \text{ m}$$

Then $w = 1816$ m, i.e. $w < 2000$

Then $Q_{1,2} = \langle U_{1,2} \rangle \cdot 26{,}900/Q_T \qquad = 2.68$

$$Q_3 = \bar{U}_3 \cdot \frac{23}{2000} \cdot w^2/Q_T \qquad = -14.07$$

$$Q_4 = \bar{U}_4 \cdot \tfrac{1}{2}(H \cdot W - \frac{23}{2000} w^2) Q_T \qquad = 10.4$$

Closing $\sum Q_{1,2} + Q_3 + Q_4 = -1.0$

5.3.7. Estimate of river induced flushing time

Although the temperature of the Lake water outside the Bay is not specifically known, there is evidence from records of

Lake Superior surveillance cruises 1964 through 1973 (Robertson, 1982) indicating that during March and April no significant temperature difference would be expected between the Bay water and near shore Lake water. Thus, at the lower levels at least the Bay may reasonably be considered open ended. If this were the case, then the plumes observed at the 18 m level at the current meter station, might reasonably be considered to depict an exchange flow with the Lake.

Accepting these arguments, it may be estimated that a Bay flushing time is

$$\frac{\text{Bay Volume}}{Q_3 \cdot Q_T}$$

which is approximately 214 days. Because of the simplifications and assumptions used to arrive at it, this number must be recognized as having validity only as a comparative figure of merit in assessing Bay flushing due to river flow, against flushing due to other mechanisms.

5.3.8 A tidal oscillation

The spectral analysis of current data over the ice-covered period established the existence of a major kinetic energy component at a period of 7.84 hours. An estimate of the fundamental period of oscillation of the Bay, based on a length of 45 km (from Kidd Point to

George Point) and a mean depth (volume/area) of 6.9 m gives 6.1 hours. A ratio of the peak transmitted energy to the peak impressed energy is called transmissibility. In an undamped system, this may be approximated by:

$$T = \frac{1}{(r^2-1)}$$

$$\text{where } r = \frac{\text{impressed motion period}}{\text{fundamental period of the Bay}}$$

The transmissibility of the Lake-Bay system is then 1.57, neglecting damping.

Platzman (1972) has shown that the fundamental mode of the free oscillation of Lake Superior has a period of 7.84 hours when computed by his resonance iteration method. He cites corroborating spectral analysis results which show a period that must lie between 7.79 and 7.89 hours. It is apparent that the tidal oscillation observed in Black Bay is driven by the fundamental mode of the free oscillation of Lake Superior, and reflects some amplification of the Lake oscillation due to the proximity of the natural periods of the Lake and the Bay.

5.3.9 Estimation of tidal flushing time

This oscillation would be expected to have significant effects on the Bay flushing time. The relevant statistics from the spectral analysis program are listed in Table 5.

The kinetic energy density represents the mean square value of current over the frequency interval f and f + Δf.

By definition (Bendat, Piersol, 1971) the rms amplitude of the along channel component of tidal current observed in the spectral analysis of the current time series is calculated from

$$\overline{v} = (G_x(f) \cdot \Delta f)^{\frac{1}{2}}$$

in Table 5, and is taken to have a cross-section averaged value of 1.45 cm s^{-1}.

This tidal oscillation then represents a prism of water volume moving up and back past the meter section.

The volume of this prism may be estimated as

$$V_p = \text{Excursion of oscillation X Section Area}$$

$$V_p = 1.45 \times 10^{-2} \times 7.84 \times 3600 \times 85000$$

$$= 3.48 \times 10^7 \ m^3$$

From the monthly mass balance for the Bay, the average river discharge for February and March is $8.63 \ m^3 \ s^{-1}$. The volume of river water entering the Bay in one tidal period is then:

$$V_R = 8.63 \times 7.84 \times 3600$$

$$= 0.024 \times 10^7 \ m^3$$

If it is assumed that these two volumes are entirely mixed in the tidal cycle, and that the oscillating prism volume is entirely exchanged by a fresh lake volume at each cycle, then this volume may be taken as a flushing flow, and an estimate of tidal flushing time made as

$$t_F = \frac{\text{Volume of Bay}}{\text{Prism Volume + River Volume}} \times \text{Tidal Period}$$

$$= \frac{343 \times 10^7}{(3.48 + 0.024) \cdot 10^7} \times \frac{7.84}{24}$$

t_F = 32 days

During May and June the average river discharge increases to 74 $m^3 s^{-1}$, giving a V_R of 0.2 x 10^7 m^3 and t_F = 30.4 days. Within the limits of this estimate, the increased volume of river flow at the freshet does not significantly affect the tidal flushing time, since the river discharge is still small with respect to the volume of the tidal prism.

It is generally not valid to assume complete mixing of the river and tidal water during each cycle for the entire estuary. In addition, unless the along shore current is sufficiently strong to traverse the mouth of the Bay in one tidal period, thereby replacing the ebb tide with fresh lake water for the next flood, then it cannot be assumed that the next flood is not returning some portion of the Bay water. Consequently, the above estimated tidal flushing time represents a minimum and will always be less than the observed flushing time.

An estimate for an exchange ratio to be applied to the tidal flood might be made on the basis of the magnitude of the along shore lake current past the Bay mouth (U_s), the width of the mouth (W), and the tidal period (T), assuming the along shore lake current fully mixes with and carries away the ebb flow from the Bay mouth.

$$r \equiv \frac{\text{Tidal Period}}{\text{Time for current to traverse Bay mouth}}$$

$$r = \frac{T \cdot U_s}{W} \equiv \frac{\text{Volume of flushing input}}{\text{Tidal Volume}} \quad (0 < r < 1)$$

Bennett (1978) shows evidence that a strong relationship exists between vertical temperature structure and horizontal water currents in the near shore zone of Lake Superior. This reference suggests that rms current speed in the epilimnion may range from 7 cm s^{-1} in late May to as high as 27 cm s^{-1} in early September. For a Bay mouth width of about 7 km, this suggests that r might vary from 0.28 to 1.0 over the late spring and summer season.

Incorporating this definition, a more realistic estimate of tidal flushing time would be:

$$t_F = \frac{V}{(r\ Vp + VR)} \cdot \frac{T}{24} \text{ days}$$

The tidal flushing time might thus vary over a range of 112 days to 32 days.

It appears that of the two mechanisms of Bay - Lake exchange evident in the data during the ice-covered period, the more significant is that of tidal flushing.

5.4 Ice-Free Period

Although the river in-flows increase by a factor of 4 times between April 17 and May 1, the monthly mass balance shows that the maximum river in-flows are still small relative to the Bay volume.

The other significant event is that the removal of the ice cover opens the whole Bay surface to the direct influx of solar and atmospheric heating as well as wind stress.

5.4.1 The thermal bar

The temperature of maximum density of water is about 4°C. In consequence, the heating of surface water between 0° and 4° results in an unstable vertical density gradient. This causes a strong vertical advection of heavier (warmer) surface water down into the water column. Stability in the water column is re-established once the whole depth reaches 4°C. Where the water column is over a sloping bottom, as in the shore zone, the inshore water will reach the stable 4°C before the offshore water which remains unstable.

This boundary between stable and unstable regions has been called the "thermal bar" and is characterized by steep horizontal temperature gradients at the surface and the confluence of 4° surface water towards it, forming a sinking thermal plume. The thermal bar

has been the subject of study in large lakes (e.g. Rogers, 1966 et seq.) inlets of lakes (Spain et al., 1976), in the laboratory (Elliott, 1971) and numerically (eg. Bennett, 1971). This thermal boundary is dynamic, moving off shore commensurate with the rate at which the volume of water below the surface is heated to 4°. Thus it tends to be shore parallel, following bottom contours, moves more swiftly over shallow bottom slopes than steep bottom slopes, and is slowed by the advection of water through it due to runoff flows (Spain et al., 1976).

A major feature of the thermal bar phenomenon is that due to the large instability and the descending plume of 4° water occurring at the bar, the assumption may be made that horizontal advection and diffusion of heat entering the water surface is not of primary importance. Thus, to a first approximation, the time taken for the bar to progress from shore to some point offshore in water depth D, is the time taken to heat the water column at that point from its initial mean value to 4° when it becomes stable. Considering a water column of mass density, ρ, specific heat, c_p, unit area, depth, D, and of initial mean temperature T, the time, t, to heat it through the temperature $\Delta T = (4-T)$ may be estimated as: (Elliott and Elliott, 1970):

$$t = \frac{\rho \cdot C_p \cdot D \cdot \Delta T}{Q_t}$$

The heat flux per unit area, Q_t, is the heat going into storage. This is the balance of major heat inflows and outflows represented by a typical heat balance as

$$Q_t = Q_s - Q_r - Q_b - Q_h - Q_e$$

where Q_s = global solar radiation

Q_r = reflected incident radiation

Q_b = long wave back radiation

Q_h = sensible heat transfer

Q_e = evaporative heat transfer

An order of magnitude estimate of this heat flux for the May period, was found to be 387.1 cal cm^{-2} d^{-1} (Appendix 4).

The sub-routine Baydat in Program BAY 2 (Appendix 5) uses the Bay soundings and initial temperatures estimated from the temperature gradient for the ice-covered period at the meter station, along with the estimated value of Q_t, to estimate the progression time of the thermal bar to each 2 km square section of the Bay. The result of this calculation indicates that the thermal bar will pass through the shallow upper Bay in about 7 to 8 days from the removal of the ice cover, and will be passing the current meter station about 20 days after removal of the ice cover, (Figure 9). This compares with the

record of the temperatures at the current meter station, which show a time interval of about 24 days from ice out to a uniformly mixed 4° temperature (Figure 4), between 1 May and 24 May.

5.4.2 Progress of the thermal regime

The estimated progress of the thermal regime in a mid-channel section of the Bay is depicted in Figure 8. The down Bay movement of the thermal bar is based on the above estimate, while isotherms depicted are based on supporting temperature data and reasonable extrapolation.

During the ice covered period, the river flow passes through the Bay generally confined as a plume to its density level, with little mixing of river and Bay water (Figure 8(a)). By 10 May (Figure 8(b)) the thermal bar has traversed the shallow upper Bay. The inflowing river water is 3 to 4°C, and hence denser than the upper Bay water. This density instability would cause the river plume to seek the bottom, and flow down the bottom slope. Relatively little mixing of Bay and river water would be expected because of the density difference. The thermal bar would not affect this river plume since at the bottom, all the water is of equal density. Once past the thermal bar, the 4°C river plume would begin to lose heat to the colder Bay water so that down Bay, it would cool and eventually reach a separation depth.

The anomalies in current and temperature patterns evident in the daily average data for 4 through 10 May may reflect the river plume at this stage.

By 24 May, (Figure 8(c)), the river temperature has risen to that of the upper Bay water. The thermal bar has progressed to the current meter section as evidenced by the daily average temperatures from the current meters. There is now a significant adverse density gradient opposing river flow across the thermal bar at the upper levels. The river in-flow must therefore mix thoroughly with the upper Bay water. Since the channel confines the volume laterally, to satisfy continuity, the river inflow must be balanced by an outflowing 4° plume at the bottom of the thermal bar. As before, once down Bay of the bar, this plume must cool and reach a separation depth, mixing with the lower Bay water.

This process of river inflow mixing with the water inshore of the thermal bar and balancing outflows of 4° water at the bottom continues as the thermal bar progresses down the Bay (Figure 8(d)). As depth increases, and the thermal bar gets closer to the mouth of the Bay, the balance of densities becomes less stable in the horizontal direction. Once the thermal bar has reached the head of Montreal Channel, the Bay volume is no longer confined laterally, and the inflowing river water may now be balanced by outflow in the upper layers, along the west side of the Bay through Middlebrun Channel. By

this point the longitudinal density gradient between the Lake and the Bay has reached sufficient magnitude that a cold wedge begins to intrude into the Kidd Point-George Point transect (Figure 8(e)). In June, it appears that this intrusion is held in balance by the river outflow, but with the decline of river flow in late June, the intrusion extends into the Bay, giving it a stable stratified form.

The preceeding discussion is supported by the observed depth averaged temperatures and conforms generally to conceptions of the two dimensional thermal bar behavior developed from various laboratory models, field observations and numerical studies. It is too simplistic to explain the current observations.

5.4.3 An along shore thermal plume

In the main channel of the Bay, the bottom slopes perpendicular to the shoreline are much steeper than the along Bay bottom slope, but the sides of the Bay cannot be treated as vertical. Since the thermal bar is also progressing out from these shores, the process must be seen as three dimensional. Because the west side of the channel is shallower than the east side, the region of stable inshore water grows more quickly on the west side. As the inshore region warms, and the vertical 4° isotherm moves away from the shore, the horizontal density gradient opposing along shore down channel flow is reduced. Initially, this region will be small and even closed at the

lake end, so that along shore flows will be small, opposed both by density gradient at the lake, and by friction against the Bay shore. As heating progresses, this region will enlarge, and extend further towards the lake and around the end of the Sibley Peninsula. As this obstruction is removed, significant along shore down channel flows in the upper level would be expected to develop, bounded on one side by the shore line, and on the other side by the cold water of the deeper Montreal Channel and the lake. This out flow would be balanced for continuity by river inflow, and by intrusion in flow from the Montreal Channel at the lower level on the east side.

Some evidence for the existence of such a shore bound surface plume is seen in the higher temperatures observed on the west side by the MBT data for 30 May, 2 and 5 June, particularly at the down Bay transect between Kidd Point and George Point.

It is evident that the strength of this plume would be higher below the Kidd Point-George Point transect, and that the current meter at the 4 m level on the west side is not well placed to display it. The development of this flow might be better measured by a meter installation in the Middlebrun Channel.

5.4.4 Estimation of surface flow due to thermal wedge

From the preceding discussion, it may be assumed that during the period of peak river flow from say 28 May to 15 June, the

structure of the lower Bay is highly stratified with an arrested density wedge flow configuration. The runoff velocities in the upper layers are large. There is a significant density gradient between the warm down channel flow and the cold lake intrusion. The cold intrusion forms an up Bay wedge, which is tilted down towards the west side.

In this situation, with a large run off flow, criticial velocity may be approached, in which case an abrupt change in section, e.g. the narrow between Kidd Point and George Point, may act as a control on the net circulation volume. The configuration is analogous to flow over a sill where the intrusion of the cold wedge in the restricted channel creates a minimum depth for the surface flow, with $dH/dx = 0$, and thus becomes a control in the channel.

It may be shown that, assuming inviscid fluid,

$$F_1^2 + F_2^2 - 1 = 0$$

at such a control where

$$F^2 = \frac{Q^2}{\Delta\rho/\rho_o \cdot b^2 \cdot h^3 \cdot g} \qquad \equiv \text{internal Froude Number}$$

Q = discharge ($m^3 s^{-1}$)

$\Delta\rho/\rho_o$ = density gradient (dimensionless)

b = channel width (m)

h = channel depth (m)

g = acceleration of gravity $m \cdot sec^2$

1 = subscript for surface flow

2 = subscript for intrusion flow

If the intrusion wedge is arrested, then $Q_2 = 0$. By continuity, Q_1 is the net outflow from the Bay.

Then

$$F_1^2 = \frac{Q_1^2}{\Delta\rho/\rho_o \cdot b_1^2 h_1^3 g} = 1$$

Now

$$Q_1 = u_1 \cdot b_1 \cdot h_1$$

This assumption of rectangular channel section is justified since $b_1 \gg h_1$.

Therefore,

$$U_1^2 = \frac{\Delta\rho}{\rho_0} \cdot g \cdot h_1$$

Around 5 June the west side surface plume temperature at the Kidd Point-George Point transect is about 10°, the cold lower Bay water is about 6°, giving $\Delta\rho/\rho_0$ of 2.4×10^{-4}. The depth of the warm plume is about 6 m and g is 9.8 m s^{-2}. This suggests that the mean velocity of the warm surface plume would be about 12 cm $\cdot s^{-1}$.

5.4.5 Interpretation of PVD

Numerical studies of thermally driven lake currents during the thermal bar predict the development of shore parallel currents balancing cross stream density gradient against friction (Bennett, 1971). Such currents would be re-enforced in Black Bay by the river discharge at the head of the Bay and the density gradient between the Lake and the Bay. Thus a longitudinal circulation may be expected during the heating period of the Bay, with down channel flows at the upper levels on the west side, and up channel flows at the lower levels on the east side. This generally conforms to the evidence of the current data as reflected in the spectra of kinetic energy density. The interpretation of the PVD's of daily average currents is complicated by the occurrence of significant (daily average

15 km h^{-1}), wind episodes which were all down Bay, from 10 to 14 May, 20 May and 6 June. The development of a strong down Bay flush on the west side after the 28 May, when the thermal bar should have progressed below the Kidd Point-George Point transect, is evident, with up Bay flows on the east side.

6. A PRELIMINARY CLIMATOLOGY OF BLACK BAY

6.1 Meteorologic Background

When the daily or monthly mean values from the support data cited in Table 1, are viewed on a common time scale, (Figure 13) a general perspective of the background conditions influencing the climatology of Black Bay emerges as a representative annual cycle.

The hours of bright sunshine rise from February to April, are steady through May and June, and rise again to the highest annual level in July. The main factor, obviously, is the increasing declination of the sun with the advancing solar year. Variation in cloud cover in March, May, June and September modulate this basic pattern.

Correlated with this increase of energy input, the mean monthly air temperature rises steadily from February to May at approximately 8.1°C per month, then continues to rise at a lower rate of 3°C per month through June, reaching the annual maximum in July. Thawing degree days begin to occur at the end of March and, by 20 April, 19 thawing degree days have accumulated. These are accompanied by maximum daily temperatures from 0 to 9°C, leading to the break up of the Bay ice cover around 30 April. Similarly, in the fall, freezing degree days begin around 10 November, although below freezing daily minimum temperatures occur through much of October. It

is likely that the ice cover is established over much of the Bay by 1 December.

Mean values of thermograph records 1971 to 1975 for the Black Sturgeon and Wolf Rivers indicate the river water temperatures follow a similar cycle. It is of interest to note that this mean temperature reaches 4°C, the temperature of maximum density, in mid-May, while the temperature of the Bay water at the current meter section is still at less than 2°C.

6.2 River Flows and Lake Level

The total river discharge starts in January at 20 $m^3 s^{-1}$, but declines through mid-March to a low of about 6 $m^3 s^{-1}$. Under the influence of the rising temperatures in the spring, snow stored in the winter months December through April begins to appear as river discharge in late April. Ice leaves the Wolf River on 21 April and the Black Sturgeon on 29 April. This winter storage makes the first peak in the river hydrograph around 1 May. Thereafter, monthly average discharges for May through July correlated closely to the product of monthly average precipitation and drainage basin area for the same period, indicating that little precipitation is stored as ground water. The winter storage peak coincides with the breakup of the Bay ice cover. Precipitation discharge continues at a high level, reaching a second peak of 102 $m^3 s^{-1}$ on 3 June at the stream meter

stations. The river hydrographs are well correlated in time at each metering station. The time lag between the river metering station and the current meter station in the Bay has not been estimated. The Black Sturgeon station is about 15 km further from the Bay than the Wolf. Also, the Black Sturgeon runs into the Bay through a marshy channel, while the Wolf is over more solid terrain. It is not expected the lag would exceed a day or so, however.

Daily average Lake Superior water levels at Thunder Bay show a steady decline from January through April of about 20 cm and then a steady increase of about 5 cm/month through to the end of July.

6.3 Current Regime

The mean residence time of Bay Volume/Monthly Inflow varies widely, as shown in the Monthly Mass Balance summarized in Table 4, but it averages 47.1 months from January to August, with a minimum of 17.8 months in June.

The progressive vector diagrams of daily average currents recorded in the main channel of the Bay show two distinct regimes corresponding to the ice covered and ice free periods. The spectral analysis of the current meter records reinforce this distinction and also identify a psuedo-tide at a period of 7.8 hours, corresponding to the fundamental mode of oscillation of Lake Superior.

From early February through April, corresponding to the ice-covered period, there is a consistent pattern of current at the 18 m level, suggesting geostrophic flow. This pattern is thought to reflect an exchange flow with the Lake. During this period, however, it was found that the tidal oscillation probably is the more effective flushing mechanism. This is, in fact, probably an important flushing component year round.

This stable pattern is significantly altered in May and June, reflecting the removal of the ice cover and the increased hydrodynamic activity driven by solar and atmospheric heat input, increasing river discharge, and wind. The spectral analysis of current meter records reflect an increase of as much as 20 times in kinetic energy density over that during the ice-covered period. The tidal component is unaltered, however, suggesting that it is mainly independent of local meteorological conditions. Of the changing meteorological factors, the most significant appears to be the heat input.

6.4 Annual Temperature Structure

A general profile of the water temperature over the year in the region of the current meter station has been obtained by averaging observations from the current meters and bathythermograph profiles, (Figure 11). Isotherms reasonably substantiated by data are shown as solid lines. Dotted extrapolations are considered reasonable estimates.

The major features shown are a stable stratified cold water regime from January through April, the ice-covered period, followed by a rapid temperature rise in May. The occurrence of a single vertical 4° isotherm on 24 May, preceded by a bottom plume of 3° which peaked on 10 May, suggests the progression of a thermal bar past the meter station, with some modification by river flow at this time. This is also indicated by an approximate heat balance over the Bay, assuming the whole Bay surface to be free of ice from 1 May (Figure 9).

Following this passage of the thermal bar, and coincident with the passage of the river freshet, there is a period of rapid temperature rise throughout the full depth of the Bay section. During this period of Bay heating, a significant longnitudinal density gradient is set up between the Bay and the Lake, which appears to be held in dynamic check initially by the river outflow. As this declines in late June, an upwelling of cold lake water appears in the bottom of the channel (Figure 12).

It is expected that this cold intrusion would remain through August to October, giving the Bay a stratified form, since river flows are small and of warmer temperature, thus over-riding the intrusion. As the air temperature falls in October, surface heat loss would exceed gains, and the water temperature would fall until once more it becomes uniformly 4°C in mid-November. It is expected the ice cover would be established once more by early December.

6.5 Winds

The frequency of wind episodes where the daily average wind exceeds 15 km/hr is highest in late March and April. The wind tends to lie up-Bay through January to March, and down-Bay from April through July. There appears to be little general correlation between wind events and the temperature pattern, except in mid-May, where down-Bay winds may be a contributing factor to the general rapid thermal changes in the water column.

6.6 Summary and Conclusion

In summary, this brief review of the support data shows Black Bay to be a complex personality responding to the four major inputs of thermal energy from the atmosphere and direct solar radiation, kinetic energy from river discharge, tidal energy from Lake Superior, and kinetic energy from the wind.

An estuary has been defined as a partially enclosed body of water which receives an inflow of fresh water from land drainage and which has a free connection to the open sea. The water within the estuary consists of a mixture of fresh and saline water in proportions which vary from place to place.

Black Bay is estuary-like in that it is an enclosed body, it receives inflow of fresh water from land drainage, and it has a free connection to the open lake. It is not estuary-like in that the lake is not saline, nor is it tidal in the conventional sense.

It has been found that for a period in the spring, the heating of the Bay generates a sufficient longnitudinal density gradient to force estuarine-like longnitudinal circulations. It has also been found that the Bay responds to the fundamental mode of oscillation of Lake Superior with a tide-like seiche. It seems reasonable, therefore, that further insights into the processes involved in Black Bay may be gained by application of the analytical techniques of estuary hydraulics. In addition, it has been found that the thermal bar phenomenon may be expected to have a large influence on the mixing of river and Bay waters and in the establishment of flushing current flows in the late spring prior to stratification.

7. THE BLACK BAY HERRING FISHERY

7.1 Economic Importance

The herring fishery in Black Bay (principally with trawls during the spawning season) contributed over 50% of the total catch from Ontario waters in 1960 to 1974. They are used as fresh, frozen or smoked fish, depending on the fatness of the flesh, which is usually of excellent flavour. The eggs from females are also valuable in the production of domestic caviar. To protect the stocks, the Province of Ontario imposed an annual catch quota of 680,380 kg, which has been enforced since 1973 (Selgeby et al., 1978).

7.2 Life Cycle of Lake Herring

Lake herring (Coregonus artedii, Leseur) are pelagic and feed largely on plankton (Dyer and Beil, 1964). Maturity is attained at 3 to 4 years, and old age at 6 or 7 years. Lake Superior herring reach 300 to 330 mm in length when fully developed.

The lake herring usually forms large schools in mid waters, but depth varies with season and temperature. In Lake Superior it shows an all season range of 13 to 53 m. In general, there is a movement in spring and early summer from shallow to deep water when the lake herring moves below the thermocline. It remains in the cooler

deep water until late summer, rising to just below the thermocline. As the upper waters cool, it moves again into shallow water (Scott and Crossman, 1973).

Spawning takes place sometime between mid-November and mid-December. Spawning occurs at temperatures around 4 to 5°C, and reaches a peak in water temperatures of 3.3°C. However, it will occur even if the temperature does not drop to these levels.

In the Great Lakes, spawning may occur in shallow water or at greater depths, and pelagically in mid water (9 to 12 m) over bottoms as much as 60 m deep. Males always move into the spawning grounds a few days earlier than the females and may leave before they do or may remain a few days after they have left. Spawning may occur over any type of bottom, but often over gravel or stoney substrate (Scott and Crossman, 1973).

The eggs are deposited on the bottom and abandoned by the parents. Colby and Brooke (1970) concluded that the incubation period was 236 days at a temperature of 0.5°C, and 106 days at 5°C. The optimum temperature under experimental conditions was found to be 5.6°C at which 92 days were required for hatching. Berlin et al. (1977) observed an incubation period for coregonus clupeaformis (lake whitefish) of 104 to 146 days with 50% hatch on the 135th day when the eggs were incubated under temperatures varying from 4.4° to 1.1° to

6.8°C in simulation of typical shallow inshore waters of Lake Michigan. John and Hasler (1956) showed that young larval herring begin to feed before the yolk sac has been absorbed and that at the time of hatching they could survive 20 days of starvation and possibly a few days longer at lower temperatures. Scott and Crossman (1973) suggest that it is unlikely that hatching occurs under the ice in southern parts of Canada.

Larval herring require light to feed. John and Hasler (1956) report from experimental evidence that they will feed from the day they hatch, and that dead zooplankton (Cyclops) are eaten at first. Other evidence from Lake Ontario (Pritchard, 1930) indicates that feeding commences when about 10 days old, from food consisting of algae, copepods, and cladocera.

7.3 Temperature Preference

Most fishes are known to display a marked temperature preference. Crawshaw (1977) provides a review of the physiological and behavioral reactions of fishes to temperature change. The wide range of metabolic response to temperature change has led to the idea that the temperatures selected by fishes very likely represent temperatures at which they have evolved to carry out physiological functions with maximal efficiency. Although fishes display the ability to adjust internal conditions to different thermal environments, once a fish has

been at a particular temperature for a period of time, even rather small temperature changes lead to major shifts in metabolism. This helps to explain the survival value of behavorial temperature preference. As well, temperature serves as a proximate factor (cue, guidepost, sign stimulus or directive factor) affecting locomotor responses of fishes (Reynolds, 1977). In conjunction with nonthermal factors, this may explain the ultimate adaptive or ecological value of a temperature response, such as a migration.

In a compilation of temperature preference data for a number of species (Coutant, 1977), Coregonus artedii is listed from two sources as having a final preferendum of 10°C and 7.2°C in the large sizes. Mantelman (1958) sites work on coregonus albula "to clarify the question whether the larvae of the cisco exhibit thermal adaptation. The experiments showed that larvae whose embryonic development took place in lake water at 1 to 5° usually selected areas with a temperature of 1 to 7° in a temperature gradient. Other specimens which had been incubated in tap water at 8 to 9° usually remain in regions of higher temperature, namely 5 to 10°"(p. 31).

7.4 Black Bay as a Hatchery

The annual temperature regime in Black Bay (Figure 11) appears ideally suited to the needs of the Lake Herring. During mid and late November, the bottom water is at the preferred spawning

temperature of 3 to 5°C. Eggs laid below the 10 m depth will be incubating at a temperature between 1 and 2°C. The ice cover will be established by early December sealing the hatchery from rapid environmental changes. The tide like oscillation provides a slow but continuous exchange of Bay water with the Lake.

The incubation period is a function of water temperature to some degree so that the hatch time may vary, taking longer in colder late springs or shorter in warmer early springs. With an incubation period of 140 to 150 days, the hatch would be centered approximately from 20 to 30 April. This corresponds to the period that the ice cover on the Bay breaks up and is removed. The eggs were laid in the intruding lake water in the fall, but through the winter, the river plume sinks to the bottom, so that as the hatch occurs the larvae are exposed to the river water, which may be richer in mineral and nutrients than the lake water. A serious corollary to this is that if the river discharge is contaminated with a toxic for even a short time during the spring runoff and high precipitation period, the hatch could be seriously threatened (e.g. Smith and Oseid, 1974).

The herring hatch may be visualized as the steady release of a tracer material from the bottom of the Bay for a one or two week period around the end of April after the ice breaks up. Requiring light to feed, the larvae would tend to rise towards the surface.

Although they may be expected to show a preference for some temperature between 1 and 7°C, until the passage of the thermal bar, the vertical temperature gradient is small and would not be expected to influence the vertical distribution of the larvae.

7.5 Factors Influencing Hatch Migration

During May, it has been estimated that the tidal flushing time might be about 100 days. It has also been shown that the thermal bar will traverse the shallower upper third of the Bay within 9 or 10 days of ice breakup and then pass below Kidd Point-George Point within 25 days. The thermal bar may be conceived as a warm frontal system, representing a significant horizontal thermal gradient moving like a closing, narrowing net out from the shore and down the Bay. Assuming the larvae exhibit a temperature preference for less than 7°C, as has been reported, then it would be expected that the hatch would tend to congregate in the gradient adjacent to the thermal bar. The movement of the bar down Bay, in conjunction with the tidal flushing exchange would be a major influence in directing the migration of the hatch. It is possible that their food supply, being cold water species of algea and cladocera would also move with the bar (Stoemer, 1968) and provide further direction to the migration. In the later stages of the migration, as the bar passes the Kidd Point-George Point transect by the end of May, thermal conditions tend to develop a strong flushing current down the Middlebrun Channel, giving the hatch a final push into the lake.

If this were the case, it would be expected that by late May, the larvae population would be concentrated in the lower half of the Bay on the west side and by the second week in June would be gone almost entirely. This migration would be essentially over by late June and early July, as the river flow decreases and the Lake again intrudes into the lower levels of the Bay, almost as if in preparation for the next spawning season.

7.6 Comparison to Field Observations

The synoptic survey of larvae population conducted from May to July 1974 and reported by Selgeby et al. (1978) provides substantiation of this scenario. Sampling was reported to have started within a few days after the ice had melted. Samplings were taken on May 25 to 26 and 30, June 9, 12, 13, 19, 25, and 26, and July 6, 7 and 11. The water temperatures observed on May 25 to 30 were 3.1 to 4.5°C. This survey showed that herring larvae were wide spread over much of the lower two thirds of the Bay. Catches were largest along a band extending from the west shore below Squaw Bay, diagonally across and up the Bay to the east shore above Copper Point (Figure 13). The correspondence of this distribution to depths in Bay bathymetry is notable in its reflection of the progression of the thermal bar over this period, and the expected later development of a strong down Bay current along the lower western shore.

Density (larvae/1000 m^3) at index stations, approximately at mid channel opposite the Pearl River, were 1719 +/-400 on May 25 to 26, 810 +/-166 on May 30, 0 at the index stations after May 30 and 0 at any location after June 6. Vertical distribution was similar at dawn and dusk, with densities highest at the surface, lower at 10 m and much lower at 20 to 40 m. It was observed that the occurance of a strong north easterly wind and rough seas between May 31 and June 5 significantly reduced the catches in both the upper and lower sections of the Bay. This may have re-enforced the thermally generated down Bay current on the western shore.

7.7 Conclusion

It must be concluded that the physics of Black Bay and the biology of the Lake Herring form an intricately matched system, and that more detailed study of the Bay's behaviour is warranted to ensure the protection of this productive fishery.

Further analysis of the current meter data should be undertaken to quantify turbulent diffusion coefficients for time scales between the tidal period of 7.8 hours and 24 hours. More detailed analytical modelling of the ice free period would perhaps improve the understanding of the main flushing event due to longitudinal density gradient. More detailed temperature measurements using Fixed Temperature Profile thermistor cables during the ice covered period would provide better information about the extent of mixing of River

and Bay water, and better define the river induced circulation under the ice cover. Current meters placed at the Kidd Point-George Point transect, and in the Middlebrun Channel would give further information on the main flushing event.

REFERENCES

Bendat, J.S. and Piersol, A.G. (1971). Random Data:Analysis and Measurement Procedures, Wiley (Interscience), New York.

Bennet, E.B., 1978. Characteristics of the thermal regime of Lake Superior, J. Great Lakes Res. December 1978. IAGLR 4 (3-4):310-319.

Bennett, J.R., 1971. Thermally driven lake currents during the spring and fall transition periods, Proc. 14th Conf. Great Lakes Res. 1971. 535-544, IAGLR.

Berlin, W.H., L.T. Brooke and L.J. Stone, 1977. Verification of a model for predicting the effect of inconstant temperature on embryonic development of lake whitefish (Coregonus clupeaformis), U.S. Fish and Wildlife Service Report No. 92, Washington, D.C., 1977.

Boyce, F.M., 1978. Internal correspondence and data files for Black Bay project, National Water Research Institute, Burlington, Canada.

Canadian Hydrographic Service, 1977. Chart 2313, Black Bay, Lake Superior.

Chiocchio, F. and M. Kerman, Preliminary analysis of Black Bay current meter records, CCIW Data Files, 1978.

Colby, P.J. and L.T. Brooke, 1970. Survival and development of lake herring (Coregonus artedii) eggs at various incubation temperatures. p. 417-428. In C.C. Lindley and C.S. Woods (eds.) Biology of coregonid fishes. Univ. Manitoba Press, Winnipeg, Man. 560 pp.

Coutant, C.C. 1977. Compilation of temperature preference data. J. Fish. Res. Board. Can. 34:739-745.

Crawshaw, L.I., 1977. Physiological and behavioral reactions of fishes to temperature change. J. Fish. Res. Board Can. 34:730-734.

Danek, L.J. and J.H. Saylor, 1977. Measurements of the summer currents in Saginaw Bay, Michigan. J. Great Lakes Res. October 1977, Internat. Assoc. Great Lakes. Res. 3(1-2) 65-71.

Dyer, W.R. and J. Beil, 1964. Life history of lake herring in Lake Superior, U.S. Fish and Wildlife Service, Fishery Bulletin, 63(3):493-530.

Elliott, G.H. and J.A. Elliott, 1970. Laboratory studies on the thermal bar, Proc. 13th Conf. Great Lakes Res. 1970: 413-418, IAGLR.

Elliott, G.H., 1971. A mathematical model of the thermal bar, Proc. 14th Conf. Great Lakes Res. 1971:545-554. IAGLR.

Energy, Mines and Resources Canada, Surveys and Mapping Branch, National Topographic System, Sheet 52A (1977), Thunder Bay, Edition 2.

Fischer, H.B., E. John List, R.C.Y. Koh, J. Imberger, and N.H. Brooks, 1979. Mixing in inland and coastal waters, Academic Press, 1979.

Hamblin, P.F. and E.C. Carmack, 1978. River-induced currents in a fjord lake, J. Geophy. Res. Vol. 83, No. C2. February 1978:885-902.

John, K. and A.D. Hasler, 1956. Observations on some factors affecting the hatching of eggs and the survival of young shallow water cisco (Leuchichthys atedii, Leseur) in Lake Mendota, Wisconsin. Limnol. Oceanogr. 1(3):176-194.

MacCallum, W.R., 1976. Letter to Dr. J. Kelso, Environment Canada outlining the puzzle of rapid dispersal of herring fry in Black Bay, November 30, 1976.

Mantelman, I.I., 1960. Distribution of the young of certain species of fish in temperature gradients, Translation Series, No. 257, Fish Res. Board Can.

Phillips, D.W., 1978. Environmental Climatology of Lake Superior, J. Great Lakes Res. December 1978. IAGLR 4(3-4):288-309.

Platzman, G.W., 1972. Two dimensional free oscillations in natural basins, J. Phys. Oceanography, Vol. 2 No. 2, April 1972; 117-138.

Pritchard, A.L., 1930. Spawning habits and fry of the cisco (Leuchichthys artedii) in Lake Ontario. Biological Board of Canada, Contributions, Canadian Biology and Fisheries, N.S., Vol. 6 (1930), No. 9:227-240.

Reynolds, W.W., 1977. Temperature as a proximate factor in orientation behavior. J. Fish. Res. Board Can. 34:734-739.

Robertson, D.G., 1973. Cruise data, M.V. Karlsen, 1964 to 1973, Canada Centre for Inland Waters, Unpublished Data, File S 73 + Heat, Lake Superior, Zone 4.

Rodgers, G.K., 1966. The thermal bar in Lake Ontario, Spring 1965 and Winter 1965 to 1966, Pub. No. 15, Great Lakes Research Division, The University of Michigan, 1966.

Sato, G.K., 1969. Prediction of the Time of Disappearance of the Thermal Bar in Lake Ontario, A Master's Thesis, University of Toronto, 1969.

Schertzer, W.M., 1978. Energy budget and monthly evaporation estimates for Lake Superior, 1973. J. Great Lakes Res. December 1978, IAGLR 4(3-4):320-330.

Scott, W.B. and E.J. Crossman, 1973. Freshwater fishes of Canada, Fisheries Research Board of Canada, Bulletin 184, Ottawa, Canada.

Selgeby, J.H., W.R. MacCallum and D.V. Swedburg, 1978. Predation by rainbow smelt (Osmerus mordax) on lake herring (Coregonus artedii) in western Lake Superior. J. Fish. Res. Board Can. 35:1457-1463.

Smith Jr., L.L. and D.M. Oseid, 1974. Effect of hydrogen sulphide on development and survival of eight freshwater fish species. In Blaxten (Ed.). The early life history of fish, Springer-Verlag, 1974.

Spain, J.D., G.M. Wernert and D.W. Hubbard, 1976. The Structure of the spring thermal bar in Lake Superior. J. Great Lakes Res. December 1976, IAGLR 2(2):296-306.

Stoermer, E.F., 1968. Nearshore phytoplankton populations in the Grand Haven, Michigan vicinity during thermal bar conditions. Proc. 11th Conf. Great Lakes Res. 1968:137-150. Internat. Assoc. Great Lakes Res.

Water Survey of Canada, 1976. Water Temperatures of selected streams in Ontario, Water Survey of Canada, WRB/IWD/Ontario Region, Guelph, 1976.

LIST OF FIGURES

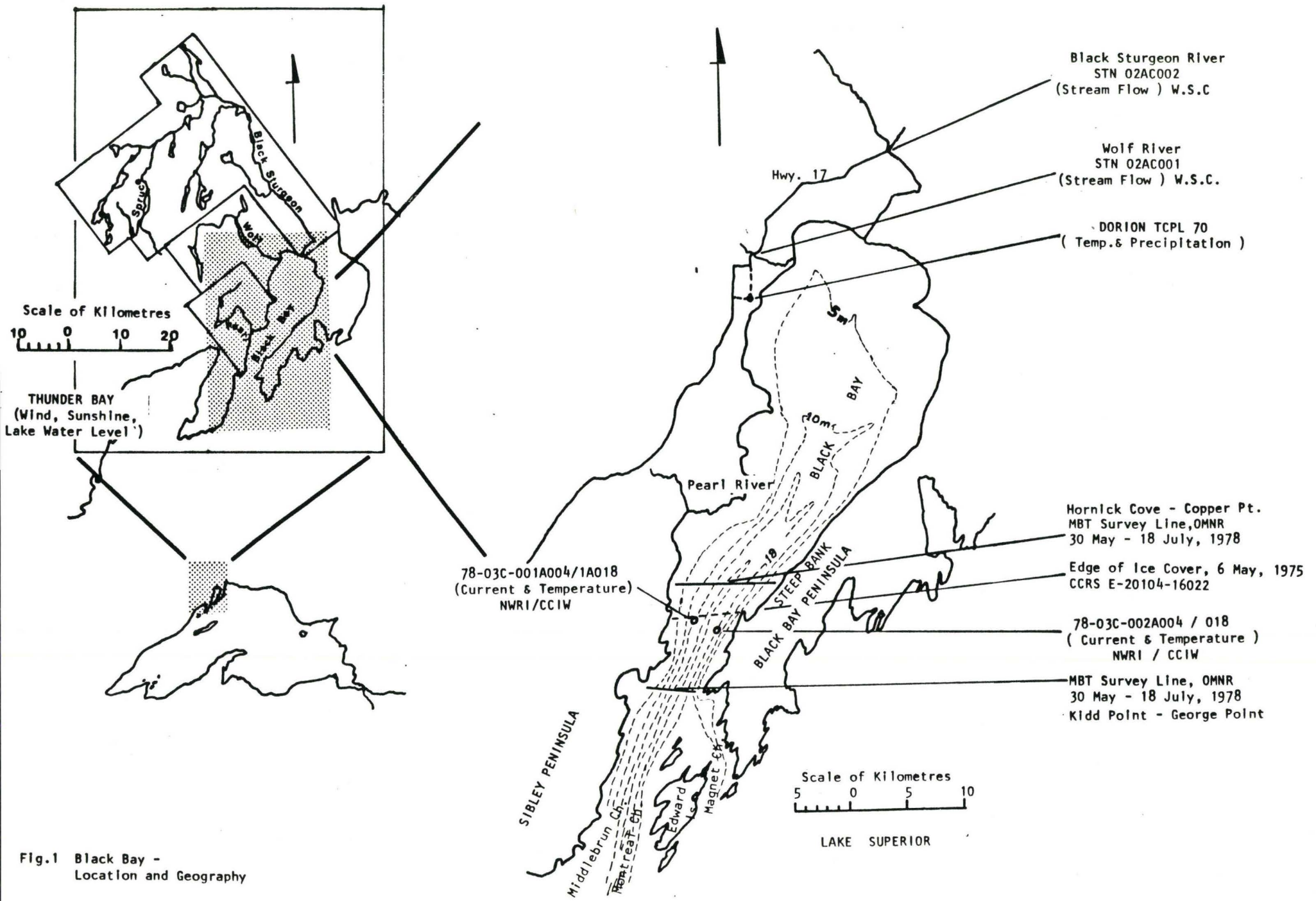

Fig.1 Black Bay -
Location and Geography

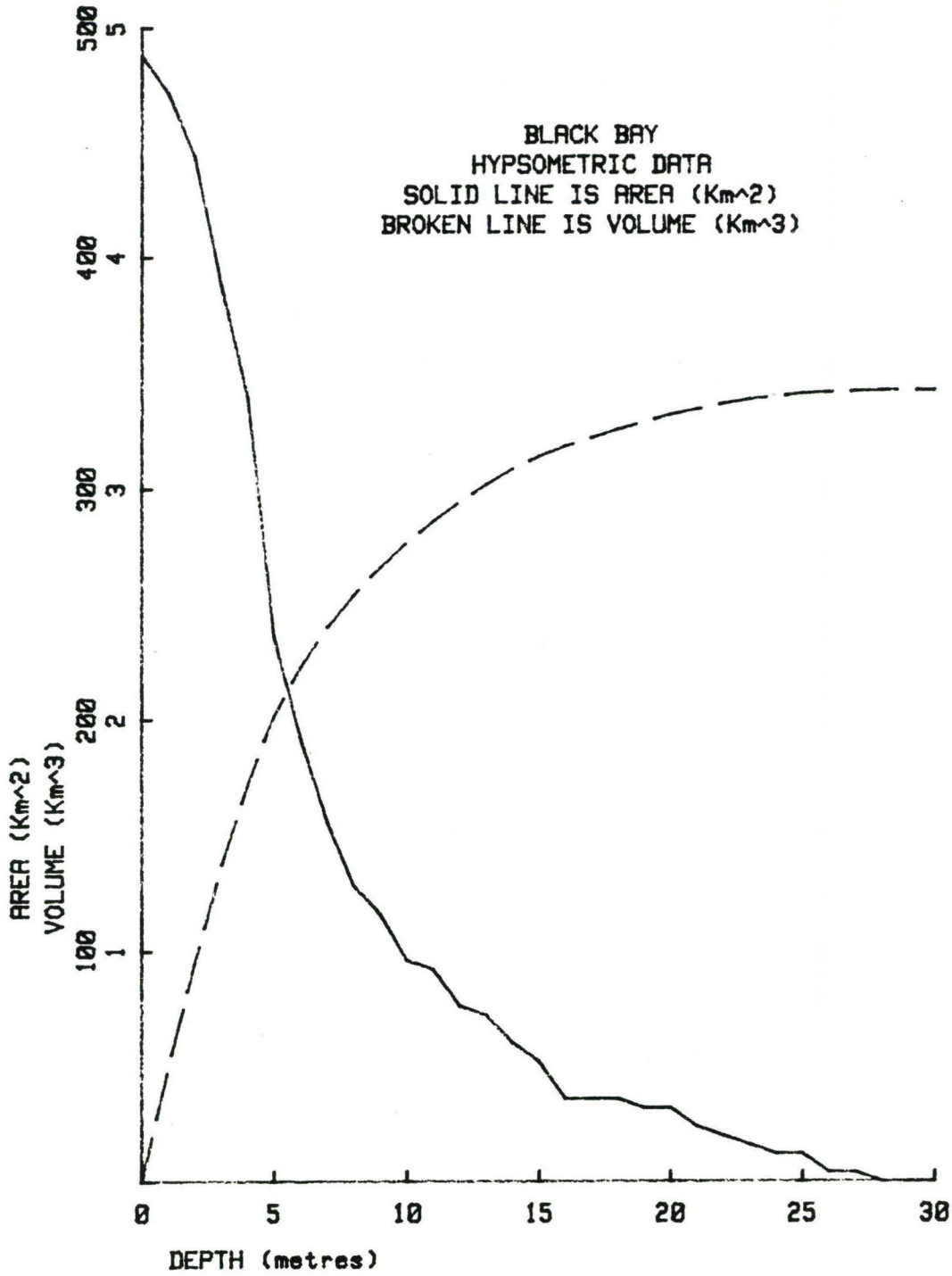

Fig. 2 Black Bay -
Hypsometric Data Plot

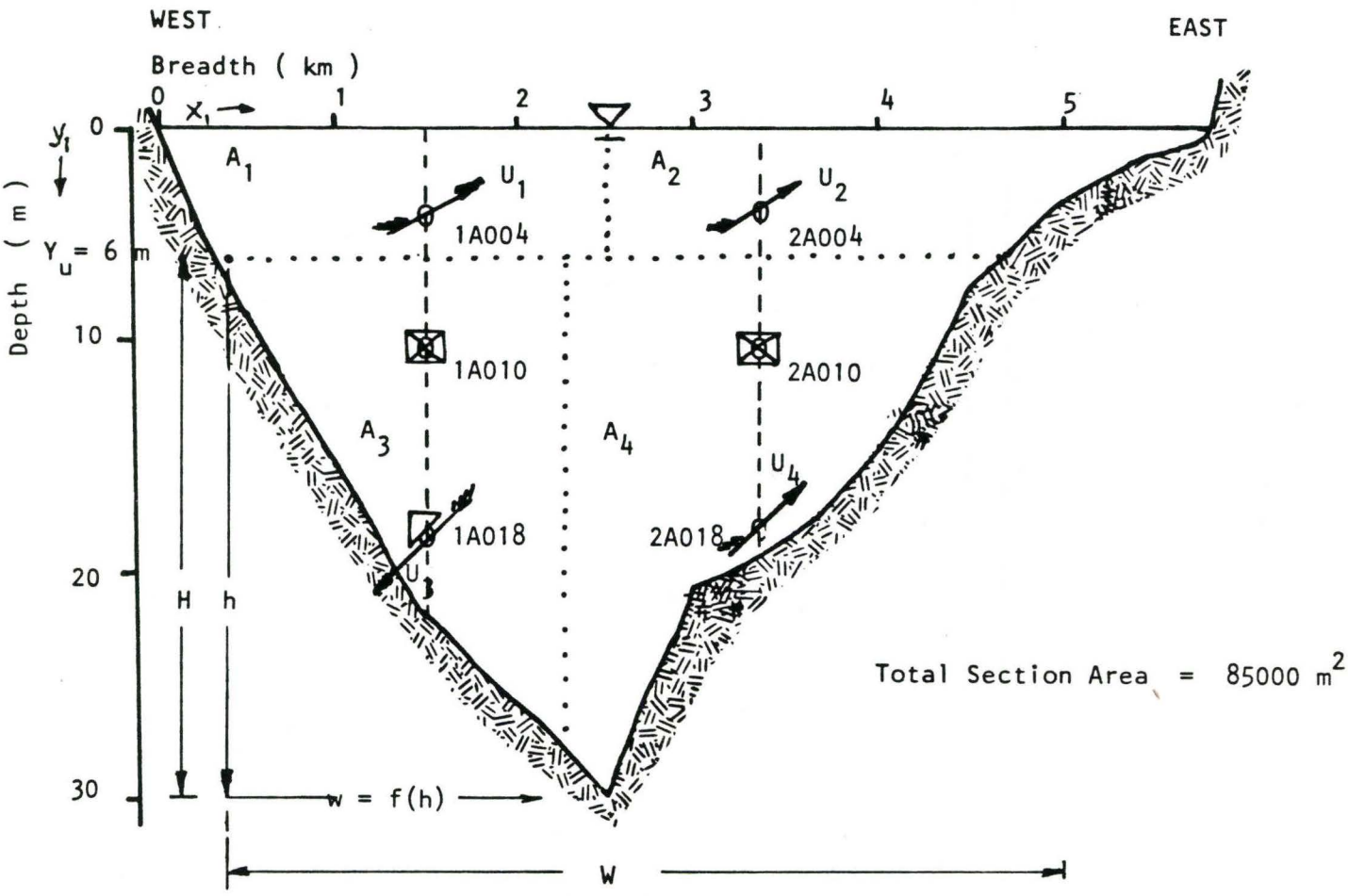

Fig. 3 Black Bay -
Current Meter Section

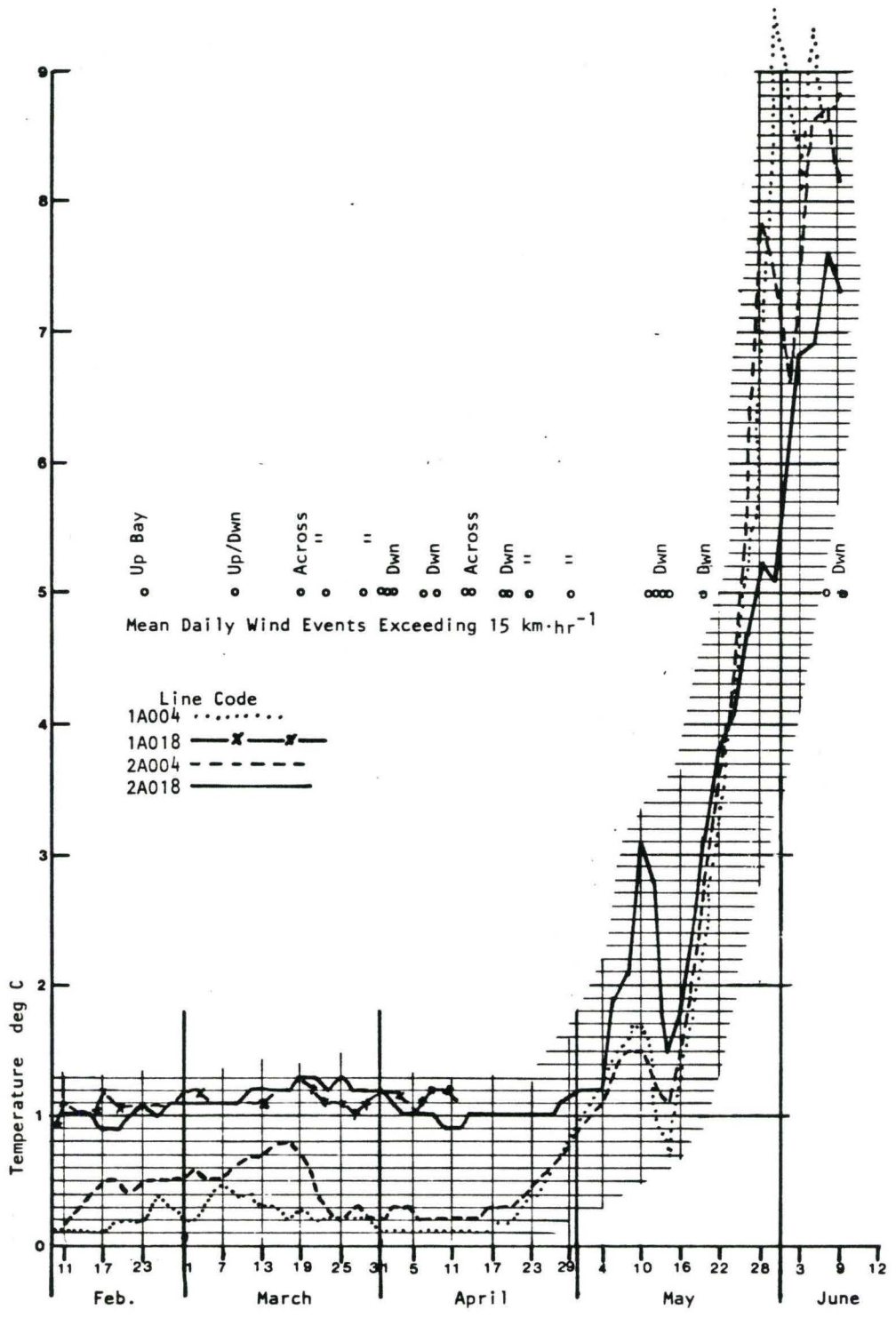

Fig. 4 Black Bay -
Daily Average Temperature
at the Current Meters

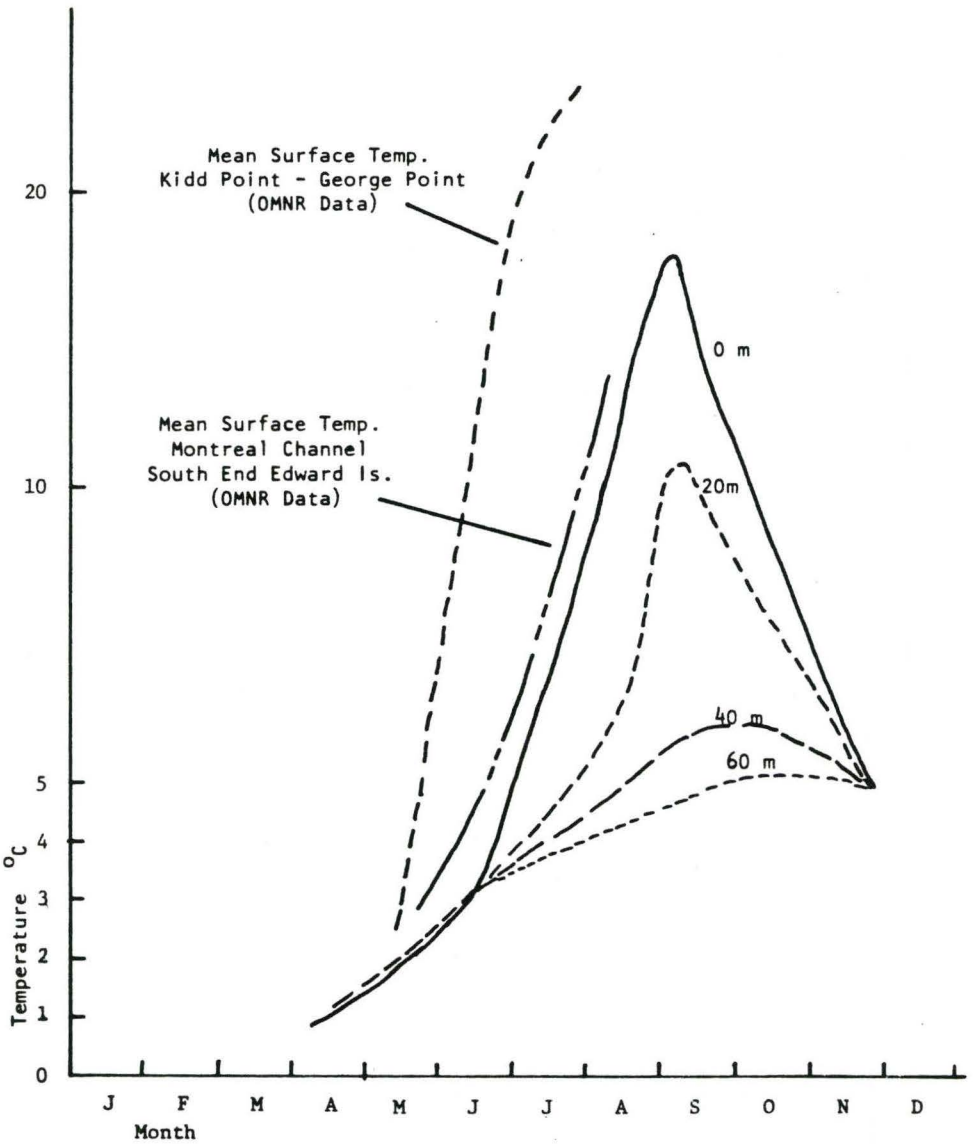

Fig.5 Black Bay -
Lake Superior, Zone 4,
Historical Temperature Data

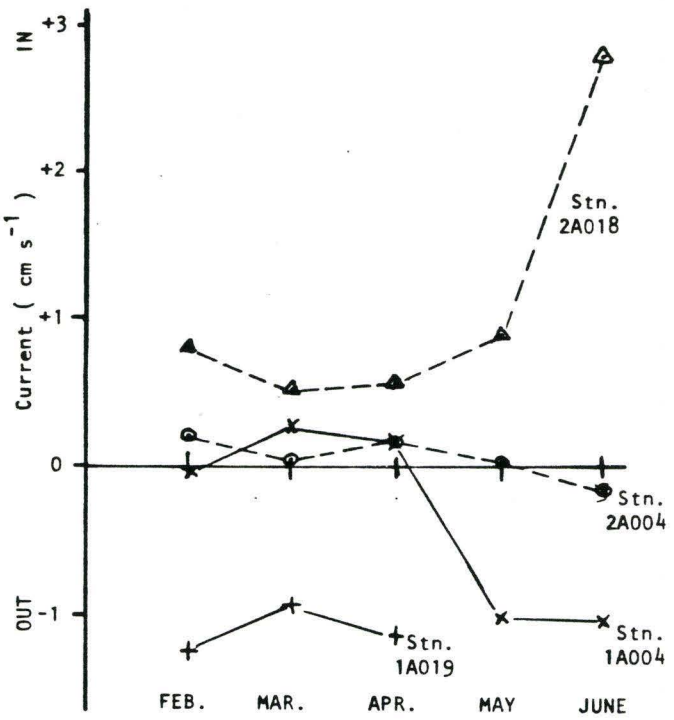

Fig. 6 Black Bay -
Monthly Average Along Bay Current

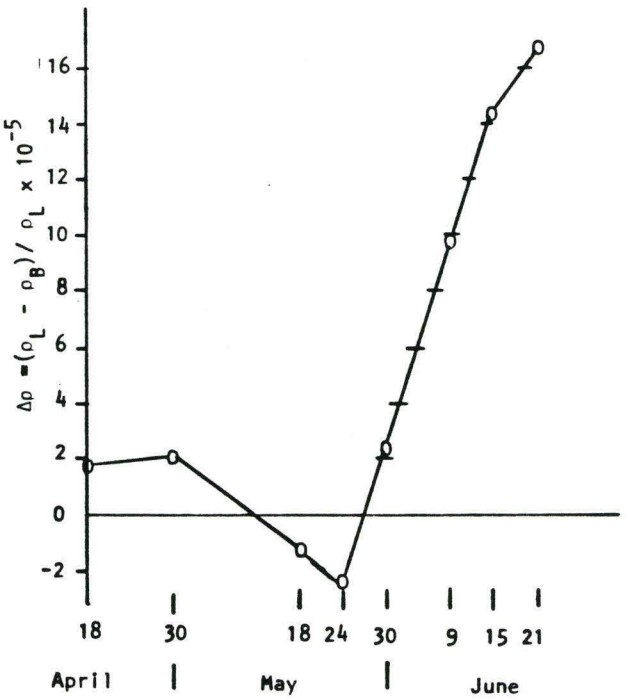

Fig. 7 Black Bay -
Density Anomaly between Lake Superior
(at 40 m depth) and the Bay .

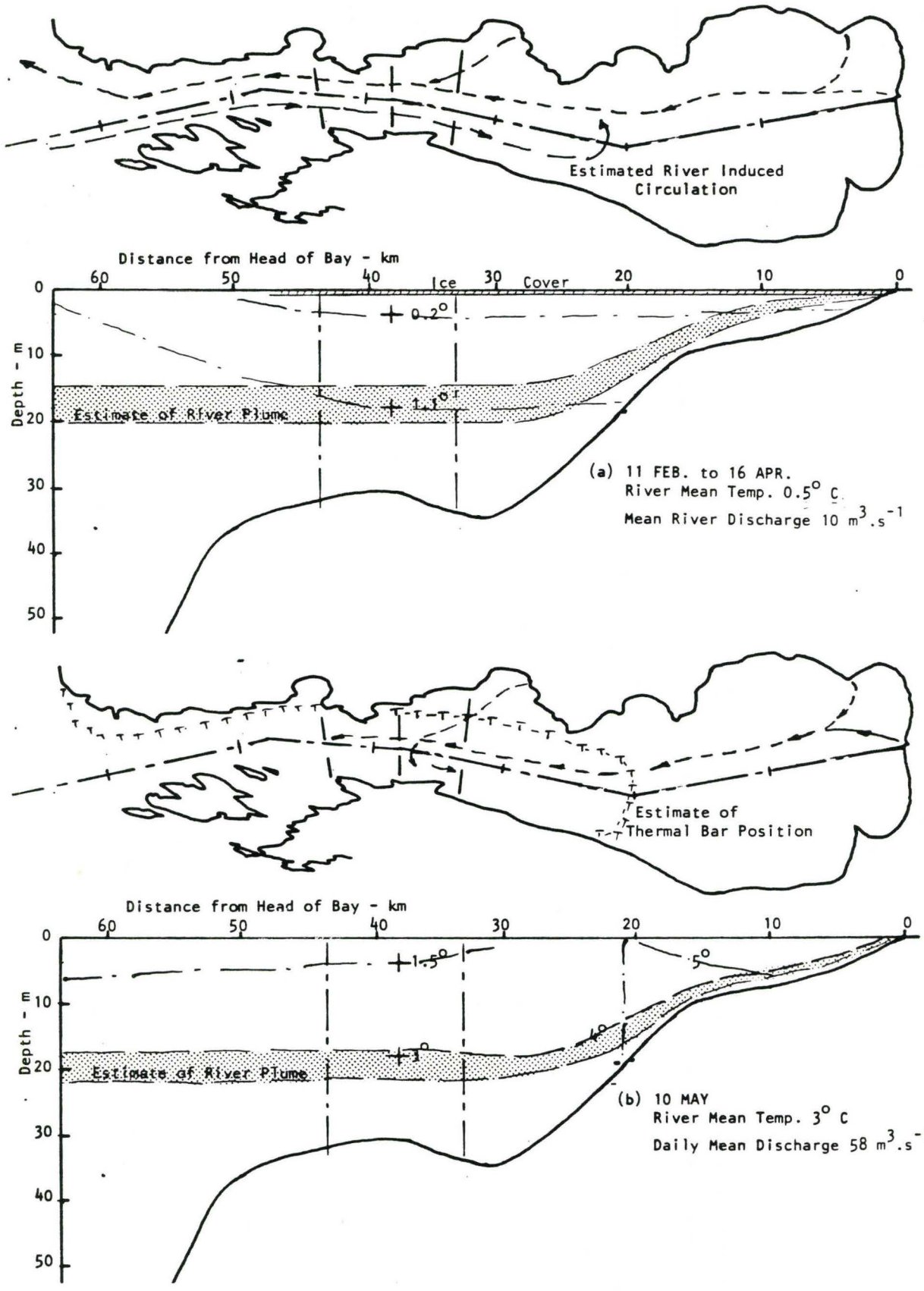

Fig. 8/1 Black Bay -
Development of the Thermal Regime

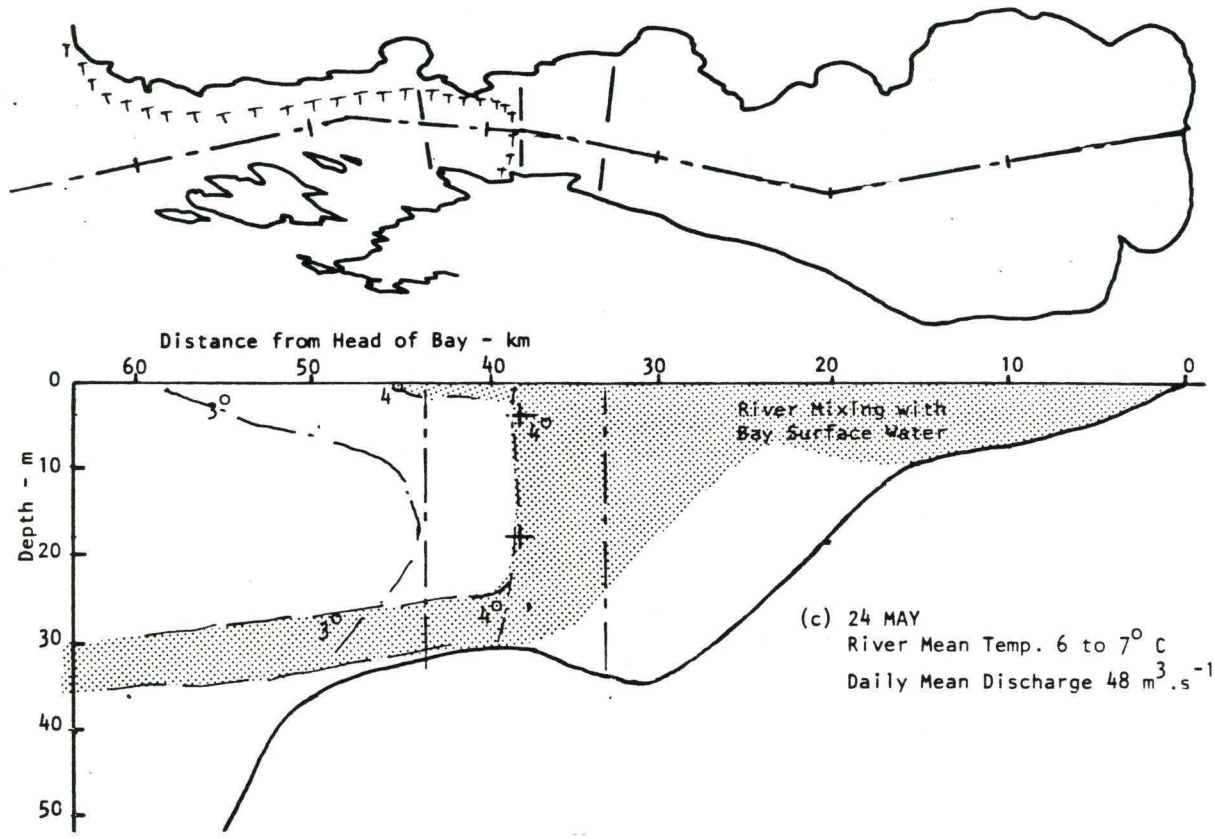

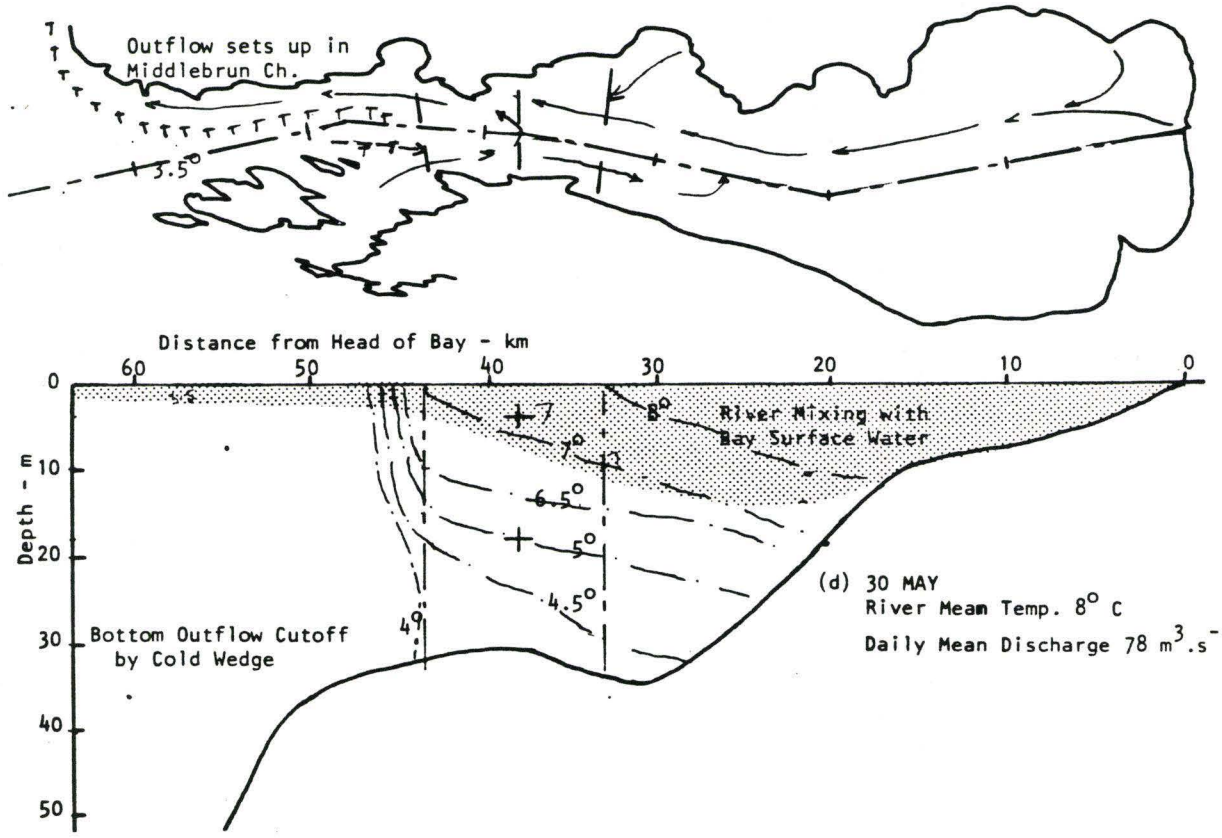

Fig. 8/2 Black Bay -
Development of the Thermal Regime

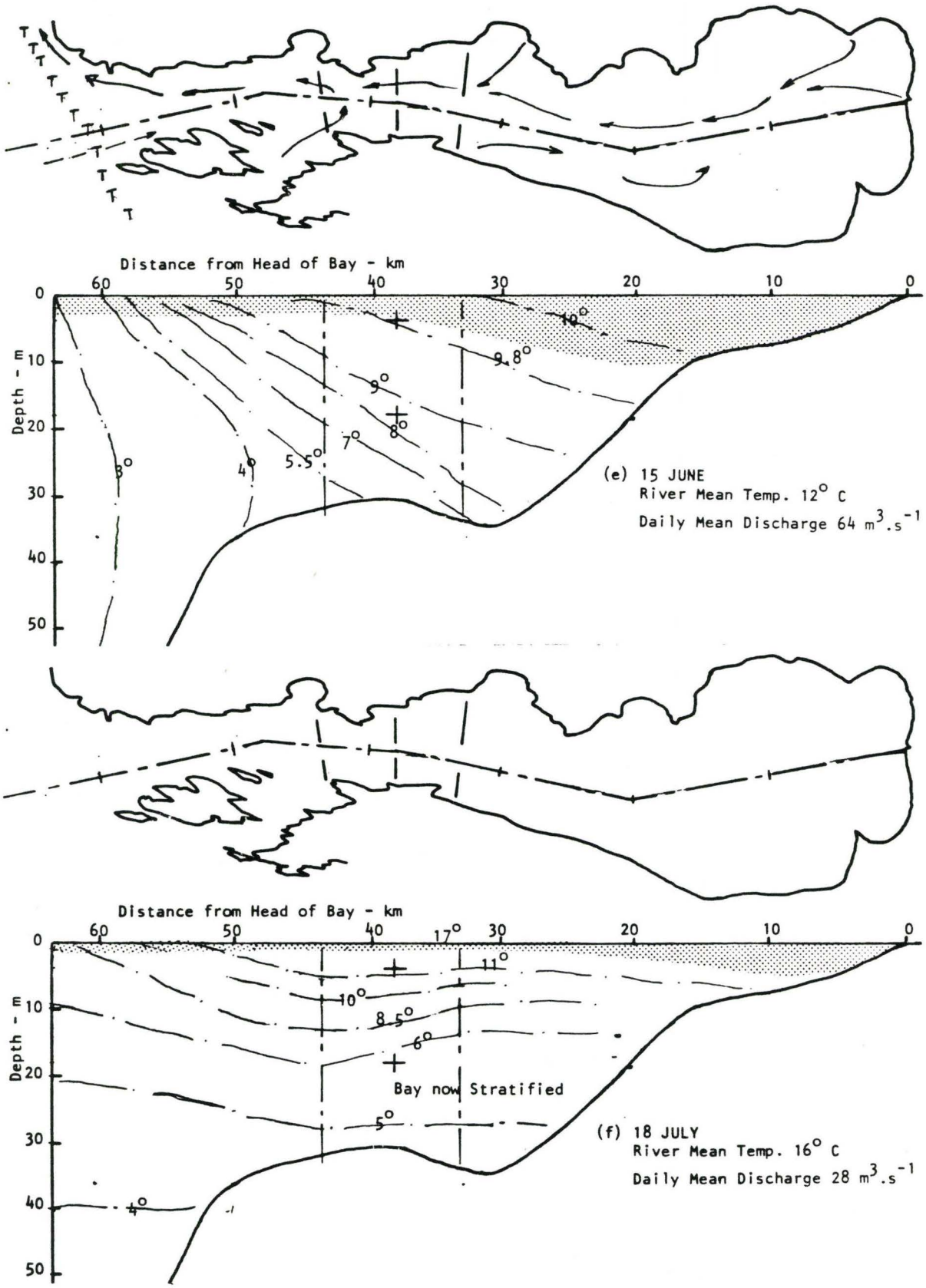

Fig. 8/3 Black Bay -
Development of the Thermal Regime

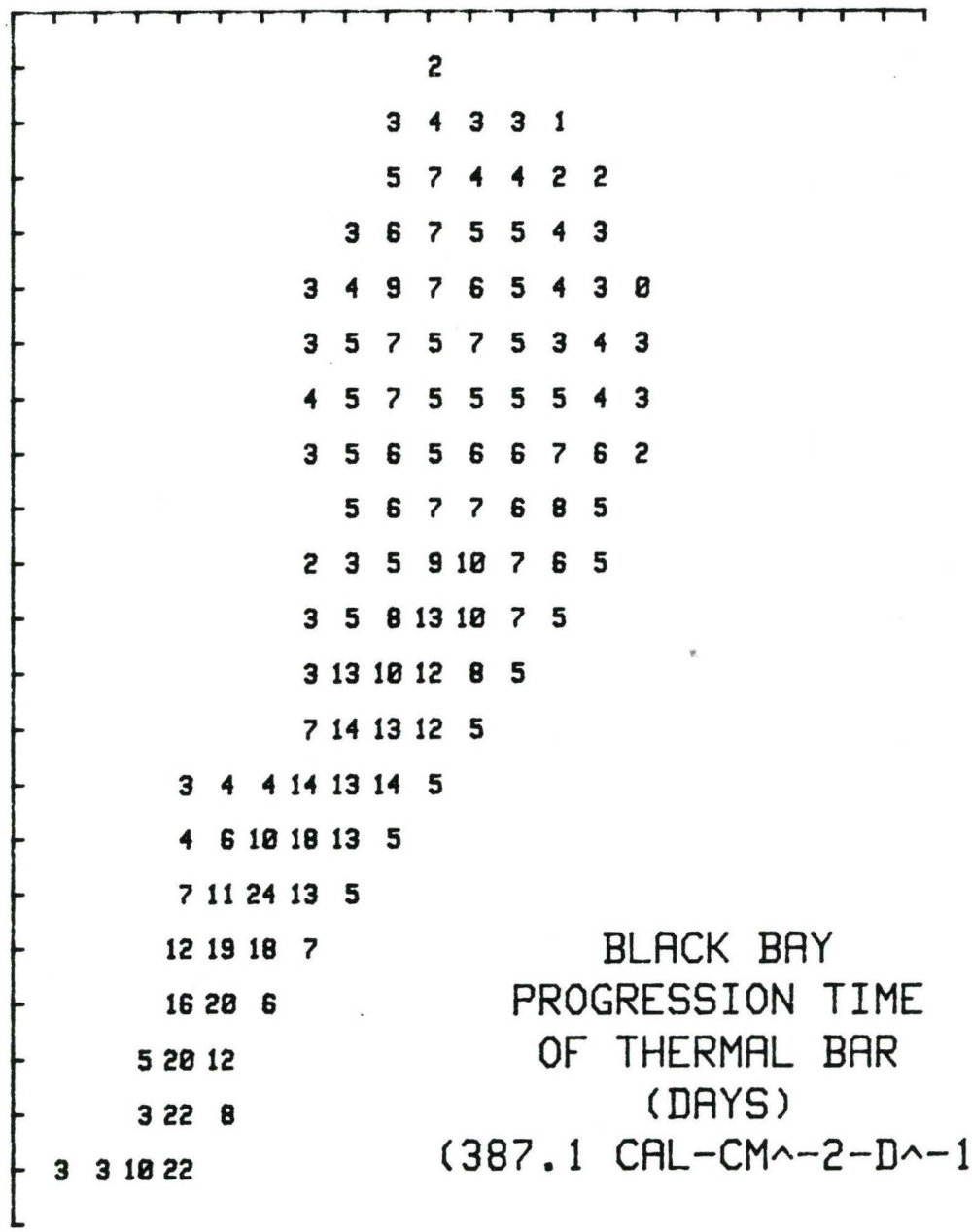

Fig. 9 Black Bay -
Progression of the Thermal Bar

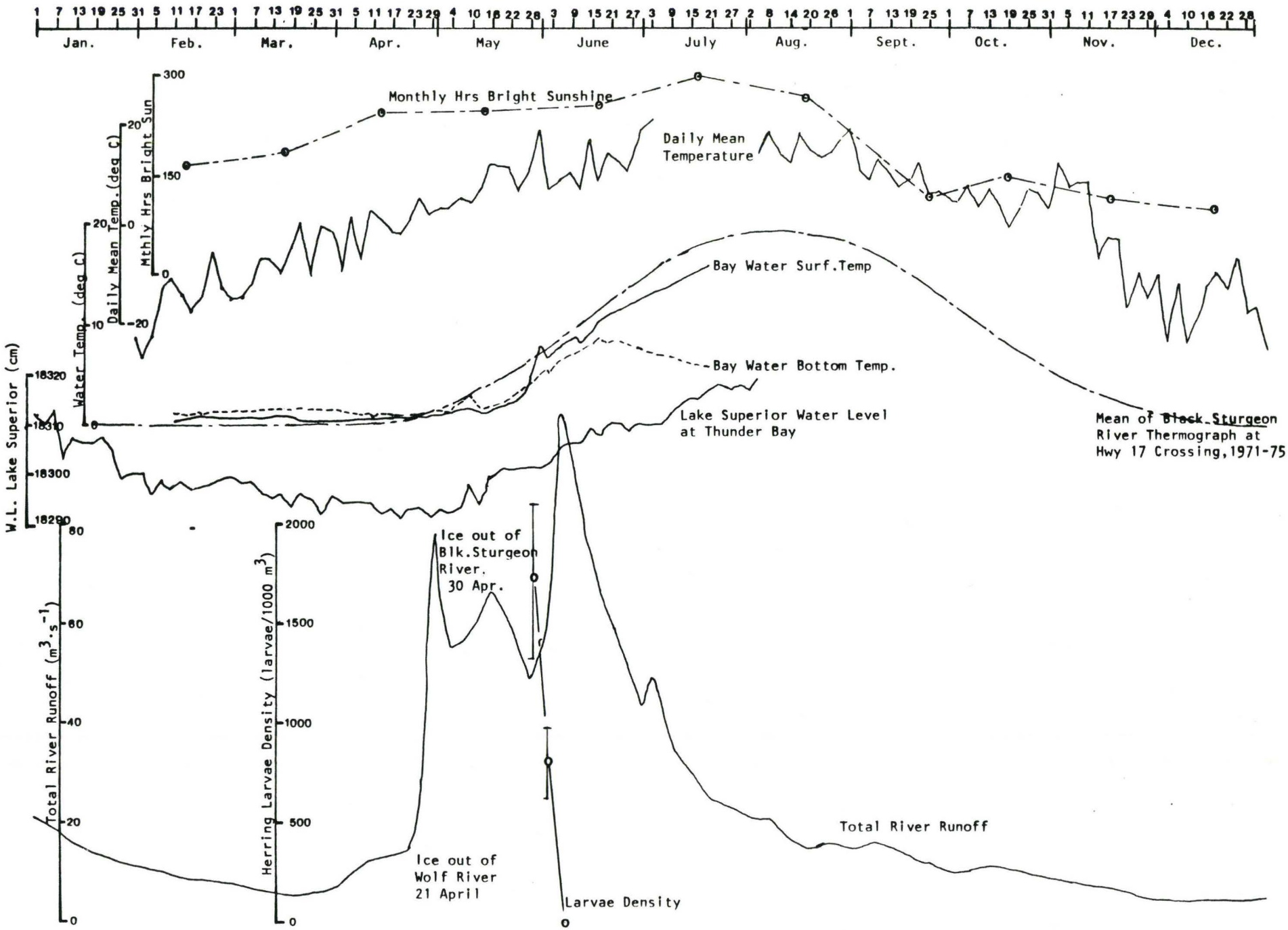

Fig. 10 Black Bay -
Climatological Data Over the Year

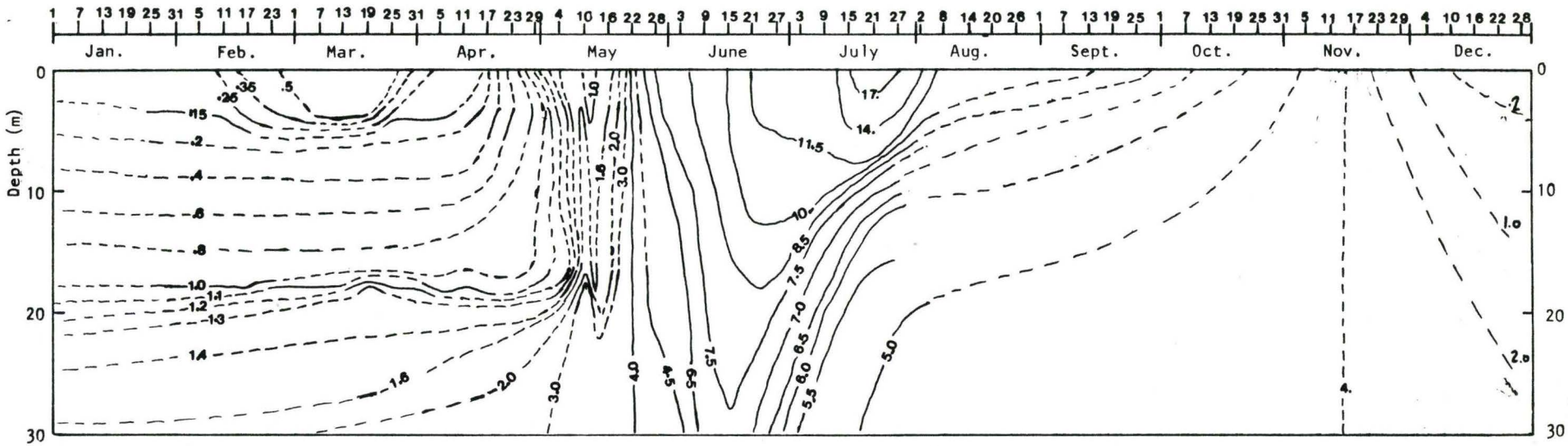

Fig. 11 Black Bay -
Annual Profile of Water Temperature
at the Current Metering Section.

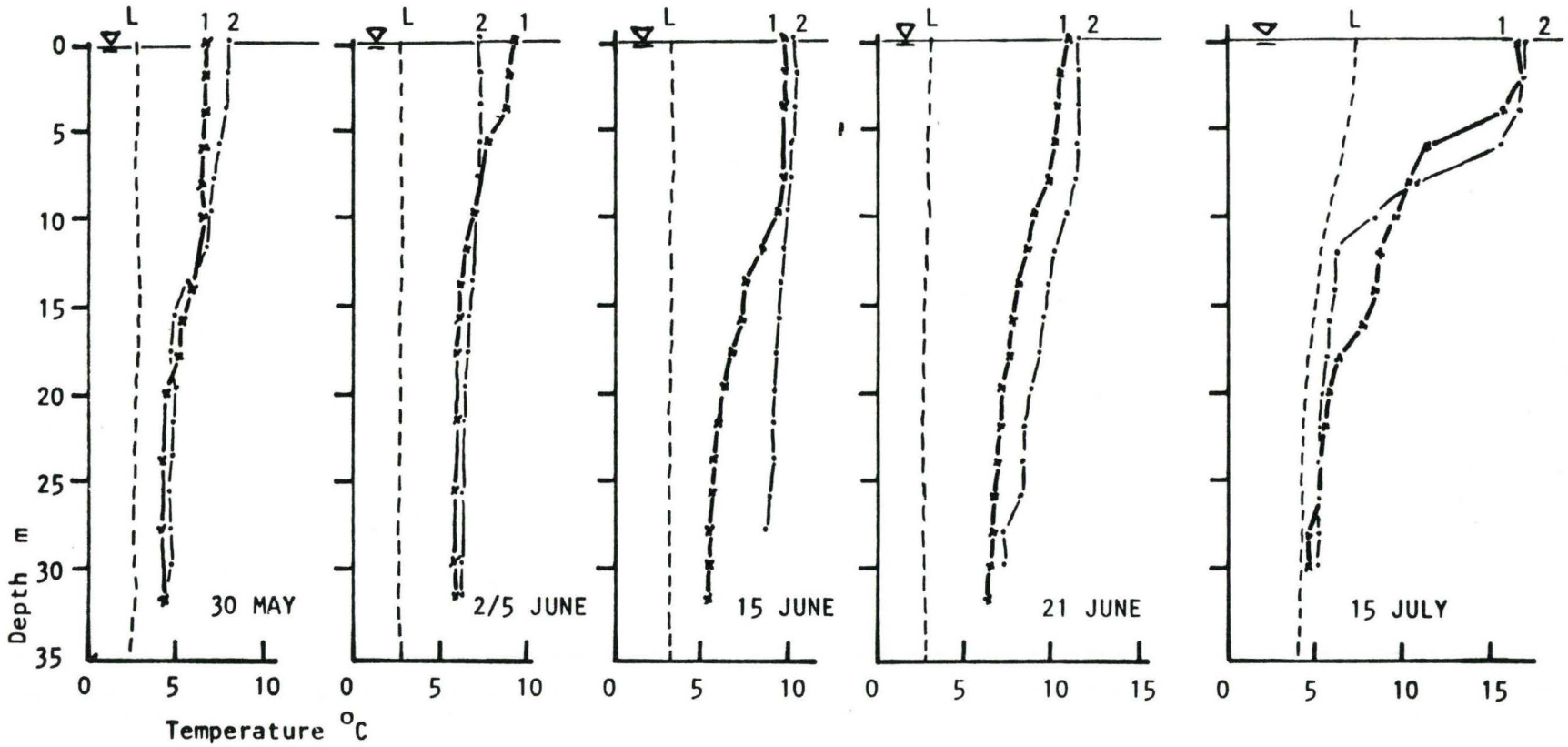

Code:
L Lake - From Fig. 6 Data
1 Kidd Pt. - George Pt. Transect - From OMNR MBT Survey, Centre Channel
2 Hornick Cove - Copper Pt. Transect - From OMNR MBT Survey, Centre Channel

Fig.12 Black Bay -
Temperature Profiles Showing Lake
Intrusion, and Early Summer Stratification
in the Mid-Channel Section

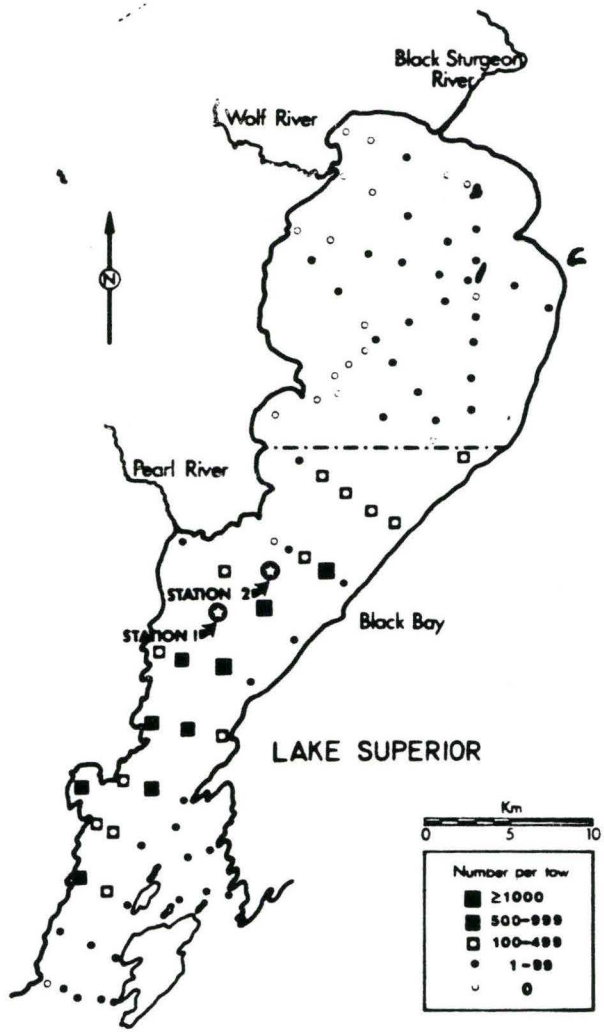

FIG. 2. Horizontal distribution of lake herring larvae in Black Bay May 27–June 5, 1974. SELGEBY ET AL.

Fig. 13 Black Bay -
Larvae Catch Sample Distribution
(Selgeby, 1978)

LIST OF TABLES

Table 1. Support Data Sources, Black Bay Study

Parameter	Type of Data	Meter Location	Period	Source
Stream Discharge Black Sturgeon River	Daily Average	Stn. 02AC001 - Hwy. 17 crossing	Jan 1 - Dec 31 1978	Water Survey of Canada
Steam Discharge Wolf River	Daily Average	Stn. 02AC002 - Hwy. 17 crossing	Jan 1 - Dec 31 1978	Water Survey of Canada
Air Temperature Precipitation	Daily min., max., Average	Dorion TCPL 70, Hwy. 17, 3.5 km South of Wolf River Crossing	Jan 1 - Dec 31 1978	Monthly Record Eastern Canada Volume 63,1978 Environment Canada
Sunshine	Hours/month	Thunder Bay Airport	Jan 1 - Dec 31 1978	Monthly Record Volume 63,1978
Wind Speed, Direction	Hourly Average	Thunder Bay Airport	Jan 1 - Dec 31 1978	Canadian Climate Centre Atmospheric Environment
Lake Superior Water Level	Hourly Average Daily Average	Thunder Bay Stn. 2/4824/08913	Jan - July 1978	MEDS, Tidal Data Section Hydrographic Survey of Canada

Table 2. Summary of Current Meter/Temperatures Data Return
See Figure 3 for Meter Location

Meter	Location/Depth	Record Period (Local Time)
1A004	West, 4 m	78/02/1900 to 78/06/09/
1A010	West, 10 m	Nil
1A018	West, 18 m	78/02/10/1900 to 78/04/12/
2A004	East, 4 m	78/02/10/1900 to 78/06/09/
2A010	East, 10 m	Nil
2A019	East, 19 m	78/02/10/1900 to 78/06/09/

Table 3. Summary of OMNR Temperature Survey, MBT Slides

Date	MBT Slide No.	Location (Ref. Figure 1)	Surface Bucket Taken
?	1, 2		
28/05/80	3 through 6	Line 1*	
	7, 8	Line 2**	7, 8
78/06/02	9 through 12	Line 1	10, 12
	13, 14	Line 2	
	15	(Mid Channel CM sect)	
78/06/05	16 through 18	Line 1	16, 17, 18
	19 through 24	Line 2	22, 23, 24
78/06/06	25 through 31	Line 1	
78/06/15	32 through 37	Line 1	33, 34, 36, 37
	38 through 44	Line 2	38, 39, 42, 43 44
78/06/21	45 through 51	Line 1	45 through 49, 51
	52 through 57	Line 2	52, 53, 54
78/07/18	58 through 63	Line 1	59, 60, 61, 63
	64 through 69	Line 2	64 through 69

* Line 1 runs from Hornick Cove to Copper Point
** Line 2 runs from Kidd Point to George Point

Monthly Mass Balance - Black Bay 1978

Bay Dimension: Area = 48×10^7 m^2 Volume = 340×10^7 m^3 Outflow Section 82,000 m^3
Outflow = River Inflow + Precipitation Inflow - Change in Storage (-Decrease; +Increase)
*April outflow includes snow storage January, February and March

	JAN	FEB	MAR	APR	MAY	JUNE	JULY	AUG
River Inflow (10^7 m^3)								
Black Sturgeon	3.558	2.127	1.725	3.973	10.744	14.270	6.572	3.952
Wolf	0.577	0.113	0.21	2.05	5.60	3.026	0.915	0.589
Pearl (Estimate)	0.353	0.069	0.129	1.255	3.427	1.852	0.560	0.360
1. Total (10^7 m^3)	4.488	2.309	2.064	7.278	19.821	19.148	8.147	4.901
River Flow (m^3/s)	16.76	9.54	7.71	28.08	74.0	73.87	30.42	18.30
Precipitation Inflow								
Precipitation (m)	0.017	0.004	0.046	0.018	0.065	0.048	0.070	0.057
2. X Bay Area (10^7 m^3)	0.82(s) →	0.19(s) →	2.21(s) →	0.86 ↓	3.12	2.30	3.36	2.74
Change in WL (m)	-0.12	-0.05	-0.03	+0.02	+0.11	+0.05	+0.08	+0.05
3. X Bay Area (10^7 m^3)	-5.76	-2.40	-1.44	0.96	5.28	2.40	3.84	2.40
Outflow (10^7 m^3) (1 + 2 - 3)	10.25	4.71	3.50	12.32*	17.66	19.05	7.67	5.24
Bay Vol/Outflow (months)	33.2	72.2	97.1	27.6	19.3	17.8	44.3	64.9
Discharge Rate (m^3/s)	38.27	19.47	13.07	47.53	65.93	73.50	28.64	19.56
Section Average Current (cm/s)	0.047	0.24	0.016	0.058	0.080	0.090	0.035	0.24
Monthly Average Current (cm/s)								
1A004		0.06	-0.23	-0.18	1.02	1.05		
1A018		1.26	0.97	1.17	--	--		
2A004		-0.20	-0.03	-0.17	-0.02	0.22		
2A018		-0.80	-0.51	-0.56	-0.86	-2.77		
Section Average		0.80	0.50	0.065				

Table 5. Kinetic Energy Density - Along Channel Component

Station	Δf (hr^{-1})	Period (hr)	Total K.E. Density $(cm/s)^2$/c.p.h.	rms Amplitude cm/s
1 A004	0.0025	7.84	0.754×10^3	±1.37
1 A018	0.0025	7.84	0.897×10^3	±1.50
2 A004	0.0025	7.84	0.847×10^3	±1.46
2 A018	0.0025	7.84	0.865×10^3	±1.47
			Mean	1.45

LIST OF APPENDICES

APPENDIX 1

Progressive Vector Diagrams of Daily Average Current

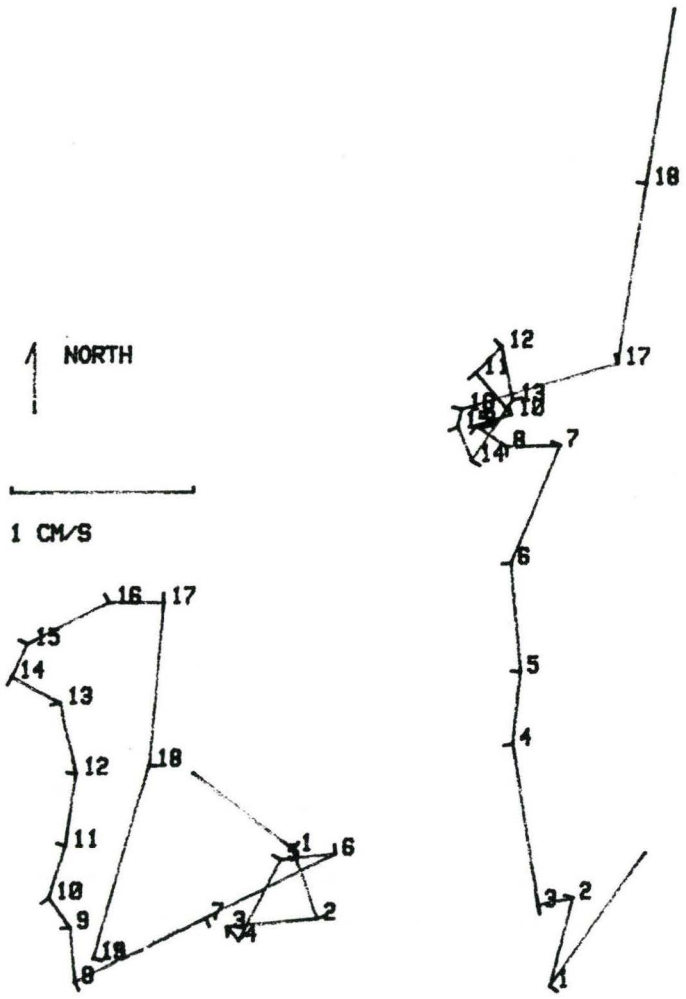

P.V.D. OF CURRENTS,STA. 1 AND 2 ;4M; FEB'78

Left is Station 1 (West Side).
Right is Station 2 (East Side).

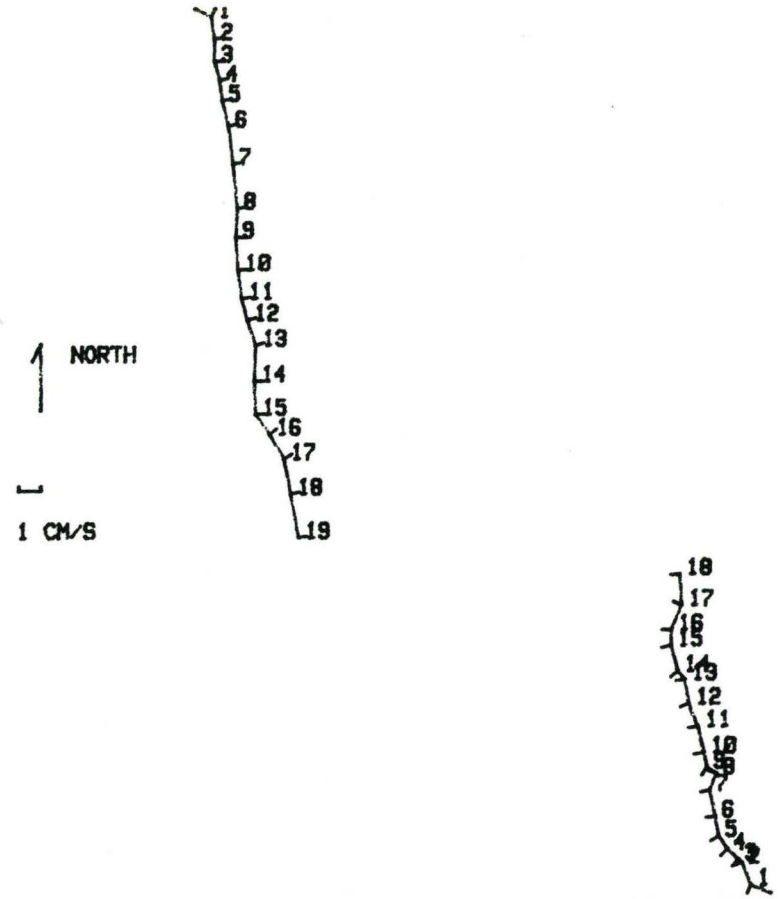

P.V.D. OF CURRENTS,STA. 1 AND 2 ;18M; FEB'78

Left is Station 1 (West Side).
Right is Station 2 (East Side).

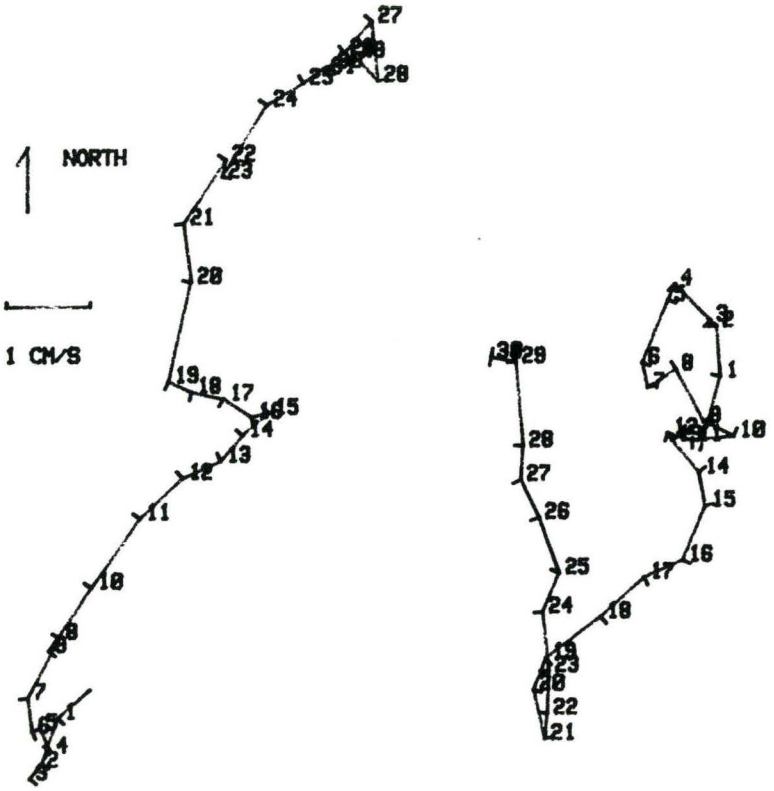

P.V.D. OF CURRENTS,STA. 1 AND 2 ;4M ; MAR'78

Left is Station 1 (West Side).
Right is Station 2 (East Side).

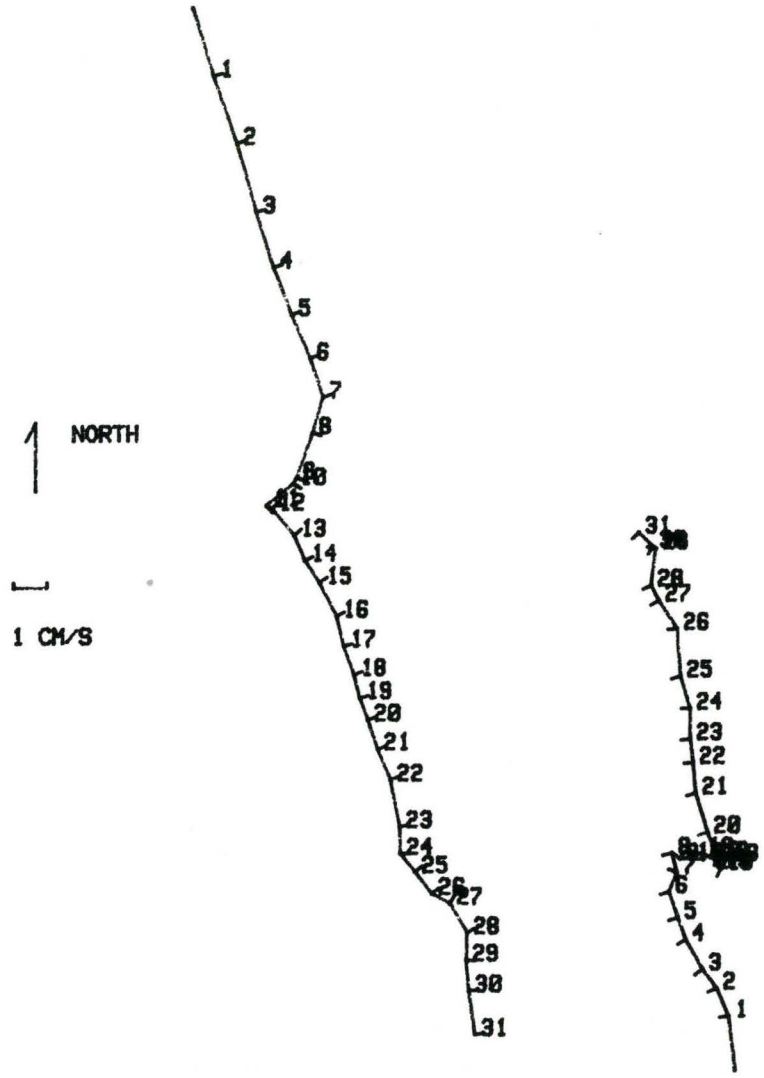

P.V.D. OF CURRENTS,STA. 1 AND 2 ;18M ; MAR'78

Left is Station 1 (West Side).
Right is Station 2 (East Side).

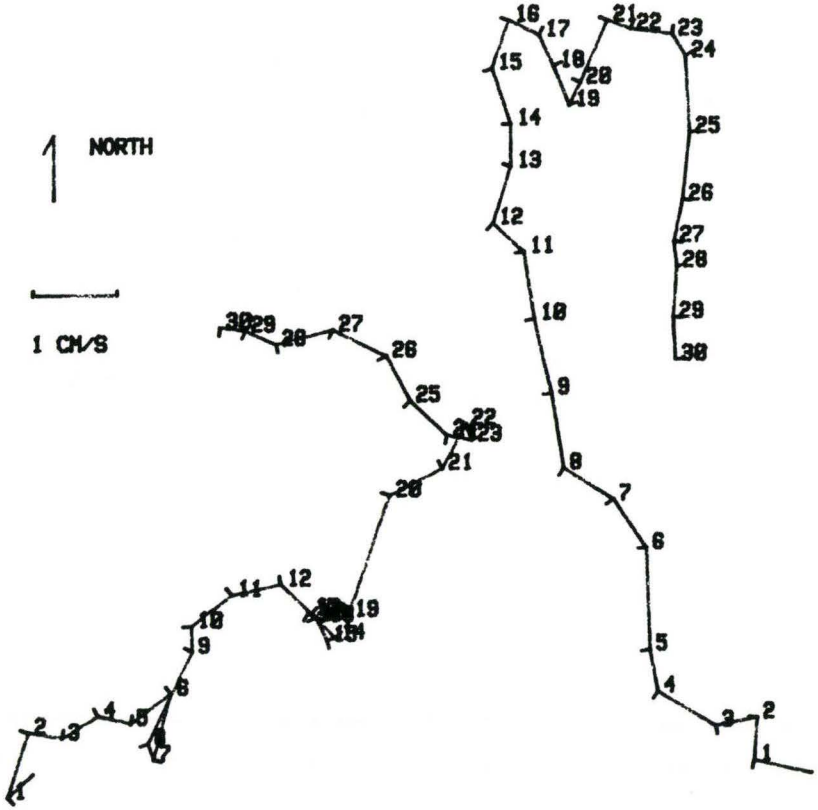

P.V.D. OF CURRENTS,STA. 1 AND 2 ;4M ; APR'78

Left is Station 1 (West Side).
Right is Station 2 (East Side).

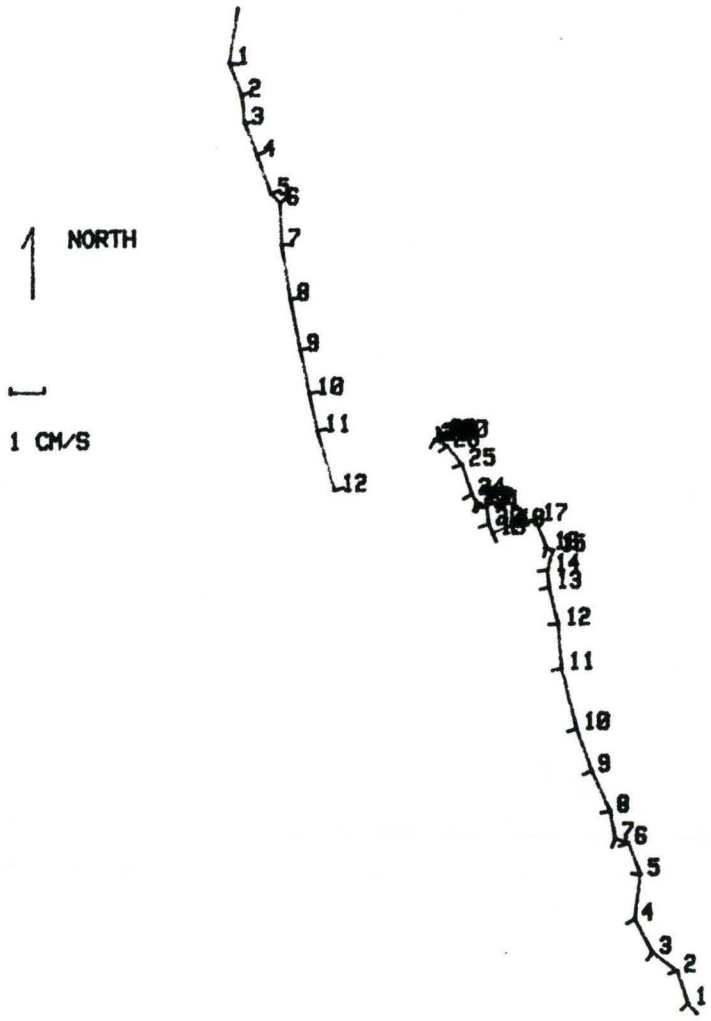

P.V.D. OF CURRENTS,STA. 1 AND 2 ;18M ; APR'78

Left is Station 1 (West Side).
Right is Station 2 (East Side).

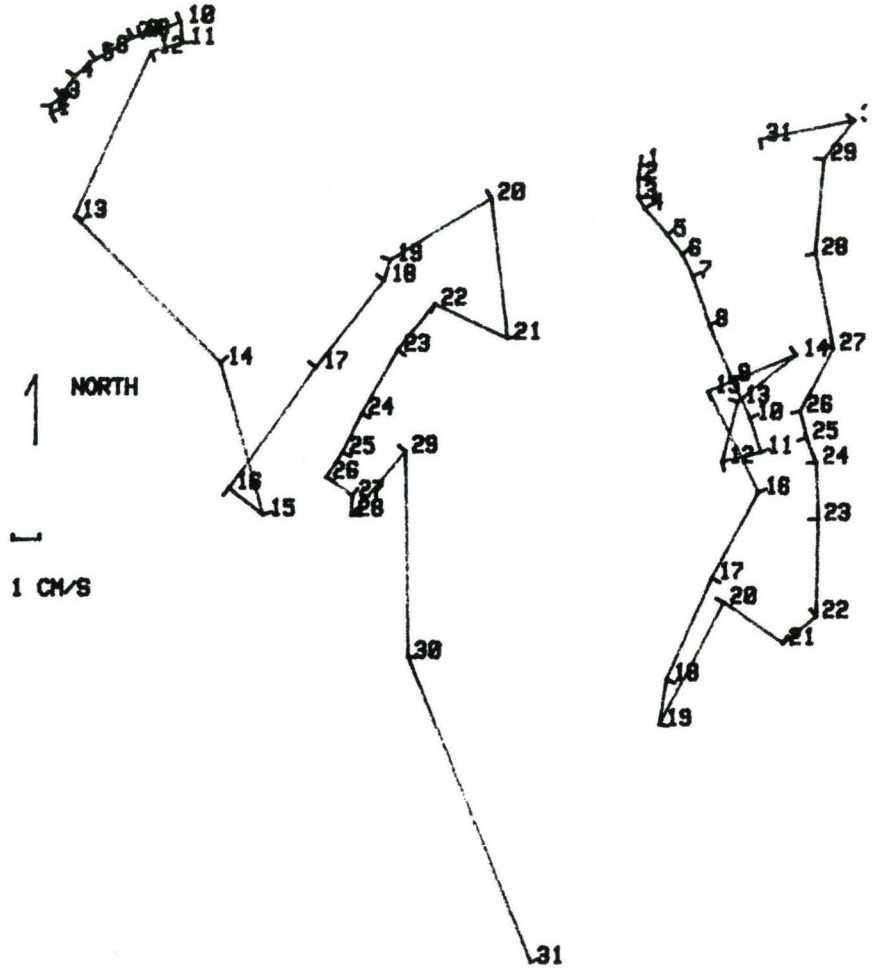

P.V.D. OF CURRENTS,STA. 1 AND 2 ;4M ; MAY'78

Left is Station 1 (West Side).
Right is Station 2 (East Side).

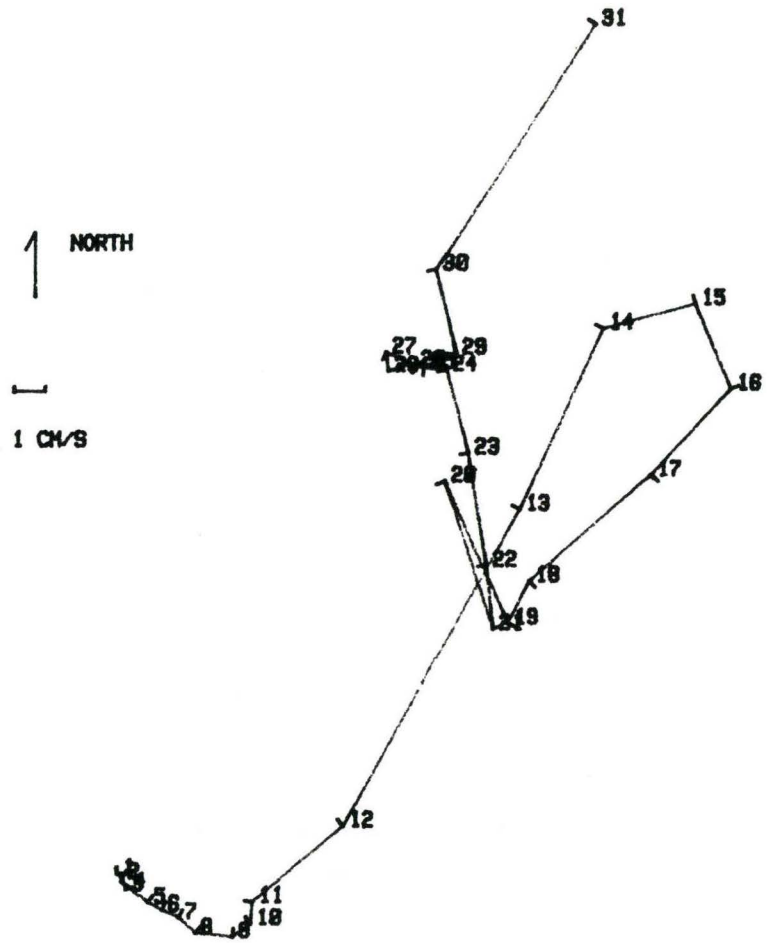

P.V.D. OF CURRENTS,STA. 1 AND 2 ;18M ; MAY'78

Left is Station 1 (West Side).
Right is Station 2 (East Side).

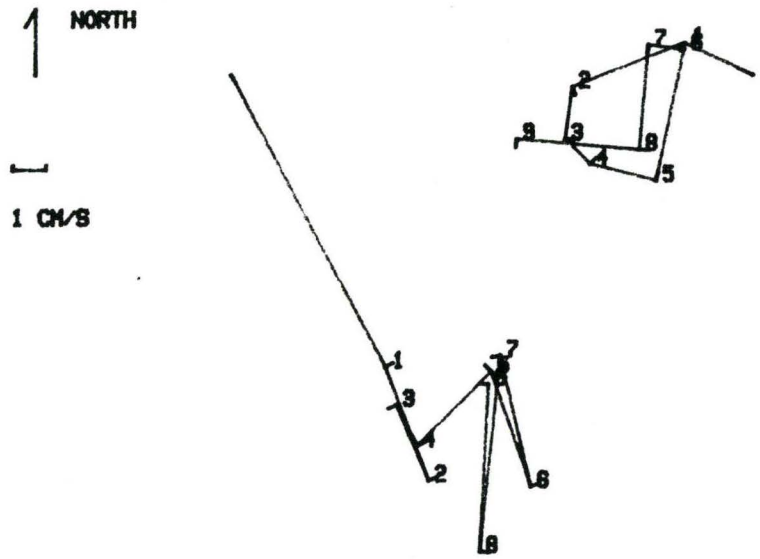

P.V.D. OF CURRENTS,STA. 1 AND 2 ;4M ; JUN'78

Left is Station 1 (West Side).
Right is Station 2 (East Side).

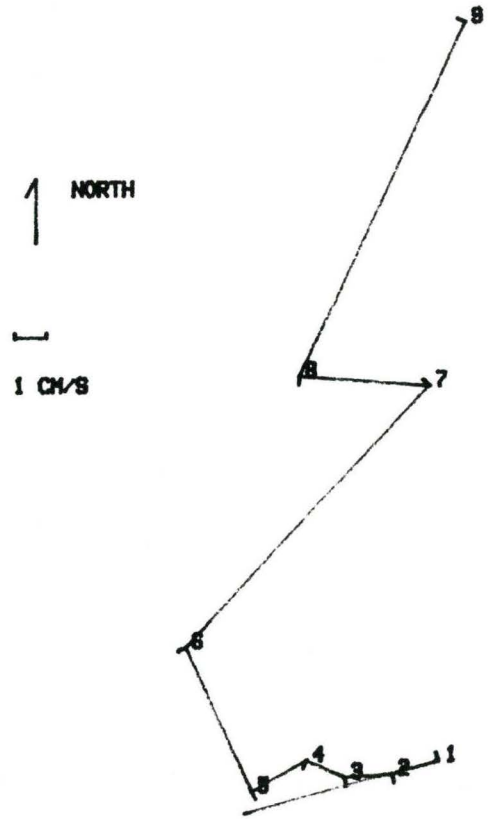

P.V.D. OF CURRENTS,STA. 1 AND 2 ;18M ; JUN'78

Left is Station 1 (West Side).
Right is Station 2 (East Side).

APPENDIX 2

Spectral Plots of Current Meter Time Series Data

KINETIC ENERGY DENSITY
Ice Free Period

4 m DEPTH

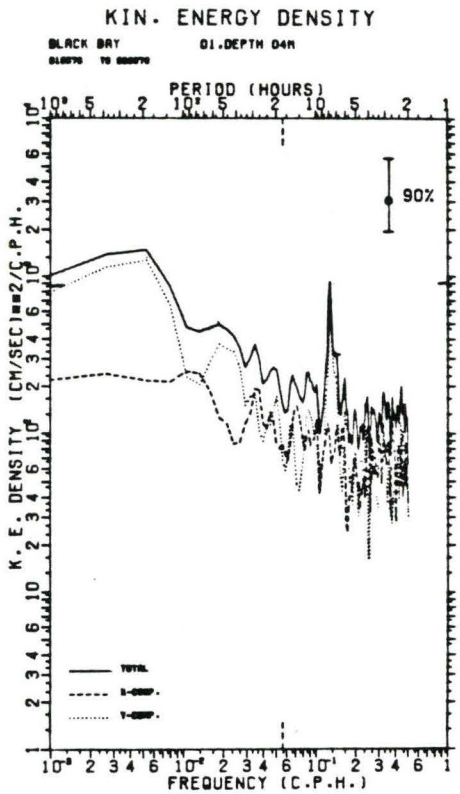

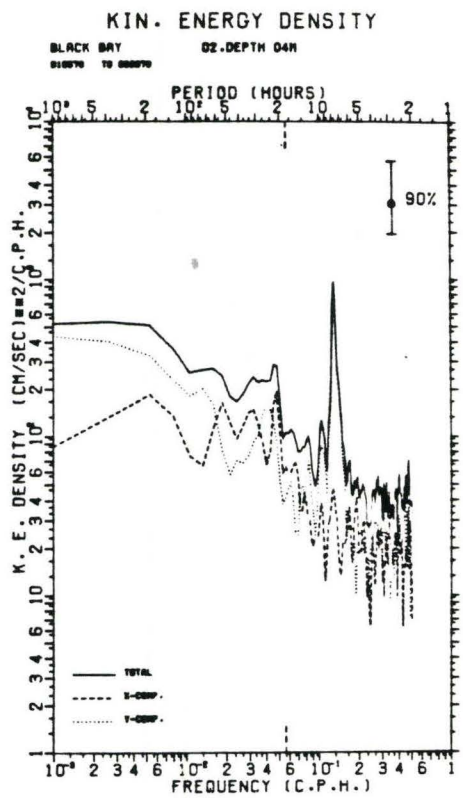

18 m DEPTH

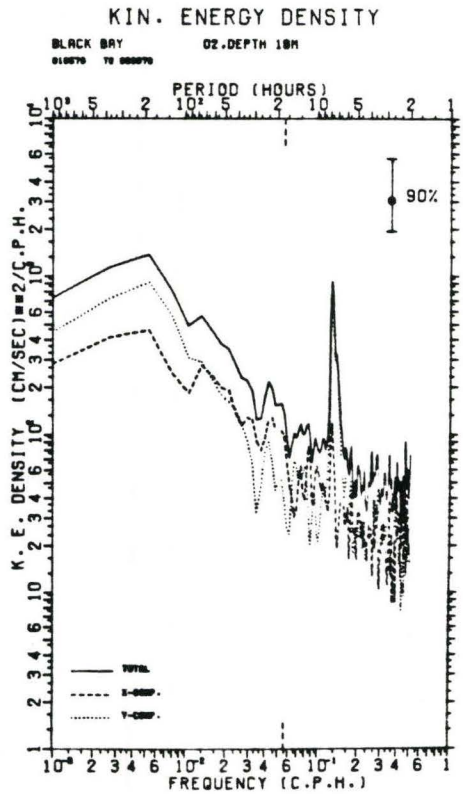

KINETIC ENERGY DENSITY
Ice Covered Period

4 m DEPTH

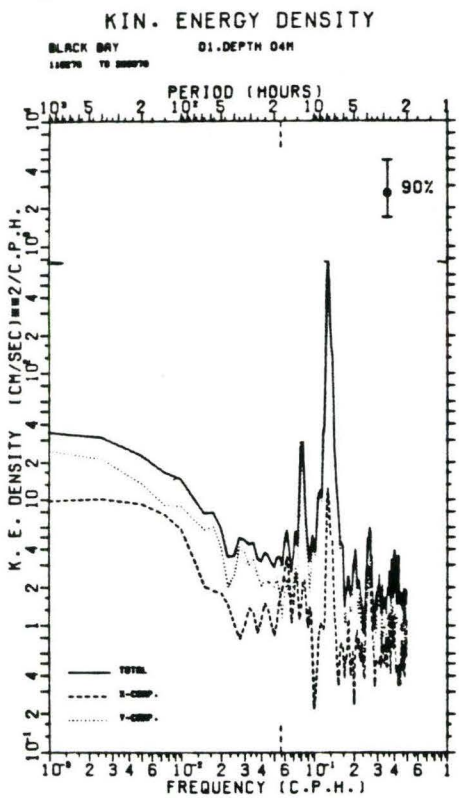

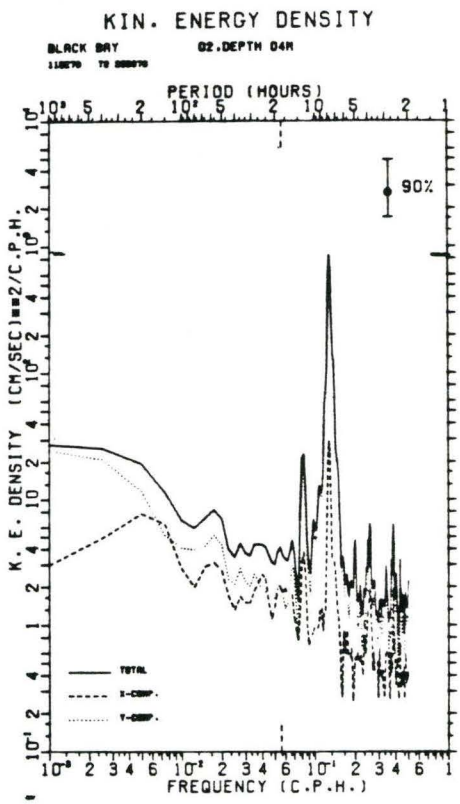

18 m DEPTH

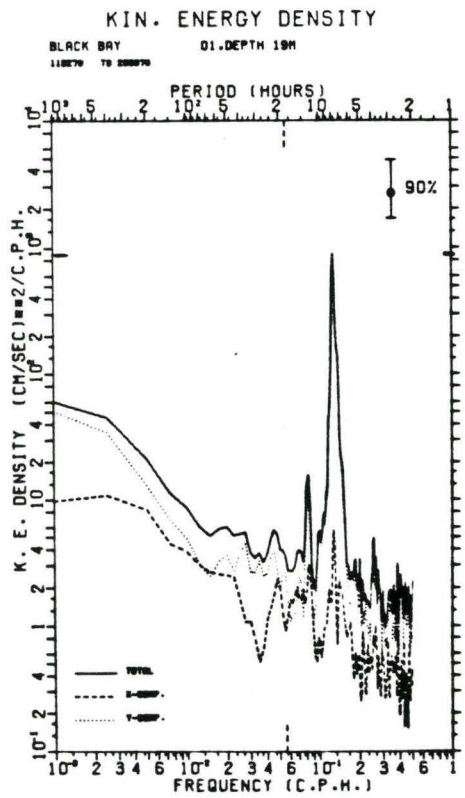

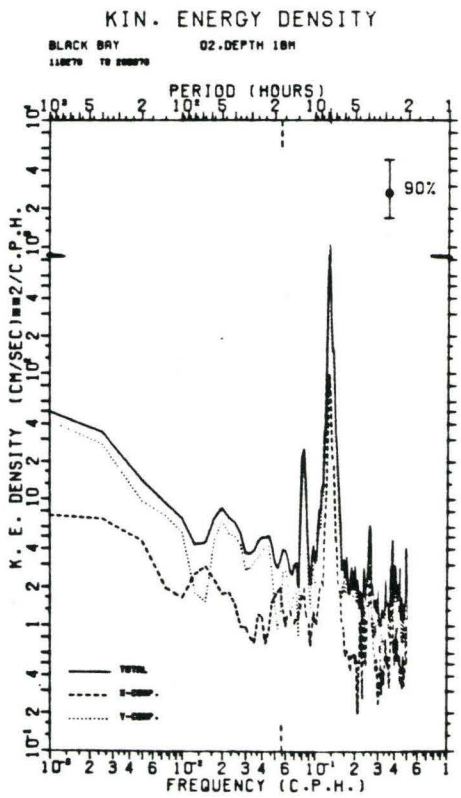

CROSS CHANNEL CORRELATION
Ice Covered Period

4 m DEPTH

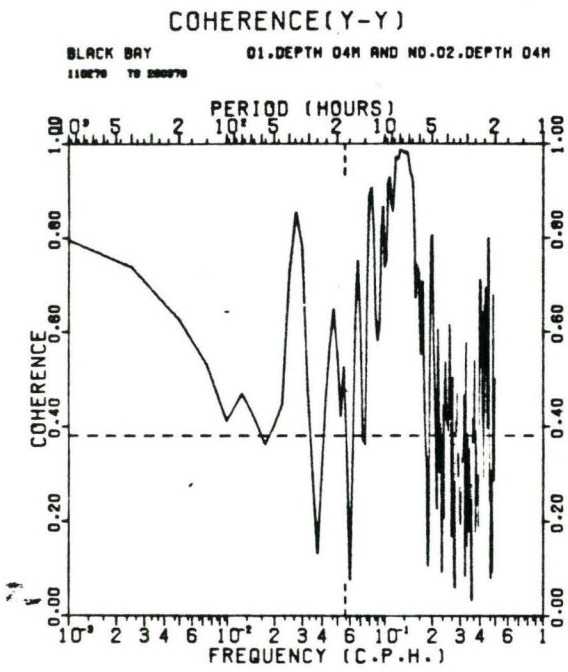

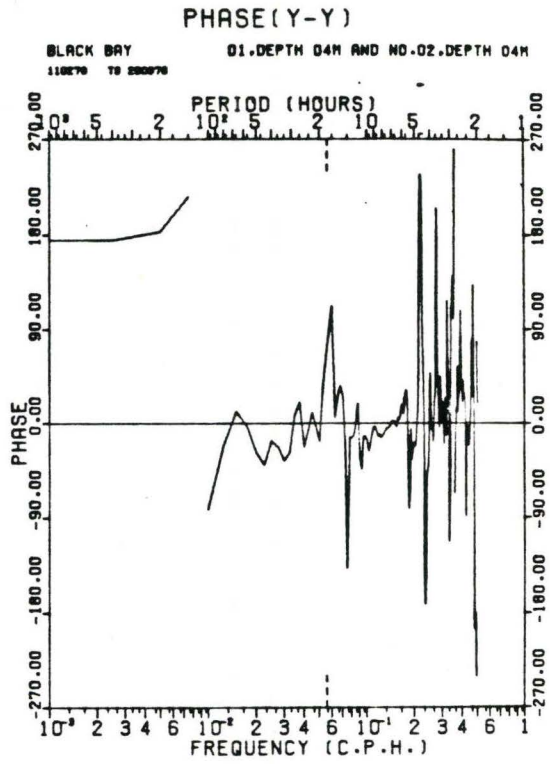

18 m DEPTH

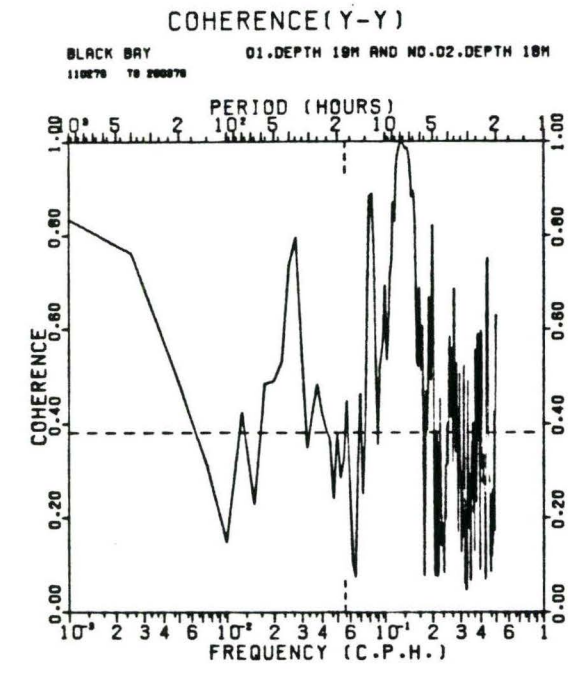

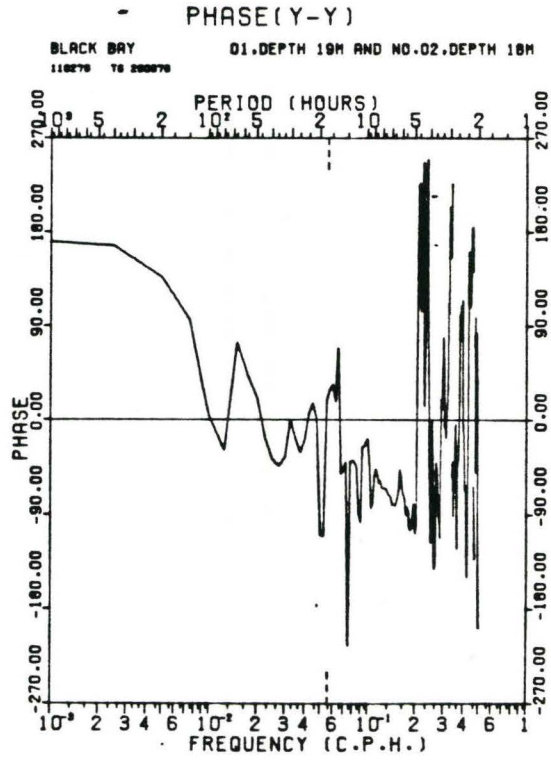

VERTICAL CORRELATION
Ice Covered Period

STN. 1

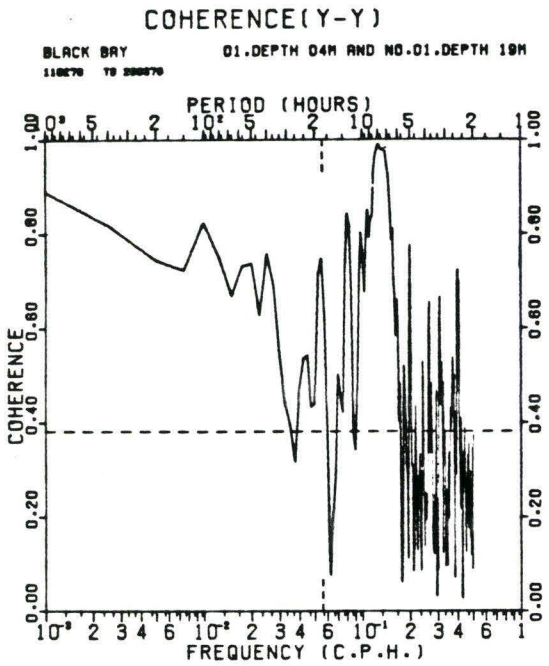

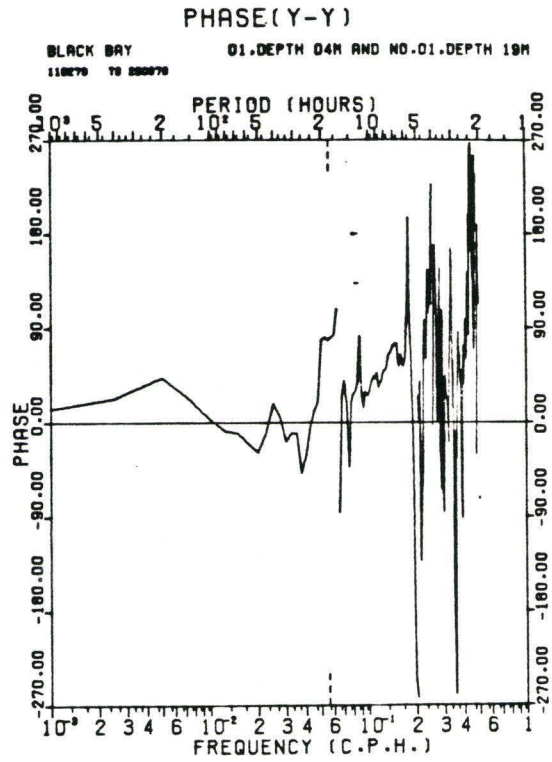

STN. 2

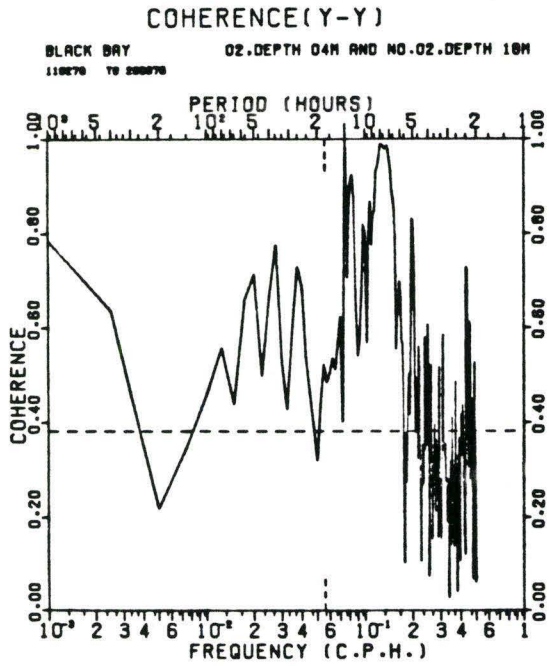

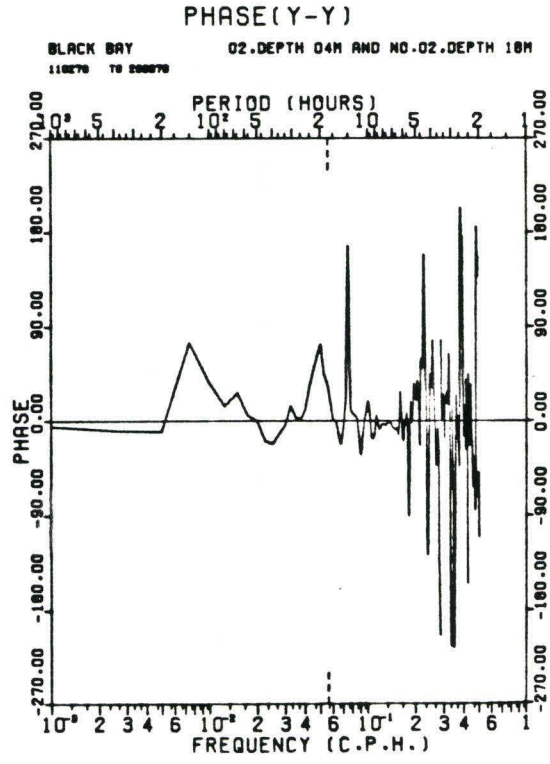

ICE FREE PERIOD

Cross Channel Correlations - 4 m Depth

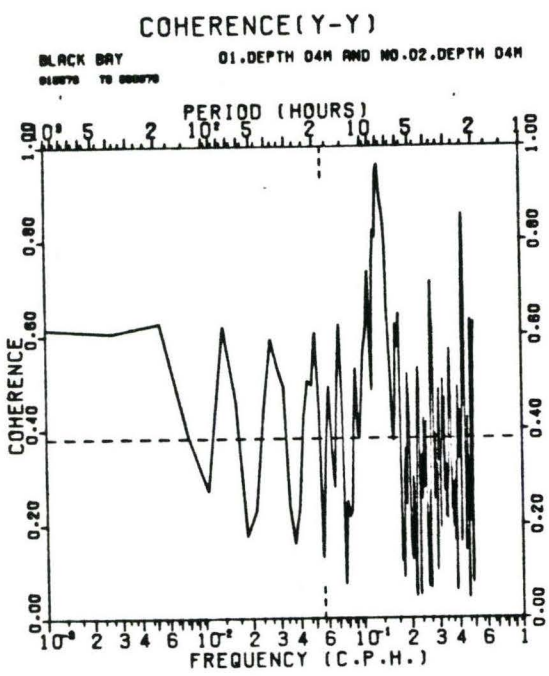

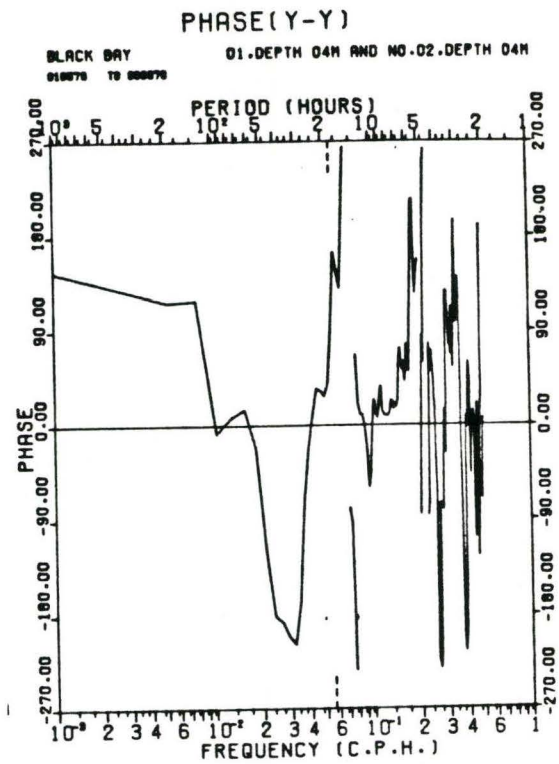

Vertical Correlations - Stn.2

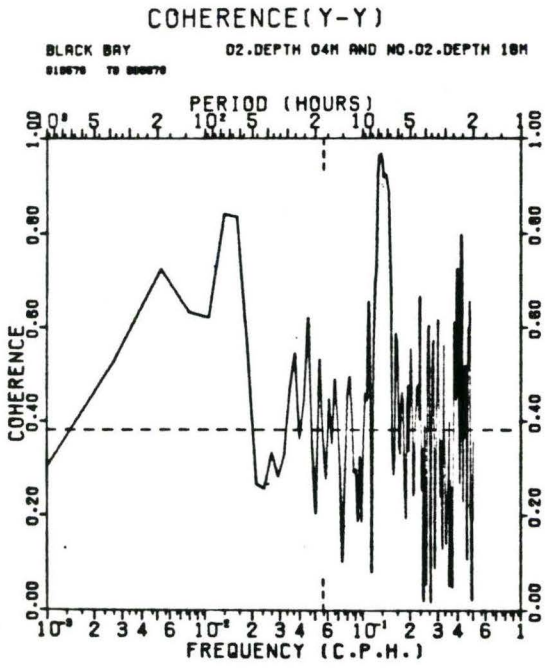

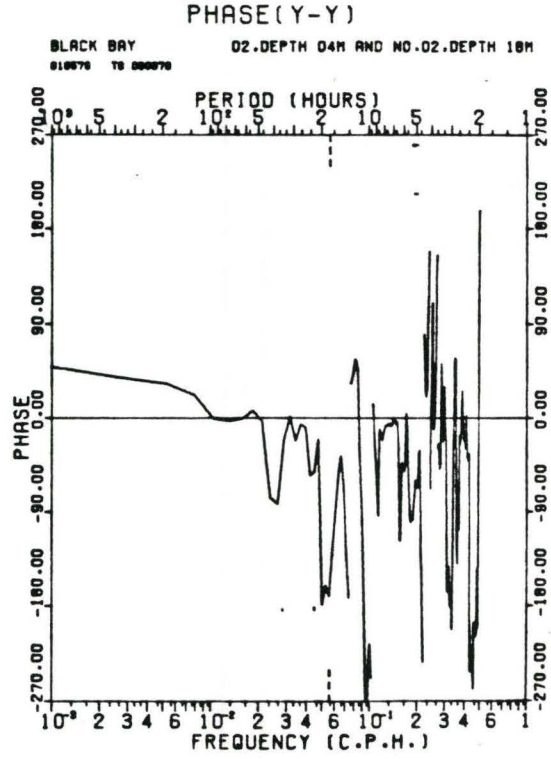

APPENDIX 3

Isothermal Maps of MBT Data

VIEW UP BAY

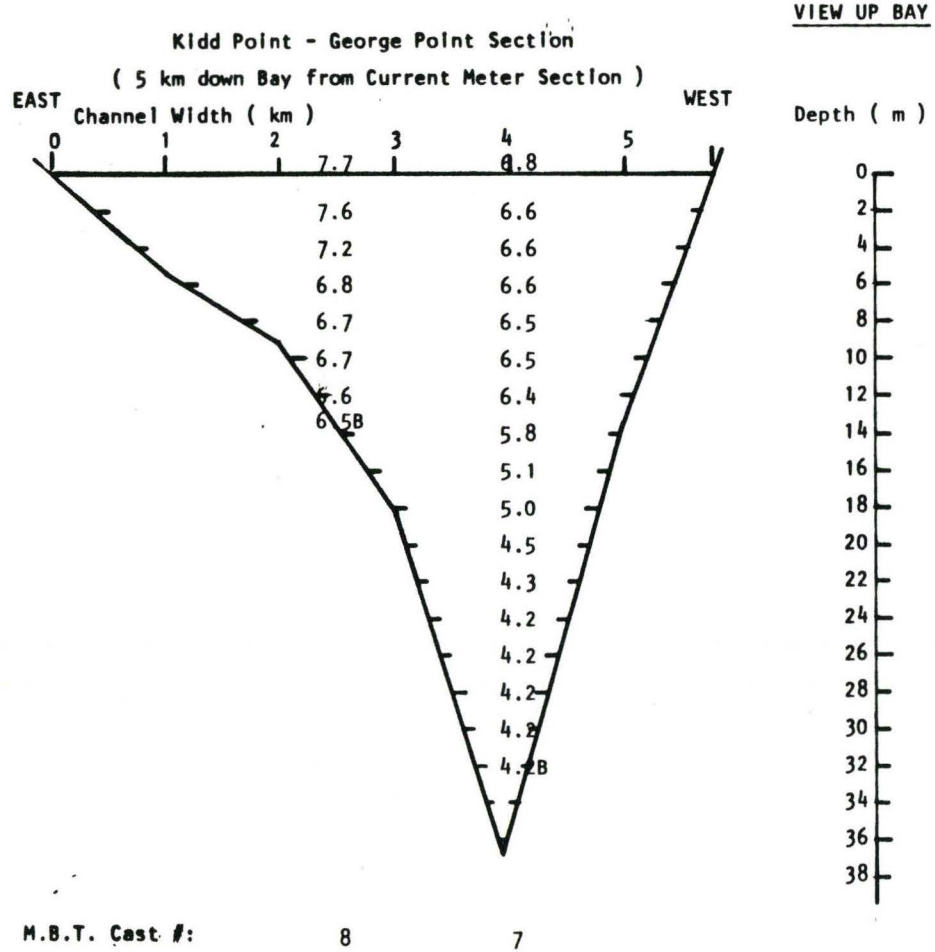

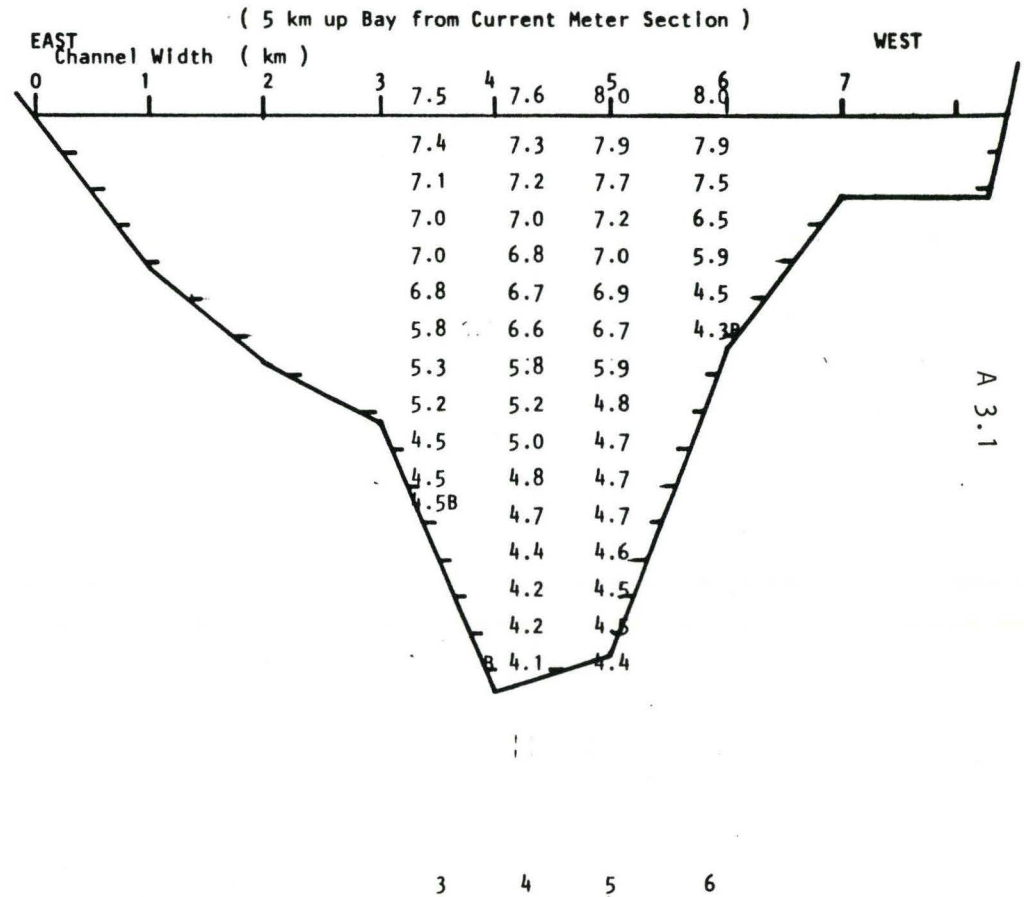

A 3.1

Date: 30 MAY 1978

Fig. A3. 1- Black Bay -
M.B.T. Temperature Profile Data. (OMNR)

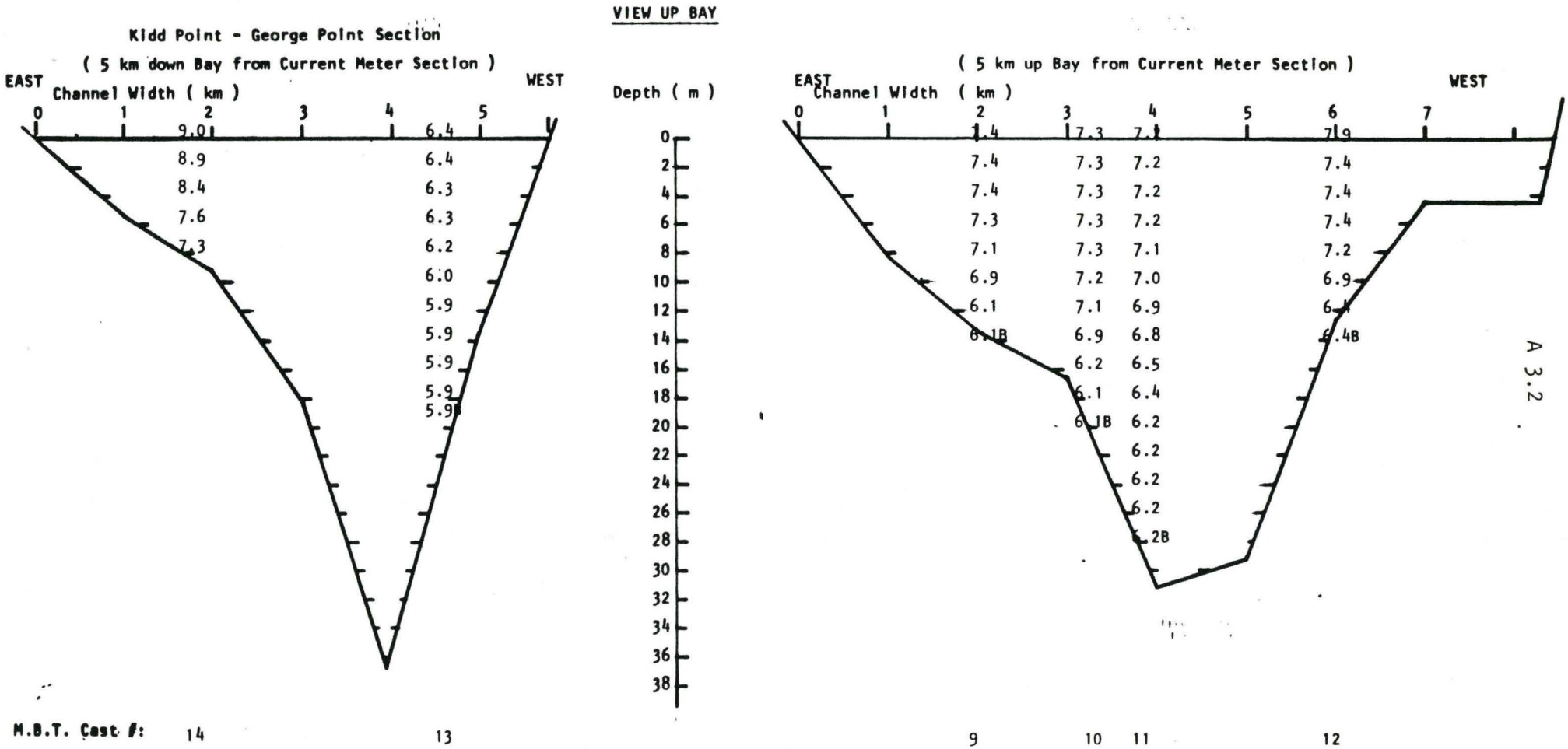

A 3.2

Fig. A3.2 - Black Bay -
M.B.T. Temperature Profile Data. (OMNR)

VIEW UP BAY

Kidd Point - George Point Section

(5 km down Bay from Current Meter Section)

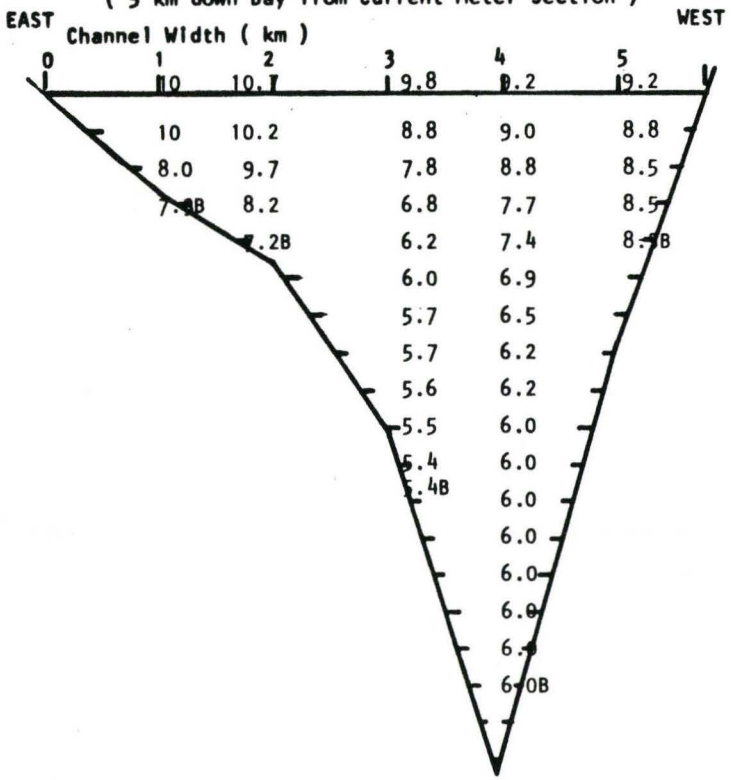

M.B.T. Cast #: 21, 20 22 19 24

Date: 5 JUNE 1978

(5 km up Bay from Current Meter Section)

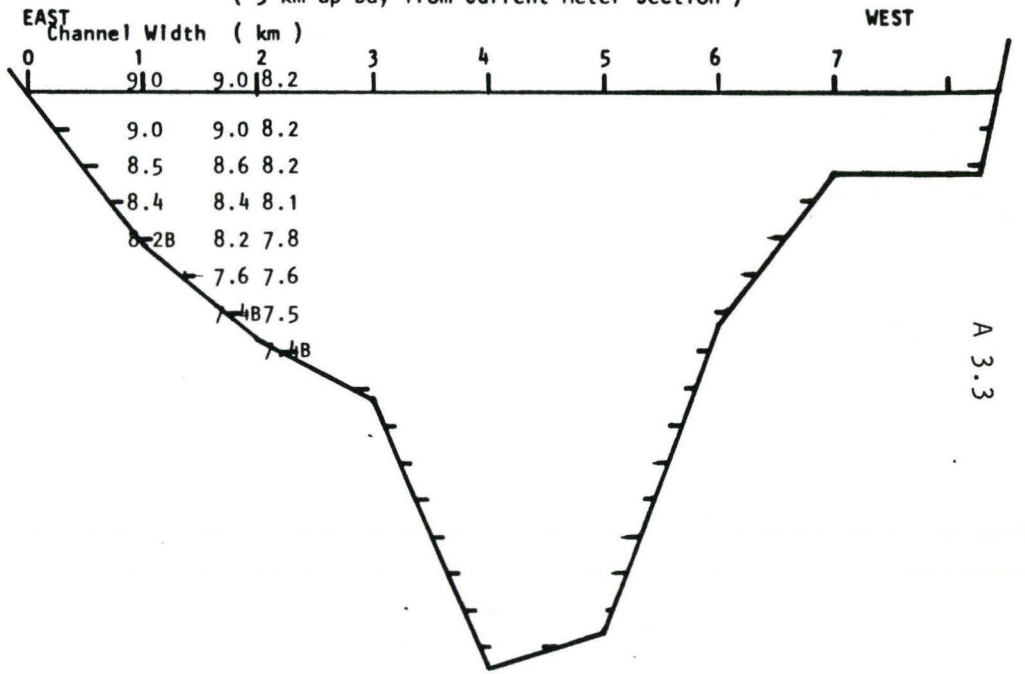

16 17 18

A 3.3

Fig. A3. 3 - Black Bay -
M.B.T. Temperature Profile Data. (OMNR)

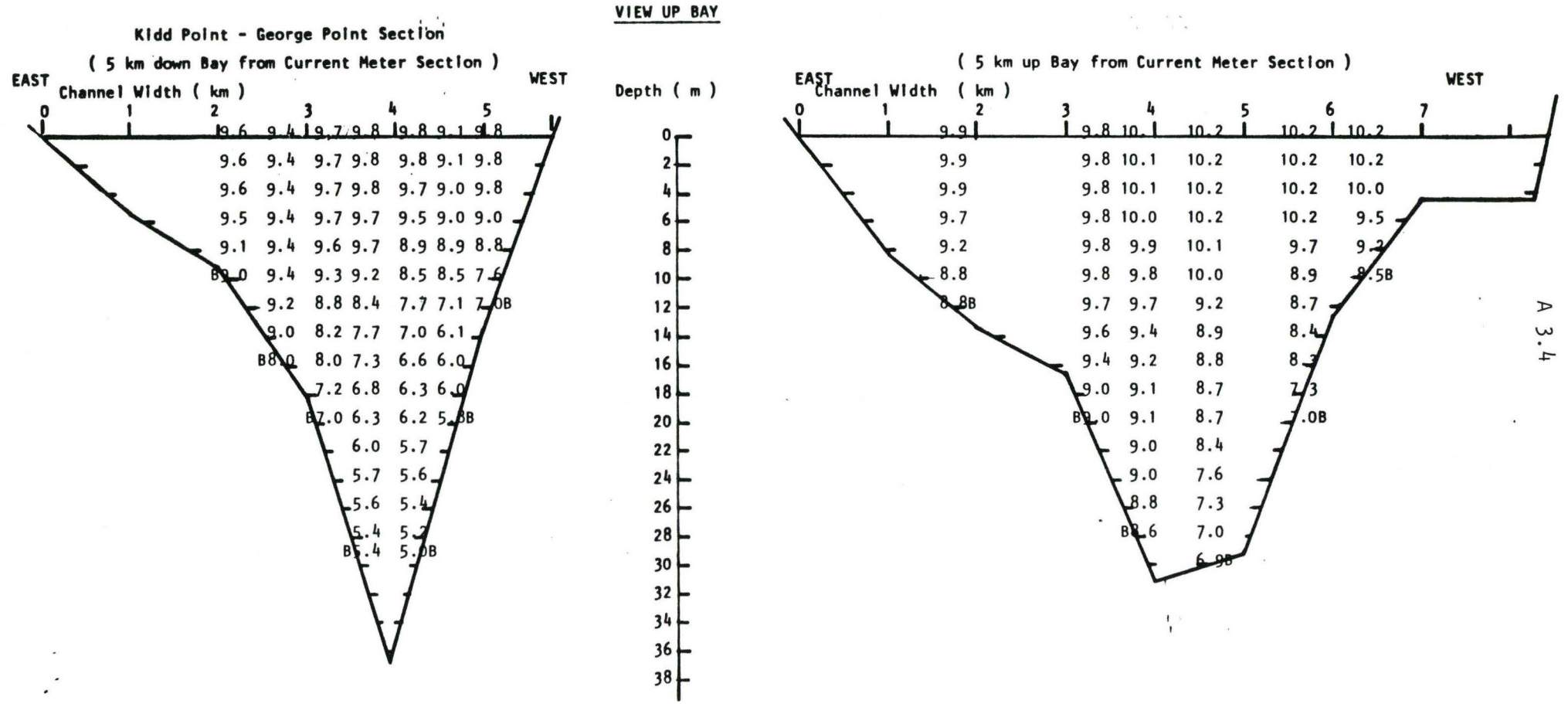

Date: 15 JUNE 1978

Fig. A3.4 - Black Bay -

VIEW UP BAY

Kidd Point - George Point Section

(5 km down Bay from Current Meter Section)

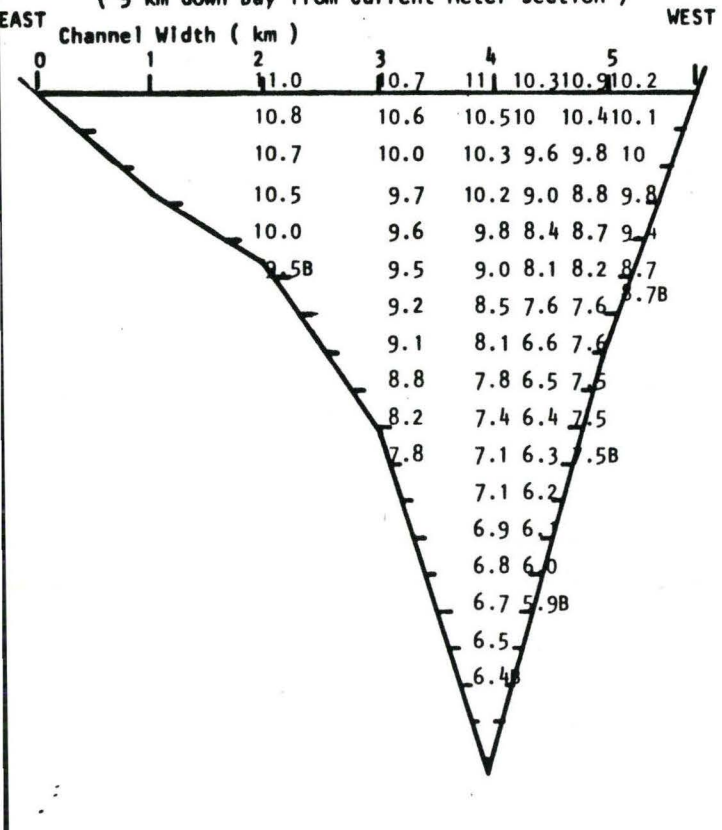

Depth (m)

M.B.T. Cast #: 52 53 54 55 56 57

Date: 21 JUNE 1978

(5 km up Bay from Current Meter Section)

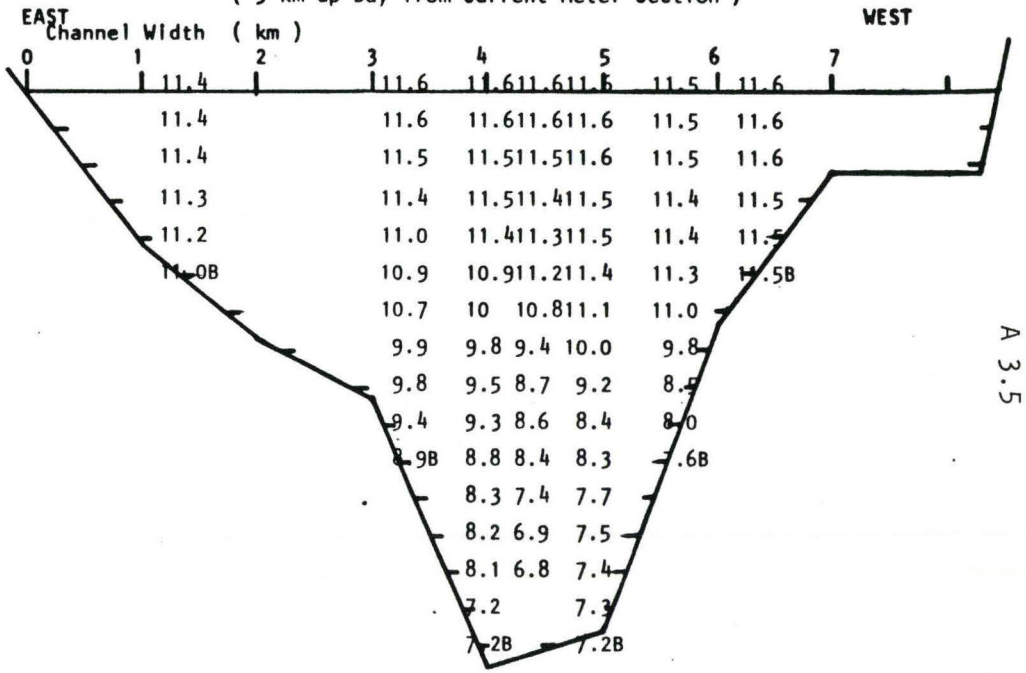

51 50 49 48 47 46 45

A 3.5

Fig. A3.5 - Black Bay -
M.B.T. Temperature Profile Data. (OMNR)

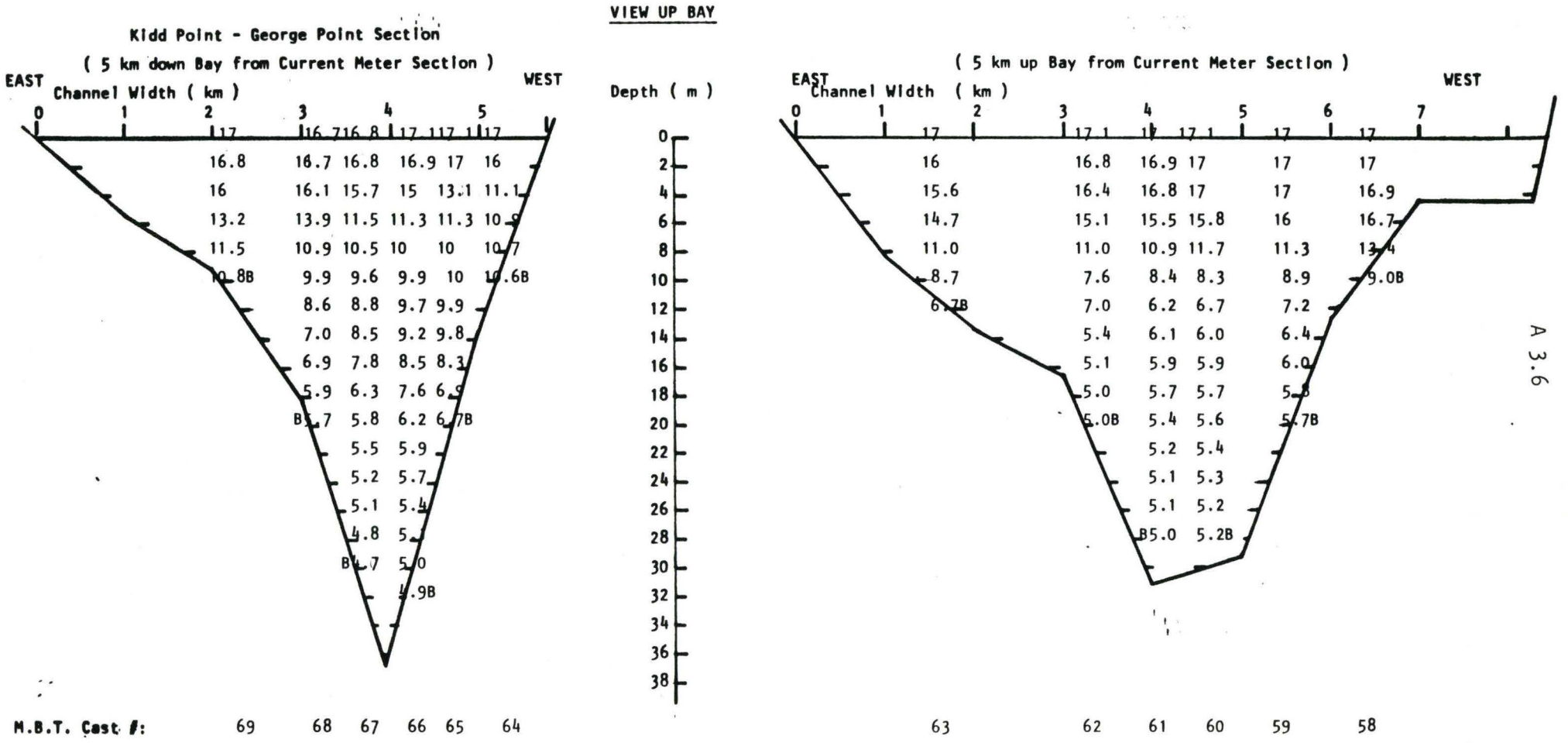

Fig. A3.6 - Black Bay -
M.B.T. Temperature Profile Data. (OMNR)

APPENDIX 4

Estimated Heat Balance for May

APPENDIX 4

Order of magnitude estimate of daily average heat flux into Black Bay during May.

The heat balance model used here is based on Sato, 1969, which is typical of many such calculations, e.g. Huber and Perez, 1970.

The heat into storage in the Bay water is the balance of heat inflows and outflows through the water boundaries.

Heat into storage = Heat in - Heat out

$$Q_t = Q_s - Q_r - Q_b - Q_e - Q_h$$

Q_s is the global solar radiation, i.e. the total short wave radiation from the whole dome of the sky received on a flat surface.

Schertzer (1978) has estimated the energy budget for Lake Superior for 1973 in some detail. Heat storage, Q_t, was computed from estimates of the heat content of Lake Superior, based on a series of 19 temperature surveys conducted from 1964 to 1973. The value obtained for May was 387 $cal \cdot cm^{-2}\ d^{-1}$. The value of global solar

radiation was computed as a lake-wide mean value based on shoreline and offshore measurements, and adjusted for cloud amount and type. This data indicates a land value of Q_s of 384.4 cal. cm^{-2} d^{-1}.

Q_r is the amount of incident radiation reflected back to the atmosphere by the water surface, and therefore, not absorbed by the water. It is the product of incident radiation and surface reflectivity. A value of lake surface reflectivity quoted by Sato, from Rogers (1964) for Lake Ontario in May, is 0.066. Thus, Q_r is approximated as:

$$Q_r = 0.066 \times 384.4 = 25.4 \text{ cal. } cm^{-2} \; d^{-1}$$

Q_b is the net back radiation of the long wave exchange between the water and the atmosphere, and is a function of air and water temperature, moisture, cloud height and cloud cover. Sato quotes Tabata (1958) that:

$$Q_b = 1.141 \left[Tw^4 - T_2{}^4 \, (atbe_2) \right] \times 10^{-7} \text{ cal. } cm^{-2} \; d^{-1}$$

For this order of magnitude estimate, we will use the following values:

T_w - water surface temperature, as the mean from 0° to 4°C, in absolute scale, i.e. 275°K

T_2 - air temperature 2 m above the water surface, as the daily mean temperature for May, 1978, from Dorion TCPL 70, in absolute scale, i.e. 9.6° + 273 = 283°K

$a \equiv 0.740 + 0.025\ c\ e^{-0.0574\ h}$

c ≡ cloud cover in tenths - take 0.64 (Thunder Bay)

h ≡ cloud height x 1000 ft - take 5

$a = 0.75$

$b \equiv 0.0049 - 0.00054\ c\ e^{-0.060h}$

$b = 0.005$

e_2 ≡ vapor pressure of water in mb two metres above the water surface.

We will assume 60% Relative Humidity at 9.6°C, and from a Steam Table, the saturation pressure is 12.3 mb.

$e_2 = 0.60 \times 12.3 = 7.4$ mb

$Q_b = 1.141\ [275^4 - 283^4\ (0.75 + 0.04)]\ 10^{-7}$

$= 74.4$ cal. $cm^{-2}\ d^{-1}$

Q_e is the heat utilized by evaporation. Sato uses the turbulent transport equation to estimate the amount of evaporation from the water.

$E = K\ W\ (e_w - e_a)$

$K \equiv$ constant ≈ 0.005

$W \equiv$ wind speed, mph, use mean speed for May from Thunder Bay, 11.1 km h^{-1} = 6.9 mph

$e_w \equiv$ saturation vapor pressure at water surface temperature in mb. We will use temperature of 2°C and 1013 mb. From a Steam Table, the saturation pressure is 7.2 mb.

$e_a \equiv$ vapor pressure of air over water in mb.

= 7.4 mb as above.

$E = 0.005 \times 6.9 \times (7.2 - 7.4)$

$= -0.007\ cm^{-3}\ d^{-1}\ cm^{-2}$

The negative sign indicates condensation, i.e. heat released to the water.

$Q_e = E\rho L$

L = latent heat of vaporization

$= 596 - 0.52\ T_w$

$T_w \equiv$ surface water temperature = 2°C

$L = 595$ cal. g^{-1}

$\rho \equiv$ water density - 1 g cm^{-3}

$Q_e = -0.007 \times 1 \times 595$

$= -4.17$ cal. $cm^{-2}\ d^{-1}$

Q_h is the sensible heat transfer due to conduction, free and forced convection. Sato quotes Bowen (1926)

$$R = \frac{Q_h}{Q_e} = 0.62 \frac{T_w - T_q}{e_w - e_a}$$

using values as defined above

$$R = 0.62 \frac{2 - 9.6}{7.2 - 7.4}$$

$$= 23.6$$

$$Q_h = 23.6 \times -4.17$$

$$= -98.3 \text{ cal. cm}^{-2} \text{ d}^{-1}$$

Totalling all the above terms

$$Q_t = 384.4 - 25.4 - 74.4 - (-4.17) - (-98.3)$$

$$= 387.1 \text{ cal. cm}^{-2} \text{ d}^{-1}$$

APPENDIX 5

Programs

1. BAY 2

2. PVD

```
10 ! Program BAY, Version 2.0, Updated 82/4/28
20 ! Stored on F.E.Roy File 1 as BAY 2.
30 !
40 !
50 ! Program BAY contains bathymetric data for Black Bay,Lake Superior
60 ! The program converts this data from fathoms to meters , lists the
70 ! metric values in chart form,and then calculates hypsometric values
80 ! of volume and surface area vs. depth. The surface area and volume
90 ! are plotted against depth.The time interval taken for the passage
100 ! of the thermal bar through each grid section of given depth is also
110 ! estimated using the arguement of Elliott and Elliott (1970).
120 !
130 !
140 ! List of Variables
150 !   A    = Depth from data file in Fathoms
160 !   Bath = Depth in metres
170 !
180 !
190 !
200  OPTION BASE 1
210  FIXED 1
220 Main:  GOSUB Init
230        GOSUB Calc
240  !     GOSUB Bardat
250  !     GOSUB Sound
260        GOSUB Pltsht
270        GOSUB Graph
280        GOSUB List
290        PAUSE
300        END
310 !
320 !
330 Init: PLOTTER IS "9872A"
340       DIM X(130),Y(130),D(130),Time(130),Depth(40),Volume(40),Area(40),Vol(4
0)
350       Dmax=30
360 !
370 !
380  DATA 0.0,0.0,0.0,0.0,0.0,0.0,0.0,0.0,0.0,1.0,0.0,0.0,0.0,0.0,0.0,0.0
390  DATA 0.0,0.0,0.0,0.0,0.0,0.0,0.0,0.0,1.5,2.25,1.75,1.5,0.75,0.0,0.0
400  DATA 0.0,0.0,0.0,0.0,0.0,0.0,0.0,0.0,2.75,4.0,2.5,2.25,1.25,1.0,0.0
410  DATA 0.0,0.0,0.0,0.0,0.0,0.0,0.0,0.0,2.0,3.5,4.5,3.0,2.75,2.25,1.75,0.0
420  DATA 0.0,0.0,0.0,0.0,0.0,0.0,0.0,2.0,2.5,5.25,4.0,3.5,3.0,2.5,2.0,.25
430  DATA 0.0,0.0,0.0,0.0,0.0,0.0,0.0,0.0,2.0,3.25,4.0,3.25,4.5,3.25,2.0,2.25,1.75
440  DATA 0.0,0.0,0.0,0.0,0.0,0.0,0.0,0.0,2.25,3.25,4.5,3.25,3.25,3.0,3.25,2.5,1.5
450  DATA 0.0,0.0,0.0,0.0,0.0,0.0,0.0,1.5,3.0,3.75,3.0,3.5,3.5,4.25,3.75,1.0
460  DATA 0.0,0.0,0.0,0.0,0.0,0.0,0.0,0.0,2.75,3.5,4.0,4.0,3.75,4.75,3.0,0.0
470  DATA 0.0,0.0,0.0,0.0,0.0,0.0,0.0,1.25,2.0,3.0,5.5,6.0,4.5,3.5,2.75,0.0
480  DATA 0.0,0.0,0.0,0.0,0.0,0.0,0.0,1.5,3.0,5.0,8.25,6.0,4.25,3.25,0.0,0.0
490  DATA 0.0,0.0,0.0,0.0,0.0,0.0,0.0,1.75,8.0,6.25,7.0,4.75,3.0,0.0,0.0,0.0
500  DATA 0.0,0.0,0.0,0.0,0.0,0.0,0.0,4.5,9.25,8.0,7.0,3.0,0.0,0.0,0.0,0.0,0.0
510  DATA 0.0,0.0,0.0,0.0,2.0,2.5,2.25,9.0,8.0,9.25,2.75,0.0,0.0,0.0,0.0,0.0,0.0
520  DATA 0.0,0.0,0.0,0.0,2.5,3.5,5.75,11.5,8.5,3.25,0.0,0.0,0.0,0.0,0.0,0.0,0.0
530  DATA 0.0,0.0,0.0,0.0,4.0,6.75,15.75,8.75,3.25,0.0,0.0,0.0,0.0,0.0,0.0,0.0,0.0,0.0
540  DATA 0.0,0.0,0.0,0.0,7.0,12.5,11.5,4.0,0.0,0.0,0.0,0.0,0.0,0.0,0.0,0.0,0.0,0.0
550  DATA 0.0,0.0,0.0,0.0,10.5,13.0,3.5,0.0,0.0,0.0,0.0,0.0,0.0,0.0,0.0,0.0,0.0,0.0
560  DATA 0.0,0.0,2.75,13.25,7.25,0.0,0.0,0.0,0.0,0.0,0.0,0.0,0.0,0.0,0.0,0.0,0.0,0.0
570  DATA 0.0,0.0,2.0,14.25,5.0,0.0,0.0,0.0,0.0,0.0,0.0,0.0,0.0,0.0,0.0,0.0,0.0,0.0
580  DATA 1.75,2.0,6.0,14.5,0.0,0.0,0.0,0.0,0.0,0.0,0.0,0.0,0.0,0.0,0.0,0.0,0.0,0.0
590  DATA 0.0,5.0,12.75,9.75,3.75,0.0,0.0,0.0,0.0,0.0,0.0,0.0,0.0,0.0,0.0,0.0,0.0,0.0
600  DATA 0.0,10.5,12.0,7.0,4.75,0.0,0.0,0.0,0.0,0.0,0.0,0.0,0.0,0.0,0.0,0.0,0.0,0.0
610  DATA 5.25,16.75,4.0,4.5,6.0,0.0,0.0,0.0,0.0,0.0,0.0,0.0,0.0,0.0,0.0,0.0,0.0,0.0
620  DATA 13.5,11.75,3.5,2.0,6.0,0.0,0.0,0.0,0.0,0.0,0.0,0.0,0.0,0.0,0.0,0.0,0.0,0.0
630  DATA 19.5,17.25,0.0,0.0,10.0,0.0,0.0,0.0,0.0,0.0,0.0,0.0,0.0,0.0,0.0,0.0,0.0,0.0
640 !
650 !
```

```
660   Vtot=0
670   Atot=0
680   Tf=100/387.1
690   K=0
700  FOR J=1 TO 21
710    FOR I=1 TO 15
720     READ A
730     IF A=0 THEN 900
740     K=K+1
750     Atot=Atot+4E6
760     X(K)=I
770     Y(K)=J
780     D=A*1.8288
790     D(K)=D
800     Vtot=Vtot+D*4E6
810     IF (D>0) AND (D<5) THEN 840
820     IF (D>5) AND (D<15) THEN 860
830     IF D>15 THEN 880
840     Td=3.7
850     GOTO 890
860     Td=3.5
870     GOTO 890
880     Td=3.25
890     Time(K)=Tf*D*Td
900    NEXT I
910  NEXT J
920 !
930 !
940 RETURN
950 !
960 Calc: FOR D=1 TO Dmax+1
970       Depth(D)=D-1
980       Area=0
990       Vol=0
1000        FOR N=1 TO K
1010          Z=D(N)-D
1020          IF Z>1 THEN 1050
1030          IF (Z<1) AND (Z>0) THEN 1070
1040          IF Z<0 THEN 1100
1050            Dinc=1
1060            GOTO 1080
1070            Dinc=Z
1080            Vol=Vol+Dinc*4E6
1090        Area=Area+4E6
1100        NEXT N
1110        Volume(D+1)=Volume(D)+Vol
1120        Area(D)=Area
1130      NEXT D
1140  RETURN
1150 !
1160 !
1170 List:INPUT "PRINTER IS 0 (Hardcopy) OR 16 (CRT)?",A
1180      PRINTER IS A
1190      IMAGE "                              Program BAY "
1200      IMAGE "            Table of Hypsometric Data for Black Bay "
1210      IMAGE "     DEPTH(m)                VOLUME(m^3)          AREA(m^2)"
1220      PRINT USING 1190
1230      PRINT LIN(2)
1240      PRINT USING 1200
1250      PRINT LIN(1)
1260      PRINT USING 1210
1270      FOR M=1 TO Dmax+1
1280        PRINT USING "6X,DD.DD,15X,DD.DDE,15X,DD.DDE";Depth(M),Volume(M),Area
(M)
1290      NEXT M
1300      PRINT LIN(2)
```

```
1310      PRINT " Total Area =";Atot
1320      PRINT " Total Volume =";Vtot
1330   INPUT "Do you want a list of data ? (1 YES,0 NO)",S
1340   IF S=1 THEN GOSUB Lisdat
1350   PRINTER IS 16
1360 RETURN
1370 Lisdat: PRINT PAGE
1380       IMAGE "                              BLACK BAY DATA           "
1390       IMAGE "     Position:    X       Y         Depth(m)      Time of Bar(d) "
1400       PRINT USING 1380
1410       PRINT LIN(2)
1420       PRINT USING 1390
1430       PRINT LIN(1)
1440       FOR N=1 TO K
1450       PRINT USING "16X,DD.D,4X,DD.D,8X,DD.DD,11X,DD.DD ";X(N),Y(N),D(N),Tim
e(N)
1460       NEXT N
1470       RETURN
1480 Pltsht: GCLEAR
1490         GRAPHICS
1500         SCALE -5,33,-.5,5.2
1510         CLIP 0,30,0,5
1520         AXES 5,1,0,0
1530         UNCLIP
1540        GOSUB Lxaxes
1550        GOSUB Lyaxes
1560        GOSUB Titles
1570         RETURN
1580 Graph:GRAPHICS
1590       PDIR 0
1600       PEN 1
1610       LINE TYPE 1
1620       MOVE 0,0
1630       FOR M=1 TO Dmax+1
1640         DRAW M-1,Area(M)/1.00E8
1650       NEXT M
1660       LINE TYPE 5
1670       MOVE 0,0
1680       FOR M=1 TO Dmax+1
1690         DRAW M-1,Volume(M)/1E9
1700       NEXT M
1710       PAUSE
1720       GCLEAR
1730     RETURN
1740 Titles:LDIR 0
1750        PEN 1
1760        MOVE 17,4.5
1770        LABEL USING "K";"BLACK BAY"
1780        LABEL USING "K";"HYPSOMETRIC DATA"
1790        LABEL USING "K";"SOLID LINE IS AREA (Km^2)"
1800        LABEL USING "K";"BROKEN LINE IS VOLUME (Km^3)"
1810      RETURN
1820 Lxaxes: !
1830 CSIZE 3,.5
1840 LDIR 0
1850 LORG 6
1860 FOR I=0 TO 6
1870   MOVE 5*I,-.1
1880   LABEL USING "K";5*I
1890 NEXT I
1900 MOVE 5,-.3
1910 IMAGE "DEPTH (metres)"
1920 LABEL USING 1910
1930 RETURN
1940 Lyaxes: !
1950 CSIZE 3,.5
```

```
1960 DEG
1970 LDIR 90
1980 FOR I=1 TO 5
1990   MOVE -1.8,I
2000   LORG 4
2010   LABEL USING "K";100*I
2020 NEXT I
2030 LORG 4
2040 MOVE -4.3,1.5
2050 LABEL USING 2120
2060 FOR I=1 TO 5
2070   MOVE -1.3,I
2080   LORG 6
2090   LABEL USING "K";I
2100 NEXT I
2110 LORG 4
2120 IMAGE "AREA (Km^2)"
2130 IMAGE "VOLUME (Km^3)"
2140 MOVE -3,1.5
2150 LABEL USING 2130
2160 RETURN
2170 Pltdat: !
2180         GRAPHICS
2190         SCALE -2,23,23,-2
2200         CLIP 0,22,0,22
2210         AXES 1,1,0,0
2220         UNCLIP
2230         LORG 5
2240         CSIZE 3,.5
2250         LDIR 0
2260         RETURN
2270 !                  -
2280 !
2290 Bardat:GOSUB Pltdat
2300         FOR M=1 TO K
2310          MOVE X(M),Y(M)
2320          LABEL USING "DD";Time(M)
2330         NEXT M
2340         CSIZE 5,.5
2350         MOVE 17,17
2360         LABEL USING "K";"BLACK BAY"
2370         LABEL USING "K";"PROGRESSION TIME"
2380         LABEL USING "K";"OF THERMAL BAR"
2390         LABEL USING "K";"(DAYS)"
2400         LABEL USING "K";"(387.1 CAL-CM^-2-D^-1)"
2410         PAUSE
2420         GCLEAR
2430         RETURN
2440 Sound:GOSUB Pltdat
2450         FOR M=1 TO K
2460          MOVE X(M),Y(M)
2470          LABEL USING "DD";D(M)
2480         NEXT M
2490         CSIZE 5,.5
2500         MOVE 17,17
2510         LABEL USING "K";"BLACK BAY"
2520         LABEL USING "K";"SOUNDINGS (m)"
2530         PAUSE
2540         GCLEAR
2550         RETURN
```

```
10    IMAGE "Program PVD,Version 1,Updated 82/3/14."
20    IMAGE "Stored on F.E.Roy File 1 as PVD1."
30    !
40    !
50    !  P.V.D. is a program to plot progressive vector diagrams.Data input
60    !  comprises up to 31 sets of magnitude and direction. Scale of diagram
70    !  to fit plotting area may be adjusted by altering scale of A in Line 160
.
80    !  Data is to be attached in space preceeding line 40.
90    !
100   !
110   ! List of Variables
120   !
130   !
140   !
150 Main:GOSUB Init
160      GOSUB Plot
170      END
180   !
190 Init: DIM V(31),D(31),Vs(31),Ds(31)
200       DEG
210       MASS STORAGE IS ":T14"
220       INPUT "PLOTTER IS CRT (1) OR 9872A (0)?",X
230       IF X=1 THEN GOTO 250
240       IF X=0 THEN GOTO 270
250       PLOTTER IS 13,"GRAPHICS"
260       GOTO 290
270       PLOTTER IS "9872A"
280       GOTO 290
290       INPUT "FILE 1,# RECORDS,FILE 2,# RECORDS,SCALE ?",A$,A,B$,B,M
300       INPUT " DEPTH,MONTH ?",D$
310       INPUT " FILE 1 ORIGIN,FILE 2 ORIGIN ? PLOT AREA IS X=200,Y=150 ",X1,Y1
,X2,Y2
320       ASSIGN #1 TO A$
330       ASSIGN #2 TO B$
340       FOR N=1 TO A
350         READ #1,N;V,D,T
360          V(N)=V*M
370          D(N)=90-D
380       NEXT N
390   ! !
400       FOR I=1 TO B
410         READ #2,I;Vs,Ds,Ts
420          Vs(I)=Vs*M
430          Ds(I)=90-Ds
440       NEXT I
450   RETURN
460 Plot: ! PLOTTER IS "9872A"
470       GRAPHICS
480       DEG
490       SCALE 0,200,0,150
500       PEN 1
510       LINE TYPE 1
520       GOSUB Plot1
530       GOSUB Plot2
540       GOSUB Title
550       RETURN
560 Plot1:!
570       MOVE X1,Y1
580       IPLOT 0,0
590       FOR J=1 TO A
600         PDIR D(J)
610         IPLOT V(J),0,-1
620         PDIR D(J)+90
630         IPLOT 2,0
640         PDIR D(J)-90
```

```
650          IPLOT 2,0
660          PDIR 0
670          WHERE Xp,Yp
680          MOVE Xp+2,Yp
690          CSIZE 3,.5
700          LABEL USING "K";J
710          MOVE Xp,Yp
720        NEXT J
730      RETURN
740 !
750 !
760 Plot2: !
770     MOVE X2,Y2
780     IPLOT 0,0
790        FOR K=1 TO B
800          PDIR Ds(K)
810          IPLOT Vs(K),0,-1
820          PDIR Ds(K)+90
830          IPLOT 2,0
840          PDIR Ds(K)-90
850          IPLOT 2,0
860          PDIR 0
870          WHERE Xp,Yp
880          MOVE Xp+2,Yp
890          CSIZE 3,.5
900          LABEL USING "K";K
910          MOVE Xp,Yp
920        NEXT K
930     RETURN
940 !
950 !
960 Title:PDIR 0
970      CSIZE 3,.5
980      PEN 1
990      MOVE 15,100
1000     IPLOT 0,0
1010     PDIR 90
1020     IPLOT 15,0
1030     IPLOT -4,1
1040     PENUP
1050     IPLOT 0,-5
1060     IMAGE "NORTH"
1070     LABEL USING 1060
1080     PENUP
1090     MOVE 10,90
1100     IPLOT 0,0
1110     IPLOT 1,0
1120     IPLOT -1,0
1130     PDIR 0
1140     IPLOT M,0
1150     PDIR 90
1160     IPLOT 1,0
1170     MOVE 10,85
1180     LORG 2
1190     LABEL "1 CM/S"
1200     MOVE 5,20
1210     CSIZE 4,.5
1220      LABEL "P.V.D. OF CURRENTS,STA. 1 AND 2 ;";D$
1230     MOVE 5,10
1240      LABEL "Left is Station 1 (West Side)."
1250     MOVE 5,5
1260      LABEL "Right is Station 2 (East Side)."
1270     PEN 0
1280 RETURN
```